PRACTICAL METHODS FOR CRITICAL LOAD DETERMINATION AND STABILITY EVALUATION OF STEEL STRUCTURES

By

PEDRO FERNANDEZ

B.S., Instituto Tecnologico y de Estudios Superiores de Occidente, 1992

A Thesis submitted to the

Faculty of the of the Graduate School of the

University of Colorado in partial fulfillment

Of the requirements for the degree of

Master of Science

Civil Engineering

2013

This thesis for the Master of Science degree by

Pedro Fernandez

has been approved for the

Civil Engineering Program

by

Fredrick Rutz, Chair

Kevin Rens

Chengyu Li

June 12, 2013

Fernandez, Pedro. (M.S., Civil Engineering)

Practical Methods for Critical Load Determination and Stability Evaluation of Steel Structures

Thesis directed by Assistant Professor Fredrick Rutz

ABSTRACT

The critical load of a column, compression member or structure, calculated from a linear elastic analysis of an idealized perfect structure, does not necessary correspond with the load at which instability of a real structure occurs. This calculated critical load does not provide sufficient information to determine when failure, due to instability of the structure as a whole, will occur. To obtain this information it is necessary to consider the initial geometrical imperfections, eccentricities of loading, and the entire nonlinear load deflection behavior of the structure. However, this process in determining the critical load is too cumbersome and time consuming to be used in practical engineering applications.

With today's computer programs that allow for the analysis of complex structures in which they incorporate advanced analytical techniques such as step-by-step large deformation analysis, buckling analysis, progressive collapse analysis, etc., it is just a natural progression that many structures are now analyzed with these tools.

The goal of this research is to propose a practical methodology for critical load determination and stability evaluation of structures that are difficult or impossible to analyze with conventional hand-calculation methods, (e.g. the

compression cord of a truss pedestrian bridge or a wind girt). The proposed methodology relies on a computer software package that has the ability to perform a second-order analysis taking in consideration end-restraints, reduced flexural stiffness (due to residual stresses in steel or cracked sections in concrete) and initial geometrical imperfections. Further, and importantly, a testing scheme was developed to validate the results from the computer in order to verify the methodology as a practical approach.

The format and content of this abstract are approved. I recommend its publication.

Approved: Fredrick R. Rutz

DEDICATION

I dedicate this work to Mary Lynne, my wife,

my parents,

my brother,

Coco and Nina

...and in the loving memory of my grandparents

ACKNOWLEDGMENTS

I would like to thank first and foremost Dr. Fredrick Rutz for the support and guidance in completion of this thesis. I would also like to thank Dr. Rens and Dr. Li for participating on my graduate advisory committee. Lastly, I would like to thank Paul Jones, the artist, who built the test models with so much precision and passion, as well as for being my fearless load operator.

TABLE OF CONTENTS

CHAPTER

I. INTRODUCTION 1

Research Program Objectives 4

Outline of Research 6

II. A HISTORICAL APPROACH ON STRUCTURAL STABILITY 9

Euler 9

Effective Length Factors 11

Inelastic Buckling Concepts 16

Tangent Modulus 19

Reduced Modulus 21

Shanley Theory 22

Amplification Factors 23

Braced Frames 25

Unbraced Frames 28

Column Strength Curves 30

Summary of Present State of Knowledge 33

III. COLUMN THEORY 34

Mechanism of Buckling 35

Critical Load Theory 37

Euler Buckling Load 40

Critical Load of Beam-Columns 45

Second Order Effects 49
Inelastic Buckling of Structures 52
Factors Controlling Column Strength and Behavior 54
Material Properties 55
Length 56
Influence of Support Conditions 57
Moment Frames 57
Members with Elastic Lateral Restraints 61
Influence of Imperfections 64
Material Imperfections 65
Geometrical Imperfections 68
IV. METHODS AND PROCEDURES FOR ANALYSIS AND DESIGN OF STEEL STRUCTURES 71
Structural and Stability Analysis 71
First-Order Elastic Analysis 73
Elastic Buckling Load 74
Second-Order Elastic Analysis 74
First-Order Inelastic Analysis 75
Second-Order Inelastic Analysis 76
Design of Compression Members 76
Determining Required Strength 79
Determining Available Strength 80
Compression Strength 82

Combined Forces 85

Current Stability Requirements (AISC Specifications) 87

The Effective Length Method 89

Direct Analysis Method 90

Imperfections 91

Reduced Flexural and Axial Stiffness 92

Advanced Analysis 93

Pony Truss Bridges 96

V. STABILITY ANALYSIS USING NONLINEAR MATRIX ANALYSIS WITH COMPUTER SOFTWARE 99

Matrix Structural Analysis 99

Direct Stiffness Method 101

Nonlinear Analysis using Matrix Methods 102

Computer Software Used 105

P-Δ and P-δ 106

Modeling Geometrical Imperfections 108

Assessment of the Computer Software with Benchmark Problems from Established Theory 109

VI. A PRACTICAL METHOD FOR CRITICAL LOAD DETERMINATION OF STRUCTURES 112

Proposed methodology: Step-by-step process 113

VII. COMPUTER SOFTWARE EVALUATION WITH BENCHMARK PROBLEMS 116

Benchmark Problem 1 118

Benchmark Problem 2 126

Discussion of Results from Benchmark Problems 133
VIII. MODEL DEVELOPMENT 134
Full-Size Analytical Study 135
Experimental Study 144
Theoretical Models 145
Bridge 1 145
Bridge 2 146
Loading 149
Geometric Imperfections 150
Procedure 151
Test Models 152
Test Setup 155
Load Testing Procedure 159
IX. EXPERIMENTAL RESULTS 161
Bridge 1 Results 164
Theoretical Results 164
Load Test Results 168
Bridge 2 Results 177
Theoretical Results 177
Load Test Results 181
X. CONCLUSIONS 187
Research Overview 187
Research Conclusions 188

General Recommendations 189

REFERENCES 191

APPENDIX 1: TEST MODELS PLANS 197

LIST OF FIGURES

Figure

1.1 Pony truss bridge (Excelbridge 2012)..... 3

2.1 (a) Cantilever Column, (b) Pinned End Column 10

2.2 Effective Column Lengths. (a) Pinned End, (b) Cantilever and (c) Fixed-end 12

2.3 Effective Length Factors *K* for centrally loaded columns (Adapted from Chen 1985)..... 14

2.4 Effective length of a moment frame with joint translation (Adapted from Geschwindner 1994)..... 14

2.5 Effective length factors (Adapted from AISC 2005)..... 16

2.6 Column Critical Stress for various slanderness ratios (*L/r*) (Adapted Gere 2009)17

2.7 Stress-strain diagram for typical structural steel in tension (Adapted from Gere 2009)..... 18

2.8 Definition of tangent modulus for nonlinear material (Adapted from Geschwindner 1994)..... 20

2.9 Stress distributions for elastic buckling: (a) tangent modulus theory; (b) reduced modulus theory (Adapted from Geschwindner 1994) 22

2.10 Load-deflection behavior for elastic and inelastic buckling (Adapted from Gere 2009)..... 23

2.11 Axial loaded column with equal and opposite end moments (Adapted from Geschwindner 1994)..... 26

2.12 Amplified moment: exact and approximate (Adapted from Geschwindner 1994) 27

2.13 Structure second-order effect: sway (Adapted from Geschwindner 1994) 28

2.14 Column strength variation (Adapted from Ziemian, 2010) 32

3.1 Elastic Stability (Adapted from Gere 2009) 36

3.2 Column Stability (Adapted from Chen 1985) 38

3.3 Beam-Column Stability (Adapted from Chen 1985) 39

3.4 Pin-ended supported column 41

3.5 Euler Curve 45

3.6 Beam-Column (Adapted from Chen 1985) 46

3.7 Elastic analysis of initially deformed column (Adapted from Chen 1985) 49

3.8 Second-order effects 52

3.9 Residual stresses and proportional stress (Chen 1985) 54

3.10 Typical stress-strain curves for different steel classifications 56

3.11 Theoretical column strength (Gere 2009) 57

3.12 Typical load-deflection curves for columns with different framing beam connections (Adapted from Ziemian 2010) 58

3.13 Column strength curves for members with different framing beam connection (Adapted from Ziemian 2010) 59

3.14 Connection flexibility (Adapted from AISC 2005) 59

3.15 Pony truss and analogous top chord (Adapted from Ziemian 2010) 63

3.16 Influence of imperfections on column behavior (Adapted from ASCE Task Committee 1997) 65

3.17 Column curve for structural steels. (a) elastic-perfectly plastic stress-strain relationship; (b) column curve (Adapted from Chen 1985) 66

3.18 Lehigh residual stress pattern (Adapted from Surovek 2012) 68

4.1 Comparison of load-deflection behavior for different analysis methods (Adapted from Geschwindner 1994) 73

4.2 Distinction between effective length and notional load approaches (Adapted from Ziemian 2010) 81

4.3 Standard column curve (Adapted from Williams 2011) 85

4.4 Interaction curve (Adapted from Williams 2011)..... 87

4.5 Lateral U-Frame (Adapted from AASHTO 2009)..... 97

5.1 Schematic representation of incremental-iterative solution procedure. (Ziemian 2011)..... 105

5.2 RISA second-order effects process (Adapted from RISA-3D 2012)..... 107

5.3 Benchmark Problem 1 (AISC 2005)..... 110

5.4 Benchmark Problem 2 (AISC 2005)..... 111

6.1 Error message from RISA-3D that *P-Δ* is no longer converging 115

7.1 Benchmark Problem 1 (AISC 2005)..... 117

7.2 Benchmark Problem 2 (AISC 2005)..... 117

7.3 Benchmark problem 1: a) undeflected shape b) deflected shape..... 121

7.4 Maximum moment values as a function of axial force for benchmark problem 1 (classical solution, Equation 7.2)..... 122

7.5 Maximum deflection values as a function of axial force for benchmark problem 1 (classical solution, Equation 7.3)..... 122

7.6 Benchmark problem 1 node arraignments a) Case 1, one additional node at mid height of the beam-column b) Case 2, two additional nodes at equal distance c) Case 3, three additional nodes at equal distance..... 123

7.7 Maximum moment values as a function of axial force for benchmark problem 1 (classical solution, with one, two and three additional nodes) 124

7.8 Maximum deflection values as a function of axial force for benchmark problem 1 classical solution, with one, two and three additional nodes)..... 125

7.9 Benchmark problem 2, a) undeflected shape b) deflected shape..... 127

7.10 Maximum moment values as a function of axial force for benchmark problem 1 (classical solution, Equation 7.5)..... 129

7.11 Maximum deflection values as a function of axial force for benchmark problem 1 (classical solution, Equation 7.6)..... 129

7.12 Benchmark problem 2 node arraignments a) Case 1, no additional node along the height of the beam-column b) Case 2, one additional node at mid height of the beam-column c) Case 3, two additional nodes at equal distance 130

7.13 Maximum moment values as a function of axial force for benchmark problem 2 (classical solution, with zero, one and two additional nodes) 131

7.14 Maximum deflection values as a function of axial force for benchmark problem 2 (solution, with zero, one and two additional nodes) 132

8.1 Actual 40 foot long pony truss bridge 137

8.2 Computer model of the 40 foot long bridge (*analytical model*) 137

8.3 Parametric study 139

8.4 Geometric imperfection 140

8.5 Deformed shape at critical load. Slender top chord 142

8.6 Deformed shape at critical load. Stiffer compression chord 142

8.7 *Bridge 1* truss geometry 147

8.8 *Bridge 1* computer model of truss 147

8.9 3D Model of *Bridge 1* 147

8.10 *Bridge 2* truss geometry 148

8.11 *Bridge 2* computer model of truss 148

8.12 3D model of *Bridge 2* 148

8.13 Load test setup diagram 149

8.14 *Bridge 1* computer model loading configuration 150

8.15 *Bridge 2*, computer model loading configuration 150

8.16 Modeling of geometric imperfections 151

8.17 *Bridge 1* Computer Model 153

8.18 *Bridge 1* Test model 153

8.19 *Bridge 2* Computer Model 154

8.20 *Bridge 2* Test Model 154

8.21 Load test setup diagram 156

8.22 Load test setup 156

8.23 Spreader beam and plates used to uniformly distribute the load on the bridge deck 157

8.24 Typical end support configuration and abutments 157

8.25 Load cell 158

8.26 Data collection setup 159

8.27 Test setup top view 160

9.1 *Bridge 1* Naming convention for top chords 162

9.2 *Bridge 2* Naming convention for the top chords 162

9.3 Top chord initial imperfection, Δ_o (a) Top view of compression chord (b) Cross-section view 163

9.4 *Bridge 1* Theoretical results 167

9.5 *Bridge 1* Theoretical and load test results 171

9.6 *Bridge 1* Deformed shape at failure 172

9.7 *Bridge 1* Theoretical (fix-ended diagonals) and load test results 174

9.8 Deformation of end-diagonal prior to buckling (test model) 175

9.9 Deformation of end-diagonal (computer model) at critical load 175

9.10 Deformation of end-diagonal at buckling (test model) 176

9.11 Deformation of end-diagonal (computer model) at critical load 176

9.12 *Bridge 2* Theoretical results 180

9.13 *Bridge 2* Theoretical and load test results 184

9.14 Deformed shape at 53% of the critical load 185
9.15 Deformed shape at 78% of critical load 185
9.16 Deformed shape at 91% of the critical load 186
9.17 Deformed shape at critical load 186

LIST OF TABLES

Table

8.1Parametric Study of Analytical Models 143

9.1 Measured initial imperfections, Δ_o, of top chords 163

9.2 *Bridge 1* Theoretical Results: Top chord ratio Δ/Δ_o 166

9.3 *Bridge 1* Theoretical Results: Critical load 166

9.4 *Bridge 1* Theoretical and Load Test Results: Top chord ratio Δ/Δ_o 170

9.5 *Bridge 1* Theoretical and Load Test Results: Critical load 170

9.6 *Bridge 1* Ratio Δ/Δ_o, theoretical results with fix-ended diagonals 173

9.7 *Bridge 1* Critical load, theoretical results with fix-ended diagonals 173

9.8 *Bridge 2* Theoretical Results: Top chord ratio Δ/Δ_o 179

9.9 *Bridge 2* Theoretical Results: Critical load 179

9.10 *Bridge 2* Theoretical and Load Test Results: Top chord ratio Δ/Δ_o 183

9.11 *Bridge 2* Theoretical and Load Test Results: Critical load 183

CHAPTER I

INTRODUCTION

A research project on stability cannot start without recognizing the contribution of Euler to the problem of stability when he published his famous Euler's equation on the elastic stability of columns back in 1744. And even though the research on the stability of structures can be traced back to 264 years ago since Euler's contribution to column stability, practical solutions are still not available for some types of structures. Stability is one of the most critical limit states for steel structures during construction and during their service life. One of the most difficult challenges in structural stability is determining the critical load under which a structure collapses due to the loss of stability; this is because of the complexity of this phenomenon and the many material properties that are influenced by geometric and material imperfections and material nonlinearity. In addition to the challenges mentioned above, the advancement in industrial processes in hot-rolled members and the use of high strength steel, which provides a competitive design solution to structural weight reduction, has resulted in increase of member slenderness, structural flexibility and therefore more vulnerability to instability.

The method proposed in this research project for the evaluation of the lateral stability of structures, and to determine their critical load at which they become instable is an innovative approach. It enables the prediction of the characteristics of stability of structures by capturing the load-deformation history and the deformed

shape of the structure at the critical load. Such critical information is generally not available through the current stability analysis methods. Although the method is oriented for analysis of 3D structures, and structures that are difficult to analyze with conventional hand-calculation methods, it can be used for any 2D structure.

Lateral stability of steel structures that are difficult to analyze with conventional hand-calculation methods include: columns under axial compression load and biaxial bending in 3D frames, stepped columns, multi-story columns of different lengths and sections, the unbraced compression chord of a wind-girt truss, and the top chord of a pony truss which due to vertical clearance requirements prohibit direct lateral bracing. Pony truss structures, while no longer as common for construction of new highway or rail bridges, are commonly used in applications similar to Figure 1.1 or as walkways and conveyor systems.

The analysis of the compression chord of a pony truss is typically accomplished by treating the chord as a column with elastic supports (Ziemian 2010). This column, with intermediate elastic restraints, will buckle in a number of half-waves depending on the stiffness of the elastic restraints. The deformed shape or buckled shape of the column will fall somewhere between the extreme limits of a half-wave of length equating the length of the chord and a number of half-waves equating the number of spans between the end restraints, that is, the number of panels. From the buckled shape, the effective length of the compression chord can be

used to determine the critical load. The method on how to determine the effective length has long been the focus of the compression chord buckling problem.

Figure 1.1 Pony truss bridge

This research will focus primarily on applying the proposed methodology for the determination of the critical load of pony truss bridges. However, it can be used for any other 3D structures, including framed structures. All structural frames in reality are geometrically imperfect, that is, lateral deflection commences as soon as the loads are applied. There are typically two types of geometric imperfections that are taken into consideration for the stability analysis of structures; out-of-straightness, which is a lateral deflection of the column relative to a straight line between its end

points, and column out-of-plumbness, which is lateral displacement of one end of the column relative to the other. In the absence of more accurate information, evaluation of imperfection effects should be based on the permissible fabrication and erection tolerances specified in the appropriate building code.

In the U.S., the initial geometric imperfections are assumed to be equal to the maximum fabrication and erection tolerances permitted by the AISC *Code of Standard Practice for Steel Building and Bridge,* AISC 303-10 (AISC 2010). For columns and frames, this implies a member out-of-straightness equal to $L/1000$, where L is the member length brace or framing points, and a frame out-of-plumbness equal to $H/500$, where H is the story height. For the critical load determination and load-deformation history evaluation in this research project, three imperfections will be considered: $L/300$, $L/450$ and $L/700$.

Research Program Objectives

The goal of this research project is to propose a practical method for stability evaluation and assessment of structures that are difficult or impossible to analyze with conventional hand-calculation methods. The proposed methodology relies on a commercially available computer program in which a second order analysis can be readily accomplished by taking into consideration end-restraints, reduced flexural stiffness, and initial geometrical imperfections or out-of-plumbness. The method can be used for any frame 3D structure or truss. The specific objectives of this research project are:

1. Develop an analytical process that is based on an iterative approach (with the help of a 3D computer program) that would facilitate the determination of the critical load and stability assessment of steel structures that are difficult or impossible to analyze with conventional hand-calculation methods.

2. Investigate the correctness of the computer program to be able to perform a rigorous second order analysis, by using benchmark problems from established theory, which are presented in AISC 360-05.

3. Conduct an analytical investigation, using the proposed approach, to determine the critical load, the effects of initial imperfections, and the characteristics of the failure mode of full size pony truss models.

4. Develop two scaled pony truss bridges based on the results from item 3 that can be load tested with available equipment.

5. Apply the proposed methodology and determine, analytically, the load-deformation history and critical load of the two scaled pony truss bridges developed in item 4.

6. Develop a testing scheme in which two scaled pony truss bridges are load tested. The testing scheme must include means to measure both of

the top chords out of plane deformations and to determine the load at any instant of the load application.

7. Verify the proposed methodology by comparing the results between the computer model results and the results from the testing scheme.

Outline of Research

In general terms, this research project consisted of a literature review, development of a methodology for critical load determination of structures, and a testing scheme to validate the proposed methodology. This thesis is organized in the following manner:

Chapter II presents a historical background on column stability, from Euler's early work on column stability and elastic critical load to the development of the column strength curves used in today's column strength equations. This historical background includes an introduction to the concept of equivalent or effective length, a review of different theories that have been used to predict column strength and an introduction on the derivation of the amplification factors.

In Chapter III, the mechanism of buckling is presented along with the derivation of the critical load for an ideal column with pin supports. An introduction to structural stability of beam-columns and second order effects (P-Δ and P-δ) is discussed. In this Chapter, some of the more critical factors that control column

strength and behavior are reviewed. This review focuses on the effects of geometrical and material imperfections.

The determination of member sizes for a structure, in general terms, is a two step process. First, a structural and stability analysis is performed in order to determine the required strength. Second, empirical equations are used to determine the available strength and then compared to the required strength. Chapter IV presents an overview of the different methods for stability analysis, as well as the procedures and requirements for the determination of the available strength in AISC *Specifications for Structural Steel Buildings, AISC* 360-05 (AISC 2005) and AASHTO *LRFD Guide Specifications for the Design of Pedestrian Bridges,* (AASHTO 2012).

Because the proposed methodology requires the use of a computer program, Chapter V presents an introduction to the methods of analysis in most computer software packages. Also in this Chapter, an introduction to the capabilities of the computer software package (RISA-3D) is presented as well as a discussion of its ability to perform a rigorous second-order analysis.

In Chapter VI the proposed methodology is presents as a step by step process with the goal of determining the load-deformation history and critical load of a structure. This process addresses the selection of the computer software package, modeling, the incorporation of geometrical imperfections in the model and the determination of the critical load.

However, it is necessary to evaluate the ability of the software package to perform a rigorous second order analysis. Given in Chapter VII are the results from the benchmark problems used for the evaluation of RISA-3D. Furthermore, in this chapter, a discussion is given on the assessment of the *P-δ* capabilities of the program.

The development of the testing scheme is given in Chapter VIII and the results are presented in Chapter IX. Conclusions of the current research and recommendations are presented in Chapter X.

CHAPTER II

A HISTORICAL APPROACH ON STRUCTURAL STABILITY

Euler

Any work on structural stability cannot start without a discussion on Leonard Euler (1707-1783), for many, Euler is considered the greatest mathematician of all time (Gere 2009). Euler made great contributions to the field of mathematics, namely, trigonometry, differential and integral calculus, infinite series, analytic geometry, differential equations, and many other subjects (Gere 2009). However, with regard to applied mechanics, Euler made one of the most important contributions to structural engineering concerning with elastic stability of structures, and which is still subject of many studies after almost 270 years: the buckling of columns. He was the first to derive the formula for the critical buckling load of an ideal, slender column.

Euler's work was published in 1744 under the title *"Methodus inveniendi lineas curvas maximi minimive proprietate gaudentes"*. His original work consisted on determining the buckling load of a cantilever column that was fixed at the bottom and free at the top as shown in Figure 2.1(a) (Timoshenko 1983).

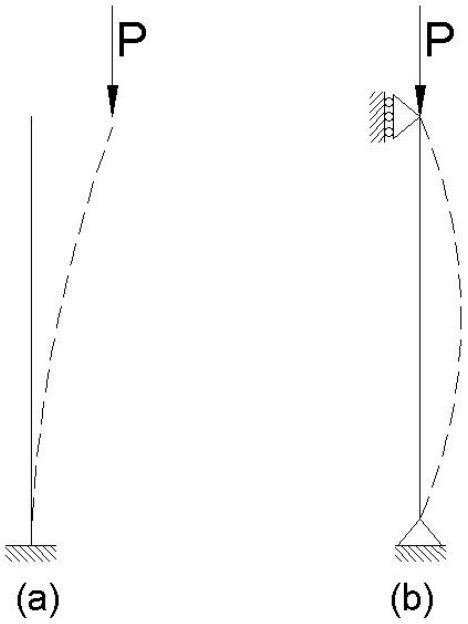

Figure 2.1 (a) Cantilever Column, (b) Pinned End Column

In this case, Figure 2.1(a), Euler shows that the equation of the elastic curve can be readily be solved and that the load at which the buckling occurs is given by Equation 2.1

$$P = \frac{C\pi^2}{4l^2} \qquad (2.1)$$

Later on, Euler expanded his work on columns to include other restraint conditions, and determined the buckling load for a column with pinned supports, Figure 2.1(b) as being

$$P = \frac{C\pi^2}{l^2} \qquad (2.2)$$

In his work, Euler did not discuss the physical significance of the constant *C* which he calls the "absolute elasticity", merely stating that it depends on the elastic properties of the material (Timoshenko 1983). One can conclude that this constant is the flexural stiffness of the column, *EI*. Euler was the first to recognize that columns could fail through bending rather than crushing. In his work he states:

> Therefore, unless the load *P* to be borne be greater than $C\pi^2/4l^2$ there will be absolutely no fear of bending; on the other hand, if the weight *P* be greater, the column will be unable to resist bending. Now when the elasticity of the column and likewise its thickness remain the same, the weight *P* which it can carry without danger will be inversely proportional to the square of the height of the column; and a column twice as high will be able to bear only one fourth of the load (Timoshenko, 1983).

Effective Length Factors

The Euler buckling load equation gives the critical load at which a pin-supported column will buckle, Figure 2.2(a). The critical load for columns with various support conditions, other than a pin-pin support, can be related to this column through the concept of an "effective length". For example, Figure 2.2(b) a fixed-end column buckles at 4 times the load for a pinned column, and because the Euler buckling load is directly proportional to the inverse square of the length, the effective length of a fixed-end column is one half of that of the same member with pinned ends. At the same time, Figure 2.2(c), a column that is fixed at the base and free at the top will have an effective length of 2*L* and will buckle at a quarter the load of the pinned-end column.

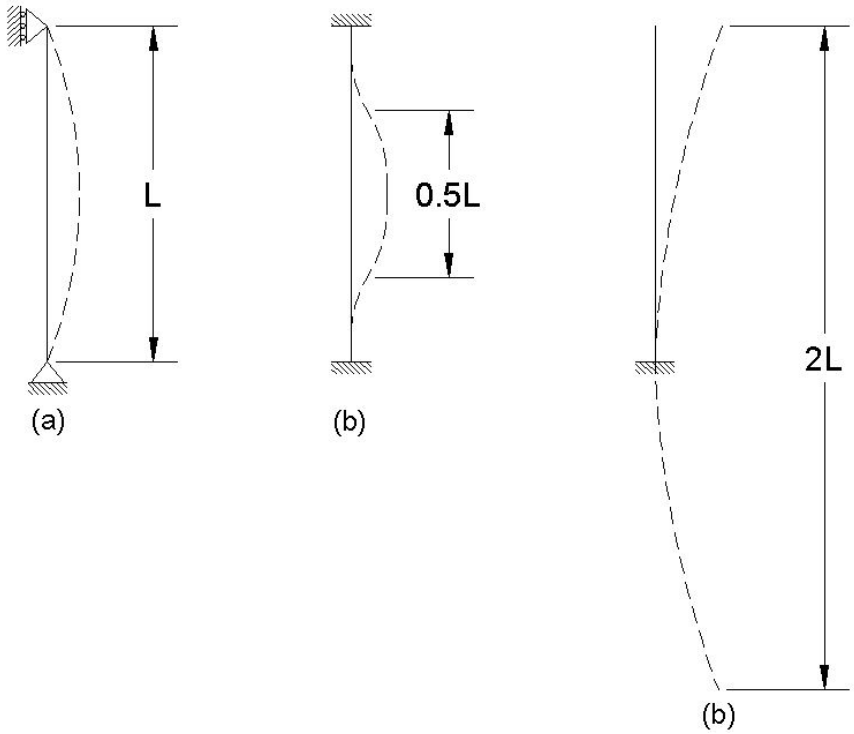

Figure 2.2 Effective Column Lengths. (a) Pinned End, (b) Cantilever and (c) Fixed-end

Because the effective length, L_e, for any column is the length of the equivalent pinned-end column, then, the general equation for critical loads, for any column with supports other than pin-pin, can be written as

$$P = \frac{\pi^2 EI}{\left(L_e^{\,2}\right)} = \frac{\pi^2 EI}{\left(Kl\right)^2} \qquad (2.3)$$

Where K is the effective length factor and is often included in design formulas for columns. That is, the Euler buckling load formula can be used to obtain the critical load of a column with different end conditions provided the correct effective length of the column is known, illustrated in Figure 2.3.

> In simplified terms the concept is merely a method of mathematically reducing the problem of evaluating the critical stress for columns in structures to that of equivalent pinned-end brace columns (Yura 1971).

So far columns with ideal boundary conditions have been discussed; however, the effective length concept is equally valid for any other set of boundary conditions not included in Figure 2.3, except that the determination for the effective length factor is not as simple or straightforward as in Figure 2.3.

For example, in the case of a column that is part of a moment frame, the effective length factor is a function of the stiffness of the beams and columns that frame into the joint. Columns or compression members can be classified based on the type of frame that they form a part. Columns that don't participate in the lateral stability of the structure are considered to be braced against sway. A braced frame is one for which sidesway or joint translation is prevented by means of bracing, shear walls or lateral support from adjoining structures. An unbraced frame depends on the stiffness of its members and the rotational rigidity of the joints between the frame members to prevent lateral buckling as shown in Figure 2.4. Theoretical mathematical analysis may be used to determine effective lengths; however, such procedures are typically too lengthy and unpractical for the average designers. Such methods include trial and error procedures with buckling equations.

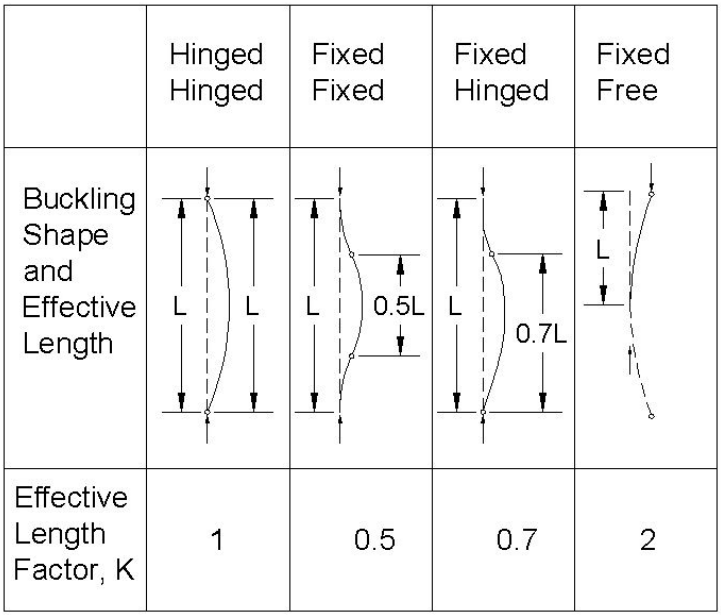

Figure 2.3 Effective Length Factors *K* for centrally loaded columns (Adapted from Chen 1985)

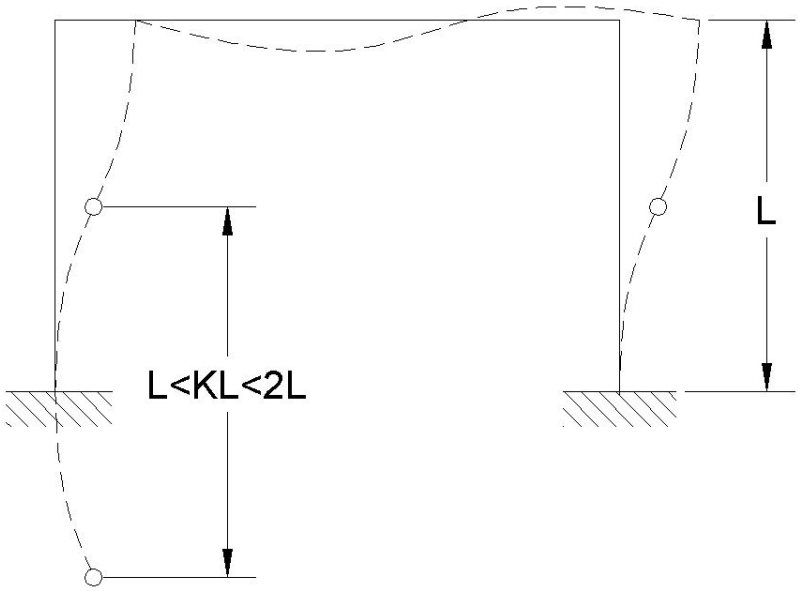

Figure 2.4 Effective length of a moment frame with joint translation (Adapted from Geschwindner 1994)

For normal design situations, it is impractical to carry out a detailed analysis for the determination of buckling strength and effective length. Since the introduction of the effective length concept in the AISC specifications for the first time in 1961 (AISC 1961), several procedures have been proposed for a more direct determination of the buckling capacity and effective length of columns in most civil engineering structures (Shanmugam 1995). The most common method for obtaining the effective length of a column or compression member and to account for the effects of the connected members is to employ the alignment charts or nomographs, originally developed by Julian and Lawrence (McCormac 2008). The alignment charts were developed from a slope-deflection analysis of a frame including the effect of column loads (McCormac 2008).

Values of K for certain idealized end conditions are given in Figure 2.5. The values of K for columns in frames, depend on the flexural rigidity of adjoining members and the manner in which sidesway is resisted. The values given in Figure 2.5 are based on the assumption that all columns in a frame will reach their individual critical loads simultaneously. In certain cases, the effective length factors are not applied correctly given that the underlying assumptions of the method do not apply. The method involves a number of major assumptions which are summarized in section C2.2b of the Commentary of the AISC Specification (AISC 2005). Some of the most significant assumptions are: members are assumed to behave elastically, all

columns buckle simultaneously, all members are prismatic and the structure is symmetric (AISC 2005).

	(a)	(b)	(c)	(d)	(e)	(f)
Buckled shape of column is shown by dashed line	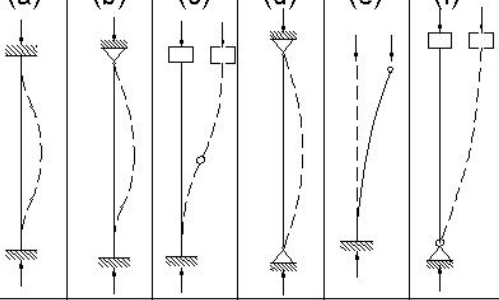					
Theoretical K value	0.5	0.7	1.0	1.0	2.0	2.0
Recommended design value when ideal conditions are approximate	0.65	0.80	1.2	1.0	2.1	2.0
End condition code		Rotation fixed and translation fixed Rotation free and translation fixed Rotation fixed and translation free Rotation free and translation free				

Figure 2.5 Effective length factors (Adapted from AISC 2005)

Inelastic Buckling Concepts

Figure 2.6 shows the theoretical stability behavior of columns as a function of the average compressive strength, *P/A* versus the slenderness ratio, *l/r*. From this figure and depending on the type of failure, columns can be classified as short columns, intermediate columns, and long columns. Short or stocky columns fail by crushing while very long columns fail by elastic buckling as described by Euler's

critical load equation. Euler determined that the critical load for a slender column does not necessary correspond to the crushing strength, but a lower values which is a function of the length of the column and the flexural rigidity as discussed earlier. However, Euler's critical load for elastic buckling is valid only for relative long columns where the stress in the column is below the proportional limit (Gere 2009).

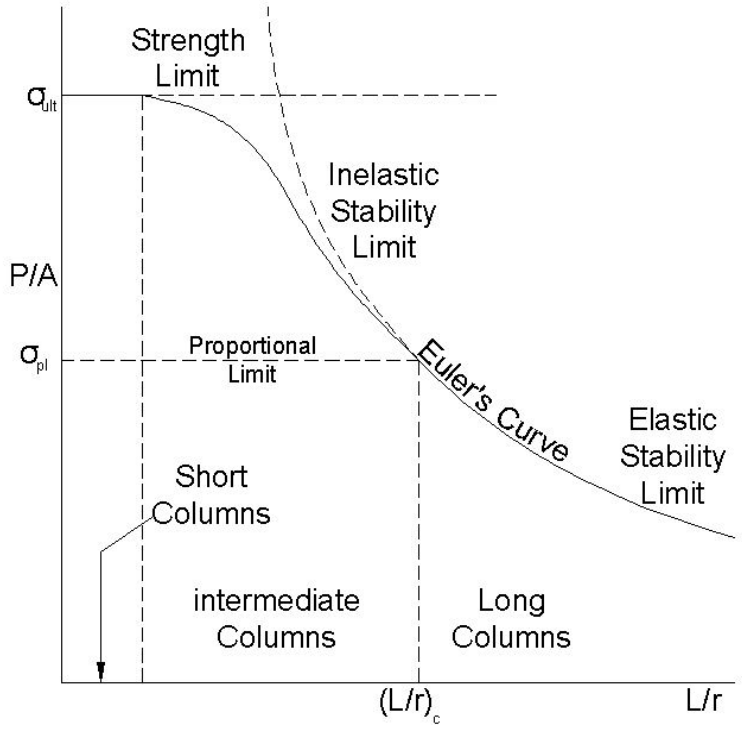

Figure 2.6 Column Critical Stress for various slanderness ratios (*L/r*) (Adapted Gere 2009)

Many practical columns are in a range of slenderness where at buckling, portions of the column are no longer linearly elastic, and thus one of the fundamental assumptions of the Euler column theory is violated due to a reduction in the stiffness of the column. This degradation of the stiffness may be the result of material

nonlinearity or it may be due to partial yielding of the cross section at certain points where compressive stresses pre-exists due to residual stress (Ziemian 2010). This range is considered as the range of the intermediate columns, thus, intermediate columns fail by inelastic buckling. For columns of intermediate length, the stress in the column will reach the proportional limit before buckling begins. The proportional limit is the limit at which not only the modulus of elasticity or the ratio of stress-strain is linear but also proportional, this can be seen in Figure 2.7. Various theories have been developed to account for this type of behavior in which columns are considered to be in the inelastic range, some of the theories are presented below.

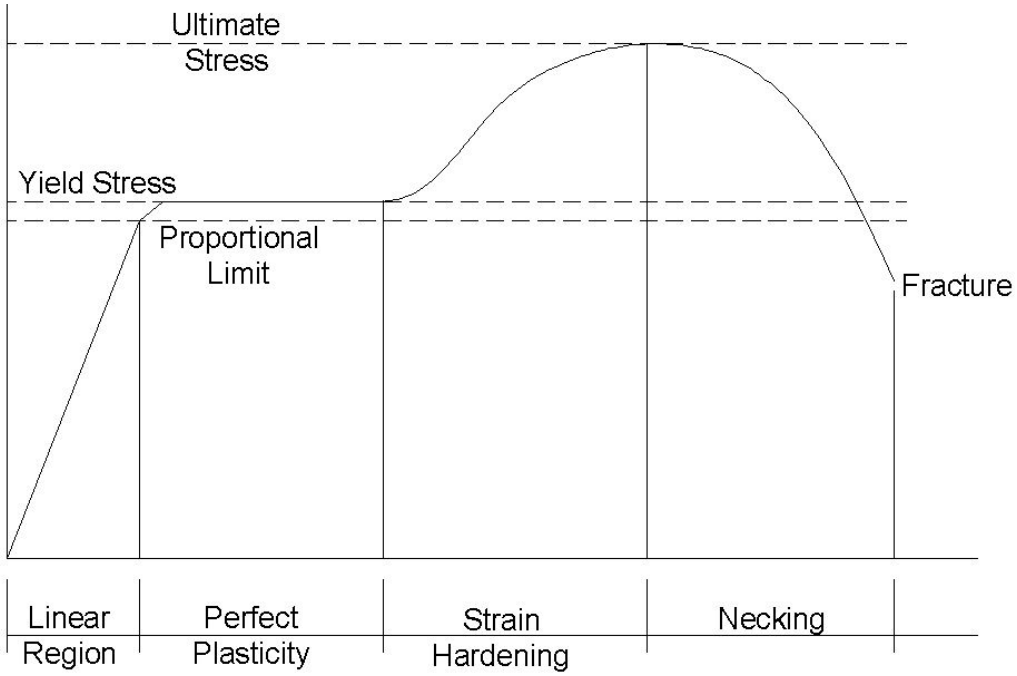

Figure 2.7 Stress-strain diagram for typical structural steel in tension (Adapted from Gere 2009)

Tangent Modulus

In the late 19th century, independent research work done by Engesser and Considère recognized the shortcomings of the Euler theory, in which Euler's buckling load was based on an elastic material response (Geschwindner 1994). During that time it was already known that various materials exhibited nonlinear characteristics. Engesser developed a theory in which he assumed that the modulus of elasticity at the instant of buckling was equal to the slope of the material stress-strain curve at the level of the buckling stress. In other words, if the load on a column is increased so that the stress is beyond the proportional limit of the material, and this increase in load is such that a small increase in stress occurs, the relationship between the increment of stress and the corresponding increment of strain is given by the slope of the stress-strain curve at point A in Figure 2.8. This slope, which is equal to the slope of the tangent line at A, is called the tangent modulus and is designated by E_T, (Geschwindner 1994) thus,

$$E_T = \frac{d\sigma}{d\varepsilon} \qquad (2.4)$$

Engesser rationalized that the fibers in tension (unloading fibers) and the fibers in compression (loading fibers), both, would behave according to the tangent modulus as shown in Figure 2.9(a). Therefore, the buckling load of a column corresponds to the load defined as the tangent modulus load. The buckling load can

then be computed from the Euler buckling expression by substituting the modulus of elasticity with the tangent modulus (Geschwindner 1994).

$$P_T = \frac{\pi^2 E_T I}{\left(l^2\right)} \qquad (2.5)$$

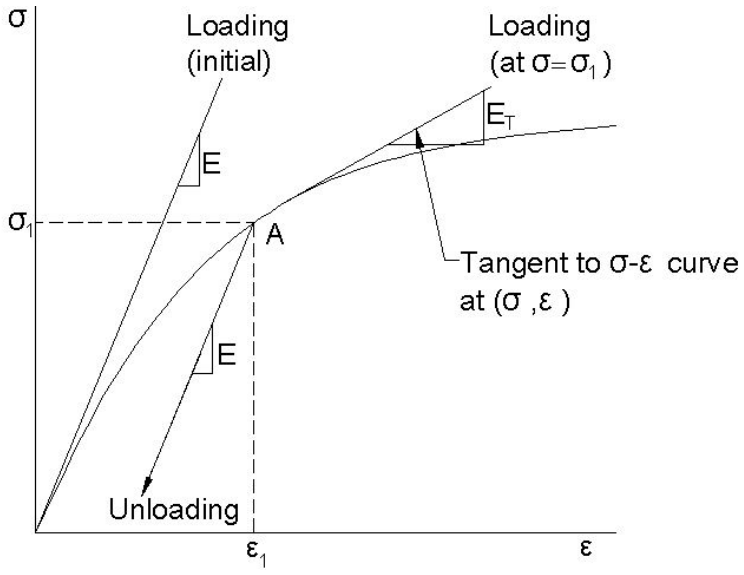

Figure 2.8 Definition of tangent modulus for nonlinear material (Adapted from Geschwindner 1994)

Because the tangent modulus, E_T, varies with the compressive stress, $\sigma = P/A$, the tangent modulus load is obtained by an iterative procedure. From Figure 2.9(a) one can think of the tangent modulus as the average modulus of elasticity of the complete cross section. Some of the fibers will be in the elastic range and others will be in the inelastic range, in other words, some fibers are responding elastically in accordance with the full modulus of elasticity, E, while other respond with a modulus of zero (Geschwindner 1994).

Reduced Modulus

The reduced modulus theory is also known as the double modulus, E_r. When a column bends under loading, in addition to the axial load, bending stresses are added to the compressive stress, P/A due to the axial load. These additional stresses are compression on the concave side and tension on the opposite side of the column. By adding the bending stresses to the axial stresses, it can be seen that on the concave side the stresses in compression are larger than the stresses in tension. Therefore, it can be assumed that on the concave side, the material follows the tangent modulus, Figure 2.9(b) and in the convex side the material follows the unloading line shown in Figure 2.8.

One can think as if this column were made of two different materials (Gere 2009). As in the tangent modulus method, the critical load can be found by replacing the modulus of elasticity, in the Euler equation, by the reduced modulus or double modulus. However, the reduced modulus theory is difficult to use in practice because E_r depends not only on the shape of the cross section of the column but the stress strain curve of that specific column. This means it needs to be evaluated for every different column section type (Gere 2009).

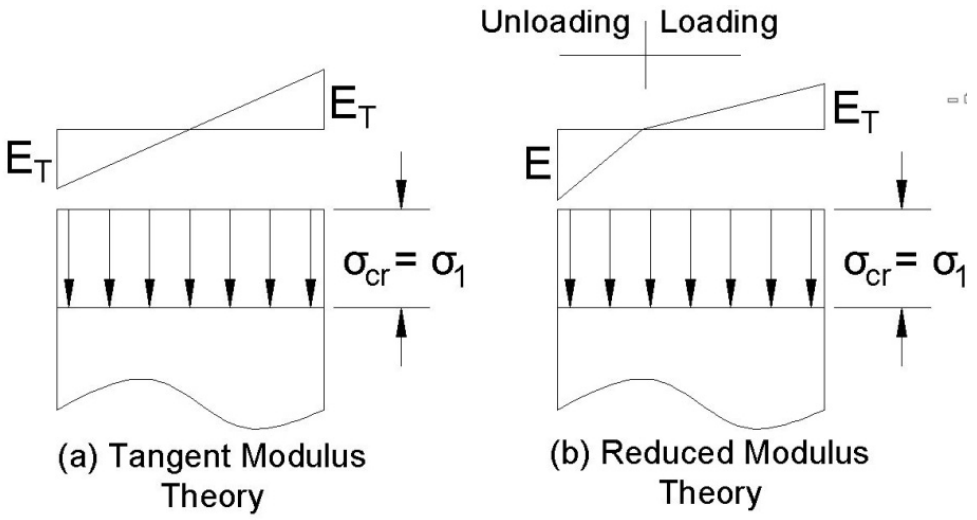

Figure 2.9 Stress distributions for elastic buckling: (a) tangent modulus theory; (b) reduced modulus theory (Adapted from Geschwindner 1994)

Shanley Theory

Tests conducted by von Karman and others over many years (Johnston 1981) have demonstrated that actual buckling loads tend to more closely follow the loads predicted by the tangent modulus equation than those from the reduced modulus equation. In 1947, an American aeronautical-engineering professor F.R. Shanley demonstrated that there would be no stress reversal in the cross section as the column reached the tangent modulus load because the initial deflection at this point was infinitesimal. Shanley proved that the tangent modulus load was the largest load at which the column will remain straight (Geschwindner 1994). Once the load exceeded the tangent modulus load, there would be a stress reversal and elastic unloading would take place and the load carrying capacity is then predicted by the reduced

modulus (Geschwindner 1994). In other words, a perfect inelastic column will begin to deflect laterally when $P = P_T$ and $P < P_{max} < P_R$, illustrated in Figure 2.10.

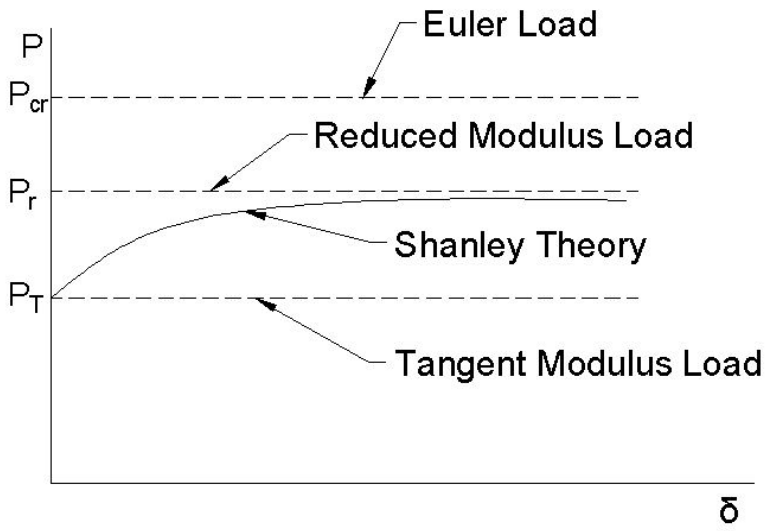

Figure 2.10 Load-deflection behavior for elastic and inelastic buckling (Adapted from Gere 2009)

Amplification Factors

Second order effects are the direct result of structural deformations. In order to account for these secondary effects, a nonlinear or second order analysis must be carried out that takes into account equilibrium on the deformed shape of the structure, rather than on the original undeformed shape as is in the case of the traditional classical methods of analysis. An alternate approach for this more rigorous and complex method of analysis, is to determine the secondary effects by amplifying the moments and forces from a first order elastic analysis. The concept of moment

magnification, to account for secondary effects, was introduced in the AISC Specifications in 1961 by including the following expression (AISC 1961):

$$\frac{C_m}{\left(1-\frac{f_a}{F'_e}\right)} \qquad (2.6)$$

for the determination of combined stresses in the following equation

$$\frac{f_a}{F_a}+\frac{C_m f_b}{\left(1-\frac{f_a}{F'_e}\right)F_b} \le 1.0 \qquad (2.7)$$

The commentary to the AISC Specification of 1961 explains the significance of the new term:

> The bending stress at any cross section subject to lateral displacement must be amplified by the factor
>
> $$\frac{C_m}{\left(1-\frac{f_a}{F'_e}\right)} \qquad (2.8)$$
>
> it recognizes the fact that such displacement, caused by applied moment, generates a secondary moment equal to the product of the resulting eccentricity and the applied axial load, which is not reflected in the computed stress, f_b (AISC 1961).

There are two different magnification factors to account for the secondary effects; one magnification factor is used for columns that are part of a braced frame and a second magnification factor for columns that are part of an unbranced frame. A frame is considered braced if a system, such as shear walls or diagonal braces, serves

to resist the lateral loads and to stabilize the frame under gravity loads. In a braced frame the moments in the column due to the gravity loads are determined through a first order elastic analysis, and the additional moments resulting from the deformation along the column length will be determined through the application of an amplification factor.

Unbraced frames depend on the stiffness of the beams and columns for lateral stability under gravity loads and combined gravity and lateral loads. Unlike braced frames, discussed earlier, there is no supplementary structure to provide lateral stability. Columns that form part of an unbraced frame are subjected to both axial forces and bending moments and will experience lateral translation. The latter will cause an additional second order effect to the one discussed earlier. This second order effect is the result from the sway or lateral displacement of the frame.

Braced Frames

In his paper titled "A Practical Method of Second Order Analysis", LeMessurier provides the full derivation of the amplification factors for both braced frames and unbraced frames (LeMessurieer 1976). A summary of the derivation is presented below.

Consider the column in Figure 2.11, the maximum moment at mid height of the column is given by equation 2.9

$$M_{\max} = M + P\delta \qquad (2.9)$$

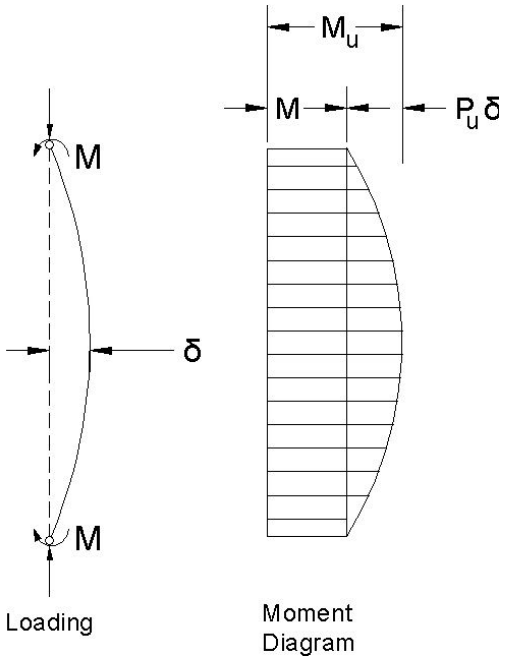

Figure 2.11 Axial loaded column with equal and opposite end moments (Adapted from Geschwindner 1994)

The moment magnification or amplification factor is given by

$$AF = \frac{M_{\max}}{M} = \frac{M + P\delta}{M} \qquad (2.10)$$

Therefore,

$$AF = \frac{1}{1 - \dfrac{P\delta}{M + P\delta}} \qquad (2.11)$$

For small deformations δ is sufficiently small that

$$\frac{\delta}{M + P\delta} \approx \frac{\delta}{M} \qquad (2.12)$$

And assuming that (Ziemian 2010)

$$\frac{M}{\delta} = \frac{8EI}{L^2} \approx \frac{\pi^2 EI}{L^2} = P_e \qquad (2.13)$$

The moment magnification factor for a column that is part of a braced frame is given by Equation 2.14

$$AF = \frac{1}{1 - \frac{P_u}{P_e}} \qquad (2.14)$$

Figure 2.12 shows the approximate amplification factor, derived above, for a pin-pin simply supported column with opposite concentrated moments at its ends. This approximate amplification factor is plotted alongside the exact solution. As it can be seen from Figure 2.12, the approximate amplification factor is slightly conservative compared to the exact solution because $\pi^2 > 8$.

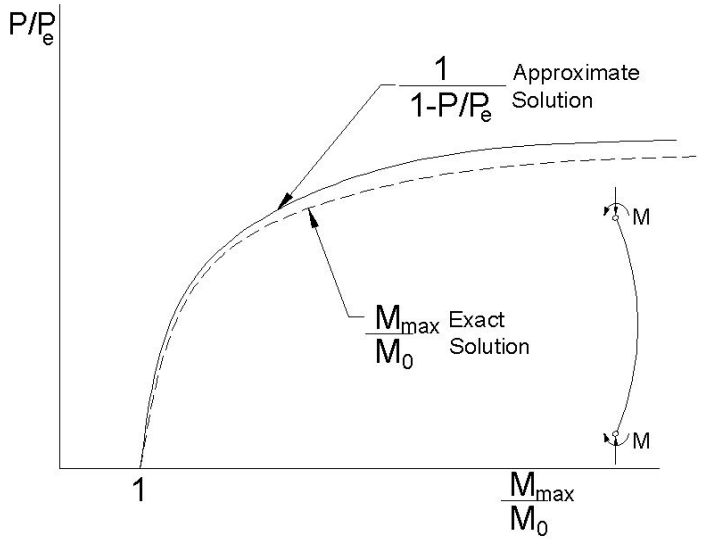

Figure 2.12 Amplified moment: exact and approximate (Adapted from Geschwindner 1994)

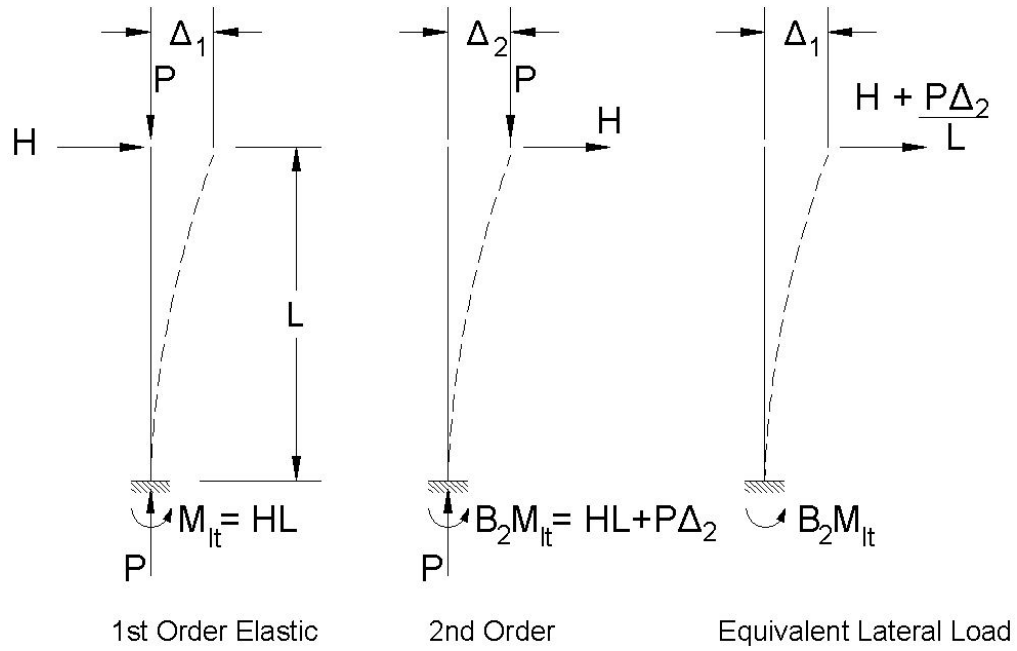

Figure 2.13 Structure second-order effect: sway (Adapted from Geschwindner 1994)

Unbraced Frames

For the case of unbraced frames, and assuming that the lateral stability for the frame in Figure 2.13 is provided by the cantilever column, the determination of the amplification factor is as follows (Geschwindner 1994):

The first order analysis moment and flexural deflections are given by

$$M = HL \qquad (2.15)$$

$$\Delta_1 = \frac{HL^3}{3EI} \qquad (2.16)$$

The displacement Δ_2 is the total displacement including secondary effects, and the total moment including second order effects is given by

$$M_{max} = HL + P\Delta_2 \qquad (2.17)$$

An equivalent load may be determined that will result in the same moment at the bottom of the column as the second order moment.

$$H + \frac{P\Delta_2}{L} \qquad (2.18)$$

It can be seen then that the moments at the bottom of the columns for the second-order and equivalent load cases in Figure 2.13 are the same, thus the second order defection is equal to

$$\Delta_2 = \left(H + \frac{P\Delta_2}{L} \right) \frac{L^3}{3EI} \qquad (2.19)$$

$$\Delta_2 = \left(H \frac{L^3}{3EI} + \frac{P\Delta_2}{L} \frac{L^3}{3EI} \right) = \left(\Delta_1 + \frac{P\Delta_2}{L} \frac{L^3}{3EI} \right)$$

$$\Delta_2 - \Delta_2 \left(\frac{P}{L} \frac{L^3}{3EI} \right) = \Delta_1$$

Solving for Δ_2

$$\Delta_2 = \frac{\Delta_1}{1 - \left(\frac{P}{L} \frac{L^3}{3EI} \right)} \qquad (2.20)$$

Because the amplification factor, B_2 is equal to Δ_2/Δ_1 and $\Delta_1 = \frac{HL^3}{3EI}$, then

$$B_2 = \frac{\Delta_2}{\Delta_1} = \frac{1}{1-\left(\frac{P}{L}\frac{L^3}{3EI}\right)} = \frac{1}{1-\left(\frac{P}{L}\frac{\Delta_1}{H}\right)}$$

$$B_2 = \frac{1}{1-\left(P\Delta_1 \big/ HL\right)} \qquad (2.22)$$

Because the frame is part of a complete structure, this equation can be modified to include all the loads in a story. Therefore the amplification factor for a sway column is given by the following equation (ASIC 2005):

$$B_2 = \frac{1}{1-\left(\sum P_u \Delta_{oh} \big/ \sum HL\right)} \qquad (2.23)$$

Column Strength Curves

After obtaining the internals forces, including secondary effects, of a structure from a structural analysis, the next step is to obtain the column compressive strength from the AISC equations in Chapter H of the AISC Specification. While the effective length factor takes into account global geometrical imperfections, that is, column out of plumbness, the column strength curve provides the strength of the column considering local geometrical imperfections and material imperfections. These imperfections are the out of straightness and residual stresses respectively.

Early versions of column strength date to the 1800's when empirical formulas based on the results of column tests were used. However these formulas were limited

to the material and geometry for which the tests were performed. Another formula for the strength determination of columns which was very popular in early 1900's, was the Perry-Robertson formula. This formula considers a column with an initial deformation and the failure of such column will occur when the maximum compression stress at the extreme fiber reaches the yield strength of the material (Ziemian 2010).

However, the studies that led to the development of the Perry-Robertson and secant formula, were based only on initial out-of-straightness and eccentrically loaded column models, along with an assumed elastic response; in addition, those expressions did not consider the presence of residual stresses. The 1961 AISC Specification presented a new formula for columns whose mode of failure was due to inelastic buckling. This new formula was based on the recommendations of the Column Research Council (CRC). The formula suggested by CRC assumes that the upper limit of elastic buckling failure is defined by an average column stress equal to one-half of yield stress. For years the column formulas found in most common specifications were strictly tangent modulus expressions combined with a safety factor (AISC 1961).

In the late 1960's and early 1970's, studies provided the basis for the development of a solution method based on an incremental, iterative numerical routine which established the load deflection curve for the column (Geschwindner 1994). These studies took into account residual stress, initial out-of-straightness,

spread of plasticity, and load-deflection curves were determined. The correlation of the computation results with full scale tests was good and in the order of 5 percent of the test values (Bjorhovde 1972).

The studies mentioned above, were part of a research program led by Lehigh University for the development of column curves in the U.S. Bjorhovde, in his PH.D dissertation "*Deterministic and probabilistic approaches to the strength of steel columns*" at Lehigh University, examined the characteristics of column strength of an extensive database for the maximum strengths of centrally loaded columns (Figure 2.14). The study encompassed a variety of different shapes, steel grades and manufacturing methods. Bjorhovde observed that there were groupings within the curves and from these, three curves were subdivided. These three column curves are known as the SSRC column strength curves 1, 2 and 3 (Bjorhovde 1972).

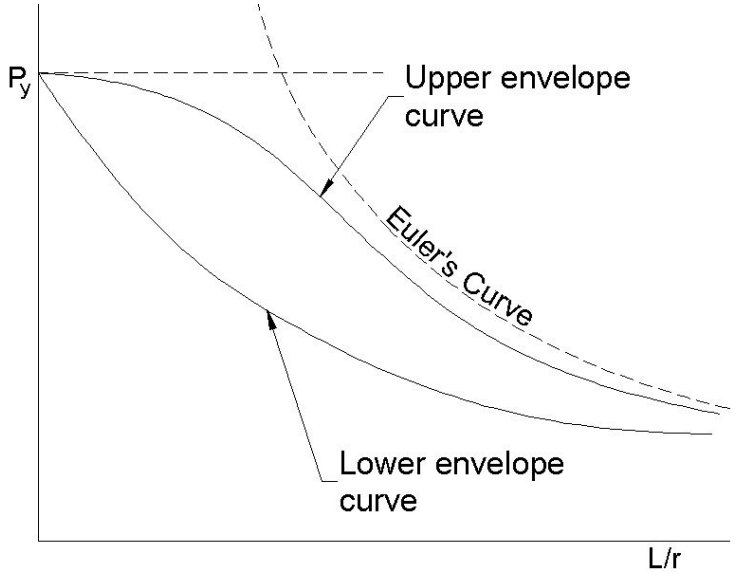

Figure 2.14 Column strength variation (Adapted from Ziemian 2010)

The commentary to the AISC Specification states that the AISC LRFD column curve represents a reasonable conversion of the research data into a single design curve and is essentially the same curve as the SSRC column curve 2P (AISC 2005). The AISC Specification column equations are actually based on the strength of an equivalent pin-ended column of length *KL*, with a mean maximum out-of-straigtness at is mid length of approximately *KL*/1500 (Ziemian 2010).

Summary of Present State of Knowledge

In addition to length, cross-section dimensions and material properties, the maximum strength of steel columns depends on the residual stress magnitude and distribution, the shape and magnitude of the initial out-of-straightness and the end restraints. The effects of these three latter variables are discussed in more detail in Chapter III.

CHAPTER III:

COLUMN THEORY

Since the beginning of human times, columns in structures were built with large cross-sectional dimensions, thus most likely carried loads well below their potential load carrying capacity, and most likely were designed with little or no engineering in the way it is understood today (Geschwindner 1994). With the introduction of steel as a construction material and the development of higher strength steels, column stability and structural stability of steel structures has become a primary concern.

A column, or compression member, is one of the most critical structural elements of a structure, because it transfer loads from one point of the structure to another, and eventually to the foundation, through compression or a combination of compression and flexural bending. Compression members are used as compression chords in trusses as well, and as in the case of pony truss bridges, may be used as pedestrian bridges. In the case of moment or sway frames, the columns and the beams that frame into, and the connections between them, provide lateral stability to those frames. However, for the most part, discussion of column strength in common literature focuses on an individual column rather than the entire system.

This basic column, which is typically used for the derivation of stability and column strength formulas, has no imperfections and is supposed to be supported by perfect hinges; in addition, this column, also known as the perfect column or ideal

column and is referred to as a pinned column, one that rarely exists in actual structures. Nonetheless, the theoretical concepts of the ideal column are important in understanding column behavior for the study of beam-columns, compression elements and stability of frames. This ideal column is loaded by a vertical force P that is applied through the centroid of the section, the column is perfectly straight and follows Hooke's law, that is, it is made of linearly elastic material.

Although a compression member or a structural column can be seen at as a simple structural member, the interaction between the responses and the characteristics of the material, the cross section, the method of fabrication, the imperfections and other geometric factors, and end conditions, make the column one of the most complex individual structural elements (Geschwindner 1994).

Mechanism of Buckling

Load carrying members of structures may fail in a variety of ways, including flexural bending, crushing, fracture and shear. Another type of failure is referred as to buckling. For an idealized column, this is called bifurcation buckling. Figure 3.1(a) shows an idealized column consisting of two rigid bars and a rotational spring. If a load *P* is applied to the end of the column, the rigid bars will rotate through small angles and a moment will develop in the spring designated as point A. This moment is called the restoring moment. If the load is relative small, the restoring moment will return the column to its initial straight position, once this load is removed. Thus, it is called stable equilibrium. If the axial force is large enough, the displacement at A will

increase and the bars will go through large angles until the column collapses. Under these conditions, the column is considered to be unstable and fails by lateral buckling (Gere 2009).

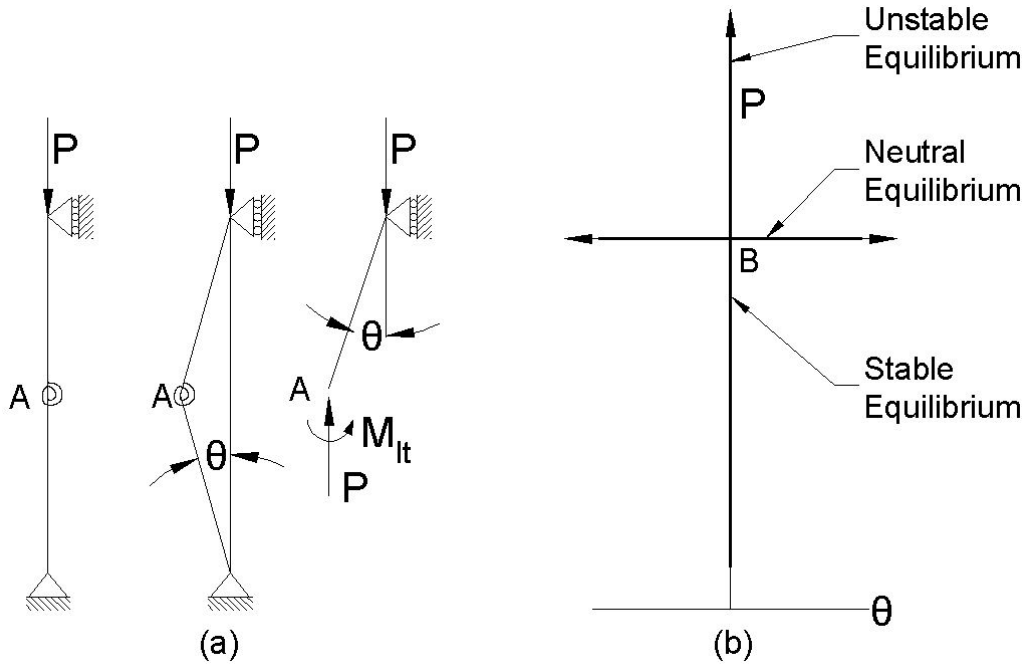

Figure 3.1 Elastic Stability (Adapted from Gere 2009)

Figure 3.1(b) shows three conditions of equilibrium for the idealized column as a function of the compressive load, P versus the angle of rotation, θ. The two heavy lines, one vertical and one horizontal, represent the equilibrium conditions. Point B, where the equilibrium diagram branches, is called a bifurcation point. That is, up to that point the column or structure remains stable and will return to its original position when the load is removed, thus, it is referred as *stable equilibrium*. If the load is removed at the critical load, point B, the column or structure would have

suffered permanent deformation but remains stable, this is called *neutral equilibrium*. If the load exceeds point B, the column or structure becomes unstable and fails due to buckling, this is called *unstable equilibrium*.

Critical Load Theory

The fundamental requirement for any column strength theory is that it must be based on the basic principles of engineering mechanics and strength of materials, while also taking into account the stress-strain relationship of the materials and reflecting geometric imperfections of all relevant kinds (Geschwindner 1994). Two basic approaches for the determination of the column critical load can be found within the basic literature for stability analysis and determination of buckling loads. The two different basic approaches are explained below and presented in this chapter.

The first or simpler approach, also known as the Euler Load or eigenvalue approach shown in Figure 3.2, attempts to determine the maximum strength of an ideal column without geometrical or material imperfections in a direct manner without calculating the deflection (Chen 1985). This approach will provide the load at which the column will buckle, in other words the load at the bifurcation point described above, without providing a full deformation history until instability occurs.

This ideal column is assumed to be loaded concentrically and the only deflections that occur at low loads are in the direction of the applied load, that is, the axial load does not produce transverse deflection until the bifurcation or buckling load is reached. This means that up to the critical load, the column remains straight

and at the critical load there exists a bifurcation of equilibrium similar to the one described above, in which the column will reach the point of instability and buckle.

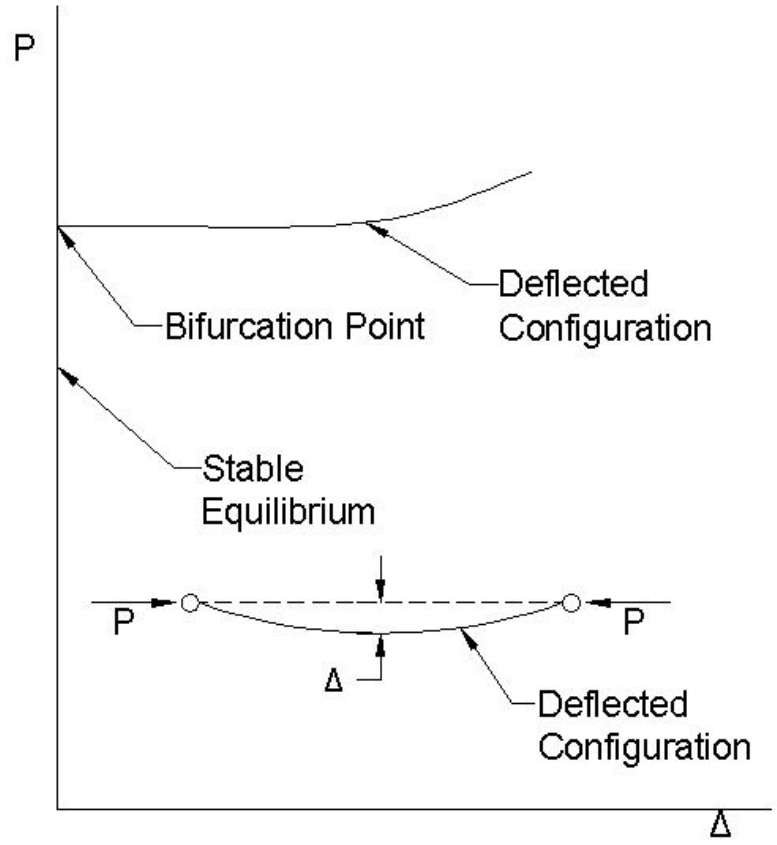

Figure 3.2 Column Stability (Adapted from Chen 1985)

A second approach for the determination of the buckling load relates to a more realistic column. A real column contains imperfections such as initial out-of-straightness (Figure 3.3), in this case, deflections start from the initial deflection, Δ_o, at the beginning of the application of the axial load and there is no bifurcation or sudden change of deflection as load increases. Therefore, the maximum load that an out-of-straightness column can support must be calculated using an alternate

approach. A suitable approach that considers this initial deflection, but it is complex due to its nature, is known as the load-deflection method. This method is also known as a rigorous second order analysis and will be presented in Chapter IV. Through this approach the solution is found by tracing the load-deflection behavior of the beam-column through the entire range of loading up to the maximum or peak load, which is also known as the strength of the column (Chen 1985).

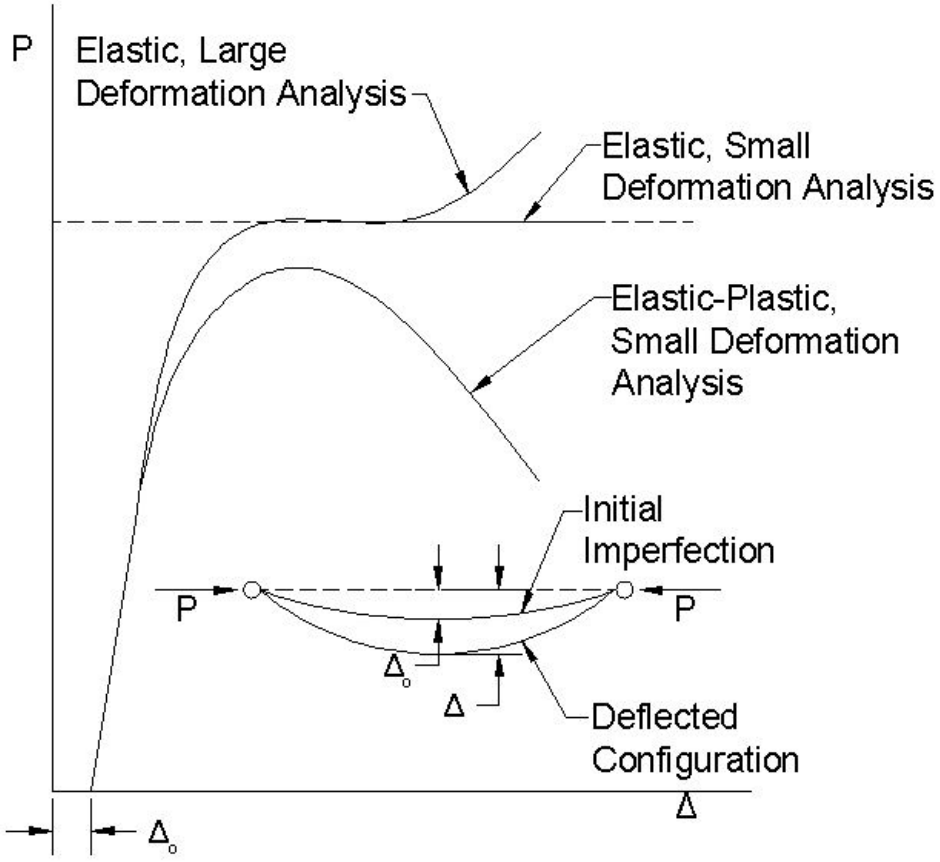

Figure 3.3 Beam-Column Stability (Adapted from Chen 1985)

Euler Buckling Load

As discussed earlier, the perfect-pinned supported column, or namely ideal column, does not exist in real structures; however, it provides a simple starting point for the stability analysis of structures that are subjected to instability buckling. For example, the column in Figure 3.4(a) will fail due to instability buckling when the column displaces as shown in Figure 3.4(b). That is, assuming the column span, L, is of sufficient length so that failure due to crushing does not take place. When the buckling load is determined for this ideal column, then the following assumptions need to be made (Chen 1985):

1. The column is perfectly straight
2. The ends of the column are simply supported
3. The compressive axial load is static and applied at the centroid of the column
4. The material follows Hook's law and is free of initial or residual stress

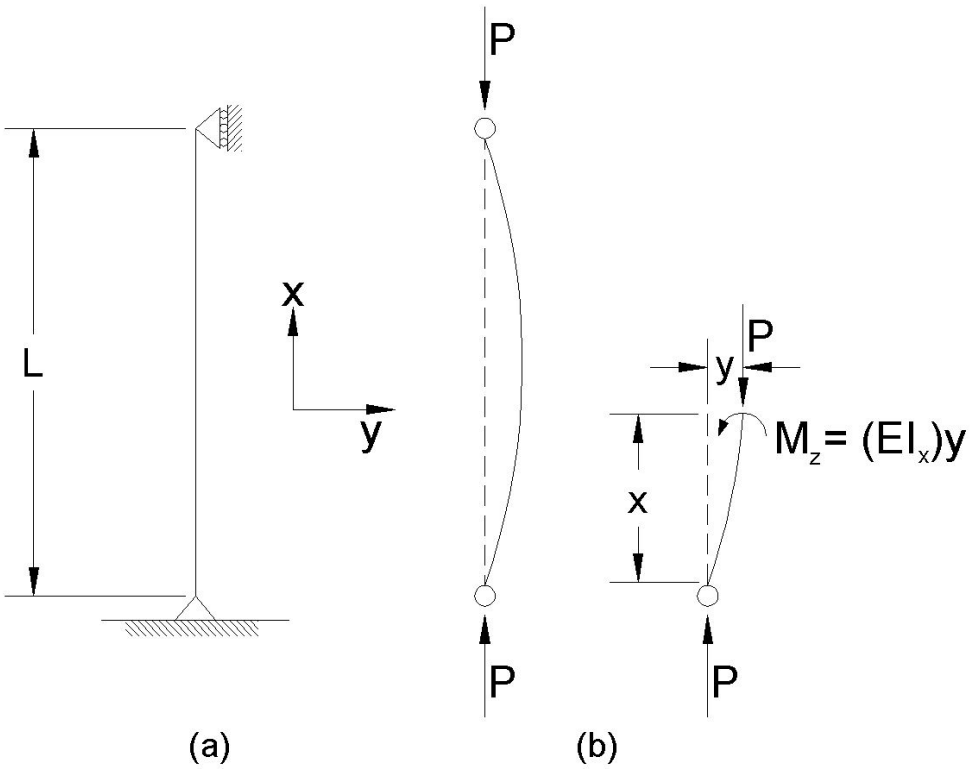

Figure 3.4 Pin-ended supported column

The critical load is that load for which equilibrium for a straight and slightly bent configuration is possible. For relative small deflections it can be seen that the state of equilibrium is given by the following equations (Chen 1985):

The external moment is given by

$$M_{Z\_external} = Py \qquad (3.1)$$

and the internal moment is given by

$$-M_{Z\_Internal} = EI_x \frac{d^2y}{dx} = -EI_x x'' \qquad (3.2)$$

Where E is Young's modulus, I the moment of inertia of the cross section and EI is the flexural rigidity.

In order to maintain equilibrium

$$-M_{Z\_Internal} + M_{Z\_External} = 0$$

The differential equation for the deflected column then becomes

$$Py - EI_X y'' = 0 \qquad (3.3)$$

Dividing the above equation by EI and re-arranging the terms we obtain the following differential equation

$$y'' - \frac{P}{EI_X} y = 0 \qquad (3.4)$$

Next, the axial parameter is defined as

$$k = \sqrt{\frac{P}{EI}} \quad \therefore \quad k^2 = \frac{P}{EI} \qquad (3.5)$$

And Equation 3.4 takes the form of a linear differential equation with constant coefficients

$$y'' + k^2 y = 0$$

A general solution is given by

$$y = A\sin(kx) + B\cos(kx) \qquad (3.6)$$

Where A and B are constants of integration. In order to determine A and B, it is necessary to apply the boundary conditions at each end of the column

$$y = 0 \text{ at } x = 0$$
$$y = 0 \text{ at } x = L$$

The first boundary condition yields

$$0 = A(0) + B(1) \therefore B = 0$$

The second boundary condition yields

$$0 = A\sin(kL) + B(0)$$

Which can be satisfied in two ways, if $A = 0$, k and P can have any value. This is known as a trivial solution.

If $sin(kL) = 0$, then

$$kL = n\pi \therefore k = \frac{n\pi}{L}$$

The deformed shape is obtained by

$$y = A\sin(kx) + 0 = A\sin\left(\frac{n\pi x}{L}\right) \qquad (3.7)$$

Where n can be any integer. The buckling load is

$$k^2 = \frac{P}{EI} \therefore P = k^2 EI$$

Then

$$P = \frac{n^2 \pi^2 EI}{L^2} \qquad (3.8)$$

However, from Figure 3.4, it can be seen that the value of critical load is given by the column bending in single curvature. The critical load is then given by

$$P_{cr} = \frac{\pi^2 EI}{L^2} \qquad (3.9)$$

From the above solution of the ideal column, one can conclude that the column strength is directly proportional to the modulus of elasticity, *E*, and the moment of inertia, *I*, of the column and inversely proportional to the square of its length. Figure 3.5, known as the Euler Curve, illustrates the buckling or Euler load as a function of the column length (Gere 2009).

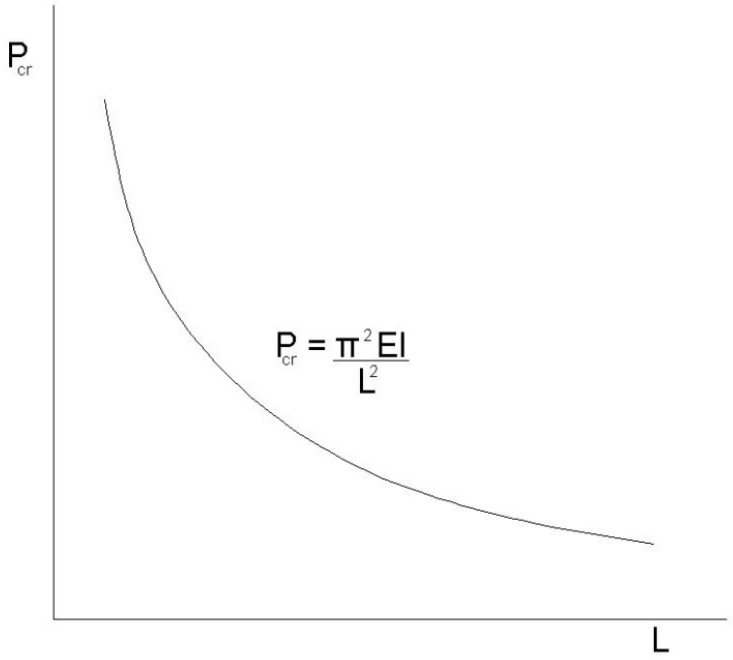

Figure 3.5 Euler Curve

Critical Load of Beam-Columns

The second approach for the maximum or critical load determination of a beam-column is obtained by a load-deflection, also known as the classical differential solution for beam-columns. Beam-columns are members that are subjected to axial forces and bending moments simultaneously. A typical load-deflection relation for beam-columns is shown in Figure 3.6. The following discussion will focus on a small deformation analysis (Chen 1985).

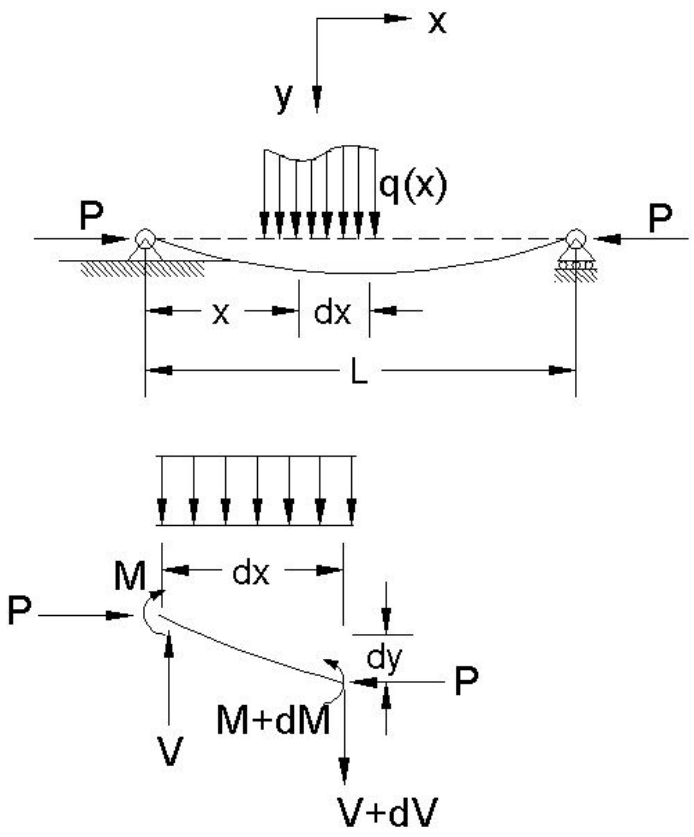

Figure 3.6 Beam-Column (Adapted from Chen 1985)

Given the beam-column in Figure 3.6, with flexural stiffness *EI*, and loaded simultaneously with an axial load, *P,* and an arbitrary distributed transverse load *q(x)*, the equations of equilibrium can be derived as follows

The transverse force is

$$V + dV - V + q(x)dx = 0 \text{ Therefore, } \frac{dV}{dx} + q(x) = 0 \qquad (3.10)$$

The moment is

$$M + dM - M - Vdx - Pdy = 0 \therefore \frac{dM}{dx} - V - P\frac{dy}{dx} = 0 \qquad (3.11)$$

Taking the derivative of the moment equation (Equation 3.11) and substituting in Equation 3.10,

$$-\frac{d^2M}{dx^2} + P\frac{d^2y}{dx^2} = q(x) \qquad (3.12)$$

From small deformation analysis and assuming that the column is loaded in the elastic range and follows Hook's law, the defection is related to the curvature by the following expression,

$$\kappa = \frac{d^2y}{dx^2} = -\frac{M}{EI} \therefore M = -\kappa EI = -\frac{d^2y}{dx^2}EI \qquad (3.13)$$

The differential equation has the form

$$EI\frac{d^4y}{dx^4} + P\frac{d^2y}{dx^2} = q(x) \qquad (3.14)$$

The axial parameter is $k = \sqrt{\frac{P}{EI}}$ $\therefore$ $k^2 = \frac{P}{EI}$ therefore,

$$\frac{d^4y}{dx^4} + k^2\frac{d^2y}{dx^2} = \frac{q(x)}{EI} \qquad (3.15)$$

Equation 3.15 is a forth-order linear differential equation that may be solved rigorously by the use of formal mathematics (Chen 1985). Figure 3.7 shows the plot of the exact solution for a beam-column with two different initial deformations.

Unlike the perfect column, which remains straight up to the Euler load, the initially deformed column begins to bend as soon as the load is applied. It can be seen that the deflection in the beam-column increases slowly at a small ratios of the applied load to the Euler load. However, as the applied load increases, the deflection increases more rapidly and it grows exponentially with no limit at load ratios near the Euler load. Thus, the carrying capacity of an imperfect column is smaller than the Euler load, regardless of how small the initial imperfection is.

The solution of Equation 3.15 is presented in Chapter VII along with the solution of a cantilever column. These two different benchmark problems, along with their rigorous differential solutions, will be used to evaluate the computer program employed throughout this research work. The two problems mentioned above are presented in the Appendix 7 of the AISC Specifications (AISC 2005), (AISC 2010). These benchmark problems are used for the evaluation of any analysis method, including computer programs that would be used as a rigorous second-order analysis method for the determination of second-order forces required by the AISC Specifications (AISC 2005), (AISC 2010).

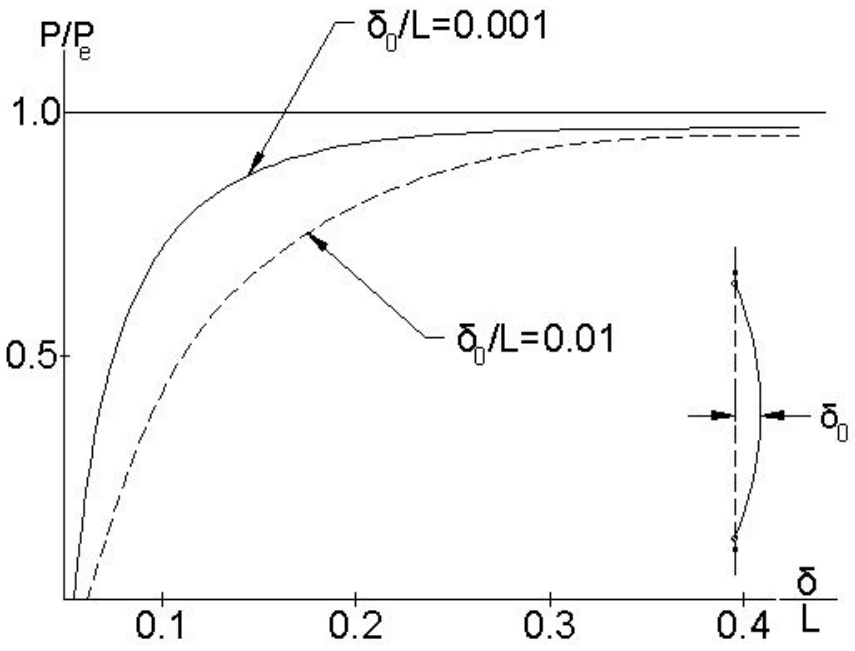

Figure 3.7 Elastic analysis of initially deformed column (Adapted from Chen 1985)

Second Order Effects

So far the critical load of an individual column has been discussed without consideration of the interaction between the column and other members that are part of a framed structure. This interaction can significantly impact the behavior of a column that is part of a frame structure. For example, the resulting moment from a beam in a moment frame structure, which is transferred to a beam-column from a rigid or moment connection, would cause an initial deformation, and together with the compressive load acting on the column, would cause an additional moment. This additional moment is the result of the eccentricity between the applied load and the centroid of the column. The additional moment would then cause additional

deflections, these deflections would cause additional moments and so forth. Therefore, second order effects are the direct result of displacements or deformations of the structure. Common elastic methods for structural analysis assume that all deformations are small and do not account for these secondary effects.

Second order effects may be determined by a complete second order inelastic analysis (also called advanced analysis and is discussed in Chapter IV) that will take into account the actual deformations of the structure and the resulting forces in addition to the sequence of loading and spread of plasticity. This approach is more complex than necessary for normal design (Geschwindner 1994). Another method which is more common for the determination of second order effects is known as a *P-Δ* analysis, which is an iterative elastic analysis to approximate the inelastic conditions. In this method a first order analysis, as described above, is carried out. The elastic deformations are determined from the resulting forces of the elastic first order analysis. Secondary moments and deformations are determined by applying the loads on the deformed structure. In order to determine the critical load of a structure, this process is repeated, incrementing the load until the analysis shows that the structure has become unstable.

A third approach used in common practice is to approximate the second order effects by amplifying the first order moments by an amplification factor. The derivation of the amplification factors was discussed previously in Chapter II

For the critical load assessment and stability analysis of a structure, it is important to understand the two different deflection components that will influence the secondary effects in the beam-column. Referring to Figure 3.8, the moment component, $P\delta$, shown in Figure 3.8(a) is the additional moment along the length of the member that results from the eccentricity between the centroid of the column and the deflected shape of the column. This eccentricity is caused by, either, the first-order moment, M, or by an initial geometrical imperfection (i.e. member out-of-straightnes). In this case the ends remain in the original position, in other words, there is no joint translation. This effect is known as the member effect or P-δ. The second component is shown in Figure 3.8b. For example, when the column is part of a sway frame (i.e. there is joint translation), the displaced structure will cause an additional moment, $M = P(\Delta)$. This secondary moment is the second order effect on the structure and is known as the structure effect *or* P-Δ. On an unbraced structure, the total second order effect on a column is given by the combined influence of the member effect (P-δ) and the structure effect $(P$-$\Delta)$. However, neglecting the effect of P-δ in the analysis of sway structures with large gravity loads can result in very erroneous second-order moments and forces. A discussion of neglecting P-δ and its effects is presented in Chapter VII.

One thing to keep in mind is that the member effect and the structure effect are not only caused by transverse or lateral forces, but also by member imperfections

and structure out-of-plumbness. These factors, also known as geometric imperfections, will be discussed later in this chapter.

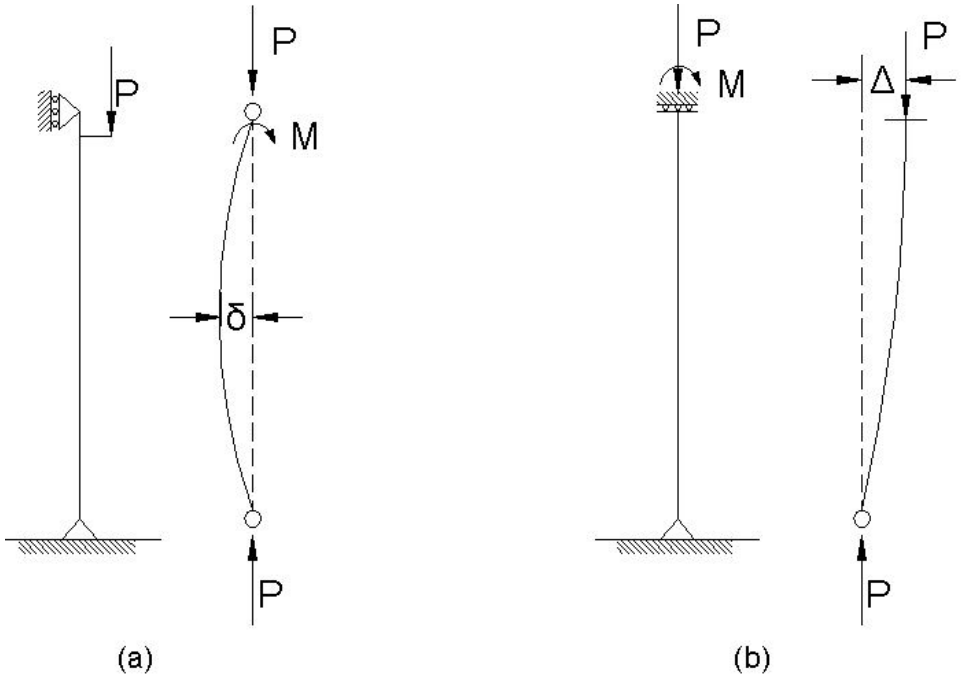

Figure 3.8 Second-order effects

Inelastic Buckling of Structures

In Chapter II, the inelastic buckling theory was presented where various theories were proposed to overcome some of shortcomings of the Euler's buckling formula. In the derivation of the Euler formula, it was assumed that the material followed Hooke's law. However, in reality a material has a proportional limit beyond which it does not behave elastically (Chen 1985). If residual stresses are present in a column cross-section, inelastic buckling can occur when the compressive stress due to applied load plus the local residual compressive stress exceed the material

proportional limit, a condition often reached at the tips or corners of wide flange steel columns. Thus, inelastic buckling includes any buckling phenomenon during which the proportional limit of the material is exceeded somewhere within the cross section before buckling occurs.

The proportional limit is the stress at which the relationship between stress and strain (i.e. modulus of elasticity) is no longer linear and proportional. The length at which a column will buckle in this range can be found in the following fashion:

From the Euler buckling load Equation, 3.9, the critical stress can be found as follows:

$$P_{cr} = \frac{\pi^2 (EI)}{(KL)^2} \quad \text{Thus} \quad \sigma_{cr} = \frac{P_{cr}}{A} = \frac{\pi^2 (EI)}{A(KL)^2} \qquad (3.16)$$

$$\sigma_{cr} = \frac{\pi^2 (E)}{\left(\frac{KL}{r}\right)^2} \qquad (3.17)$$

Where r is the radius of gyration and is given by, $r = \sqrt{I/A}$

I = Moment of inertia in the direction of bending

A = Column cross-sectional area

The critical length, KL_{cr}, can be found by substituting the critical stress, σ_{cr}, with the proportional stress, σ_{pl}, and solving for KL,

$$KL_{cr} = \pi r \sqrt{\frac{E}{\sigma_{pl}}} = \pi \sqrt{\frac{I}{A}} \sqrt{\frac{E}{\sigma_{pl}}} \qquad (3.18)$$

The proportional limit depends on the amount of residual stresses in a column cross-section as shown in Figure 3.9 (residual stresses are a type of material imperfection and are discussed later in this chapter). For example, for a circular steel-tube column of typical material properties, this type of buckling would occur at lengths of 28 to 35 times its diameter. Columns meeting this criterion will generally buckle inelastically, meaning permanent deformations will occur upon reaching the critical buckling load.

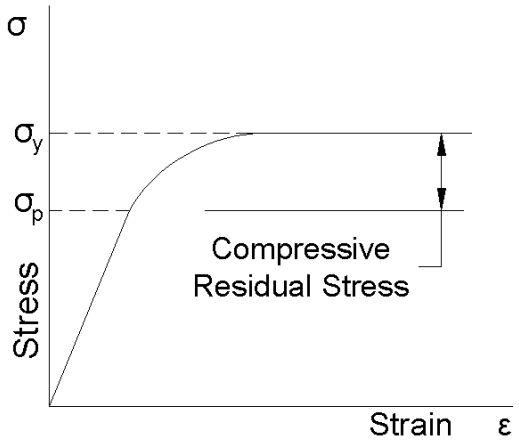

Figure 3.9 Residual stresses and proportional stress (Adapted from Chen 1985)

Factors Controlling Column Strength and Behavior

There are several factors that have an effect on column strength, for example, the characteristics of the material, and the method of fabrication, column cross section, imperfections and end conditions. However, from decades of research and

testing, the most influential factors are discussed below and include the length of the column, end support conditions, and geometric and material imperfections (Geschwindner 1994). The most critical factors that affect column behavior are summarized below.

Material Properties

From the stress strain test, Figure 3.10, two very important material properties can be derived for an elastic-plastic material, yield stress, F_y, and modulus of elasticity, E. From Figure 3.11, it can be seen that for short columns the strength of the column is directly proportional to the yield strength. However, for long columns the yield stress is irrelevant because the capacity, given in Equation 3.9, is a function of the Euler load and is influenced by the flexural stiffness. The flexural stiffness is the product of the moment of inertia and the modulus of elasticity. The strength of the material of a long column is not a factor in the determination of the column strength.

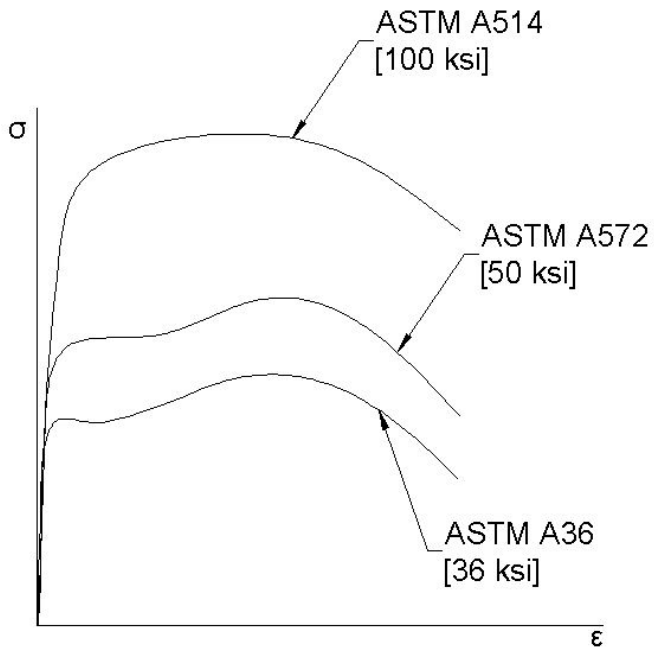

Figure 3.10 Typical stress-strain curves for different steel classifications

Length

The length of a column plays a major role on the behavior and strength of the column, as it can be seen in Figure 3.11, the behavior of the column is classified as short, intermediate and long columns. Short columns, as described earlier in this chapter, fail by crushing or compression yielding and are controlled by the yield strength. Intermediate columns fail by inelastic buckling and are controlled by inelastic or non linear behavior of the material. This nonlinear behavior is caused by material imperfections and will be discussed below. Long columns on the other hand, fail by elastic buckling and their behavior is governed by the Euler load equation.

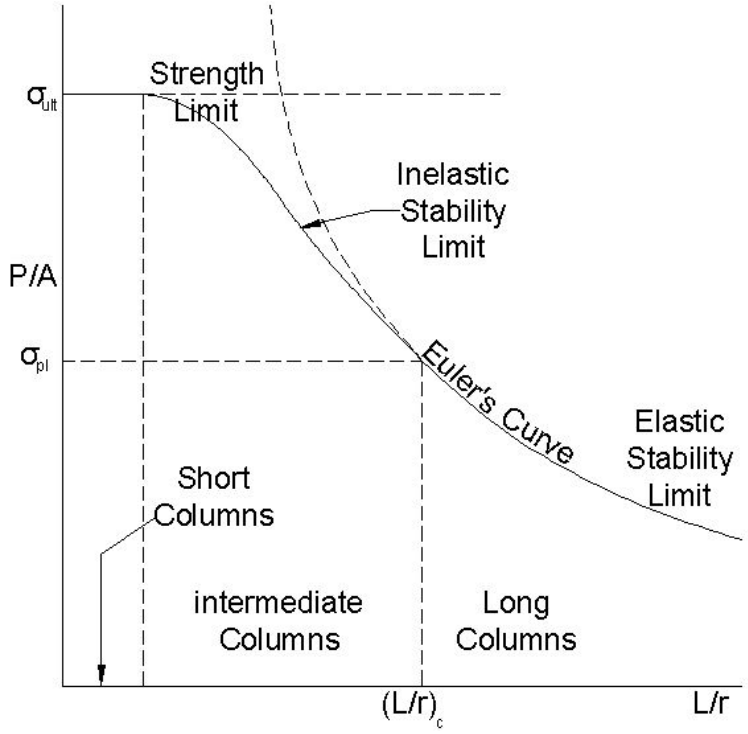

Figure 3.11 Theoretical column strength (Gere 2009)

Influence of Support Conditions

Moment Frames

Connection flexibility and member instability are closely related, and their interaction effects can have a significant influence on the overall performance of the frame. The stiffness of the beam-to-column restraining connection plays a major role on the stability behavior of columns. Figures 3.12 and 3.13 illustrate the influence of different beam-column end restraints. As is evident from Figure 3.12, the greater the connection restraint, the stiffer will be the initial response of the column and the greater the maximum load that can be carried as compared to a pin-ended column. In

addition, Figure 3.13 shows column strength curves for members with different end conditions where, the influence of end restraint for columns with different slenderness ratios can be clearly illustrated, and the fact that the influence diminishes for shorter columns. These curves are compared to the Euler curve and the SSRC column curve 2 which is used in the AISC Specifications (Ziemmian 2010). Figure 3.14 shows the moment-rotation behavior for different beam-to-column end restraints or connections.

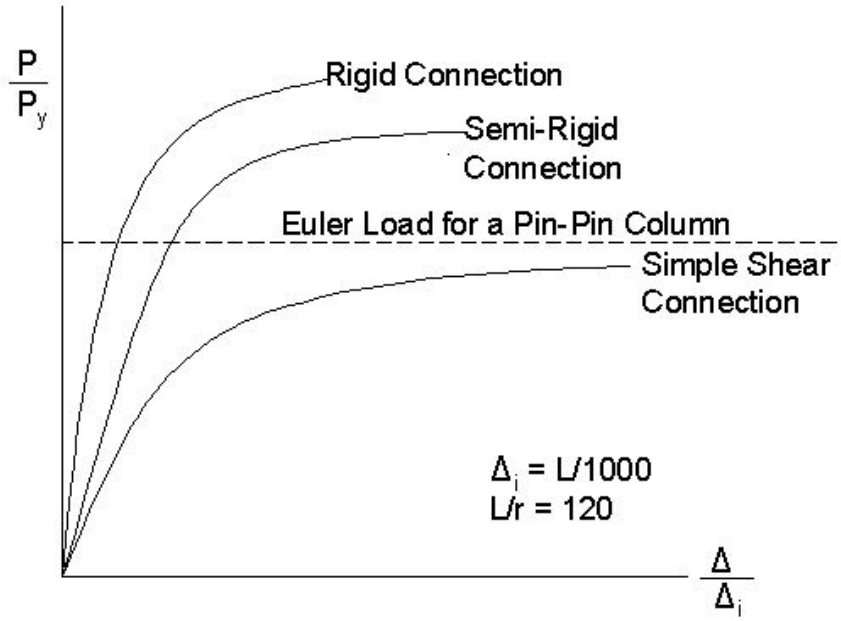

Figure 3.12 Typical load-deflection curves for columns with different framing beam connections (Adapted from Ziemian 2010)

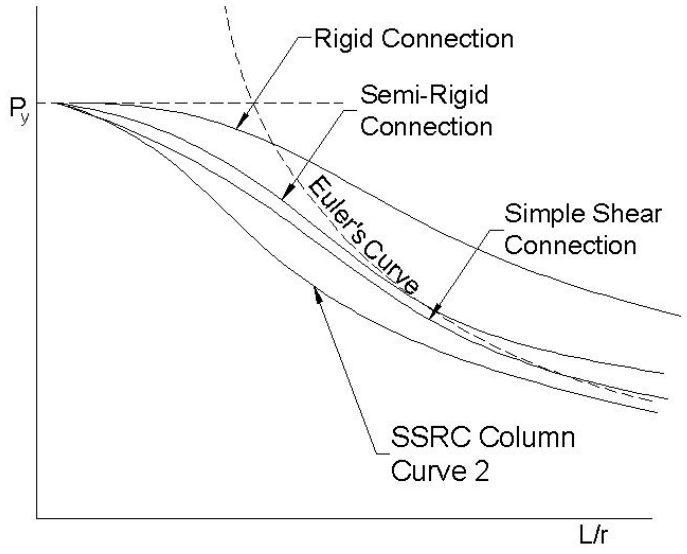

Figure 3.13 Column strength curves for members with different framing beam connection (Adapted from Ziemian 2010)

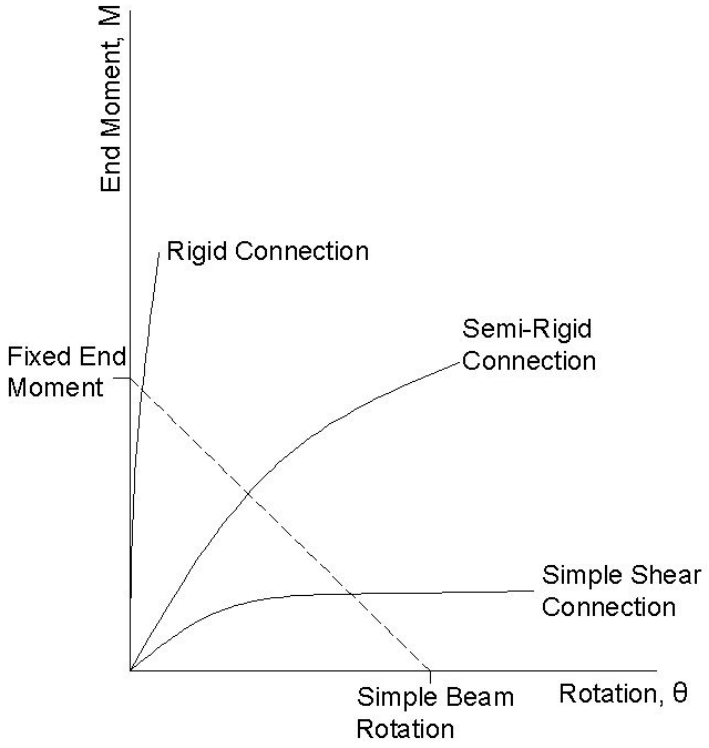

Figure 3.14 Connection flexibility (Adapted from AISC 2005)

In Chapter II the concept of "effective length" was introduced to account for column supports other than pin-pin. For moment frame structures, the alignment charts which are used for the determination of the effective length factor discussed in Chapter II, take into account the rotational restraints by upper and lower assemblages but neglect the interaction of lateral stiffness among the columns in the same story resisting lateral sway buckling of unbraced frames. LeMessurier (1977) presented a method of evaluating the *K* factor based on the concept of the story-based buckling, which accounts for the lateral restraining effect among columns in the same story. Chen and Lui (1991) modified the values of the moment of inertia of the restraining beams while using the alignment chart method in order to incorporate connection flexibility. The modification factors were derived for both the braced and unbraced frames based on the assumption that the beam-to-column connection stiffness at both ends are identical. These modification factors were developed in such a way that considered different values of connection stiffness at the ends of the beam (Bjorhovde 1984; Chen et al., 1996; Christopher and Bjorhoved 1999). The modification factors take into account actual connection stiffness and the influence of beams and effective-length factors for columns in frames by incorporating an end-restraint relative stiffness distribution factor, G_r , given by Equation 3.19 (Zieminan 2010):

$$G_r = \frac{\sum \left(EI/L \right)_{columns}}{C^*} \qquad (3.19)$$

Where C^* is the effective end restraint that is afforded to a column in a beam and column sub assemblage, using connections whose initial stiffness is C, the initial slope of the moment-rotation curve. A significant of drawback of this approach is that the value of C must be known. However, connection schemes similar to those provided by Bjorhoved and the approaches of Eurocode 3 are useful (Ziemian 2010).

Members with Elastic Lateral Restraints

The critical load assessment of structures with members that are restrained laterally between their ends by intermittent elastic lateral supports is not as straightforward as the critical load or buckling load determination of a simply supported column that has been the focus for most of the research work and studies on structural stability. Pony trusses, which are widely used as pedestrian structures, have served as the prototype through the years for the development of theory and design procedures that are sometimes utilized in other similar structures nowadays.

Early studies of compression members with elastic lateral restrains started with F.S. Jasinsky (1856-1899) in the late 1800's and with Engesser (1848-1931). Jasinky's main work on the theory of columns deals with problems encountered in bridge engineering. Jasinsky was the first to investigate the stability of the compressed diagonals and to evaluate the strengthening afforded by the diagonals in tension. In his time, several failures of open truss bridge structures (pony truss) occurred in the Western Europe and Russia (Timoshenko 1983). Jasinsky made a theoretical investigation of this problem and found a rigorous solution for this

complicated case of lateral buckling in which he calculated the critical values of compressive forces so that the upper chord and the verticals of an open bridge could be designed rationally.

Another engineer that contributed much to the theory of buckling in the same period as Jasisnky was Friedrich Engesser. He was also interested in the problem of buckling of the compressed upper chord of open truss bridges and derived some approximate formulas for calculating the proper lateral flexural rigidity of that chord. However, Egensser which in his analysis assumed an equivalent uniform elastic support, was the first to present a simple, rational and approximate formula for the required stiffness (C_{req}) of elastic supports equally spaced between ends of a hinge-ended column of constant section, Figure 3.15 (Ziemian 2010).

Engesser's approach for determining the stiffness of the elastic restraints and its effects on the pony truss compression chord was based on the assumption that the connection between the web members and the floor beam was rigid. In this theory, the transverse frame (i.e. the floor beam and the verticals) and diagonal members located at each panel point provide the lateral stiffness of the compression chord. However, this theory may result in a conservative approach for the actual frame stiffness by underestimating the true behavior of the entire system. In other words, one may argue that investigating the behavior of the bridge as a three dimensional system may result in a higher stiffness coefficient of these lateral supports.

Other earlier solutions were proposed by methods developed by Hu, Holt, Lutz and Fisher. Hu studied the problem using energy methods for elastically supported chords. He considered non-uniform axial forces, variable chord cross sections and spring stiffness for both simple and continuous pony truss bridges. Holt included the secondary effects that influence the behavior of the pony truss in his studies.

Holt presented a method of analysis for determining the critical load of a pony truss top chord (Ziemian 2010). The solution presented by Holt is used in common practice for the design of pedestrian bridges, (AASHTO 2009) and is discussed in Chapter IV.

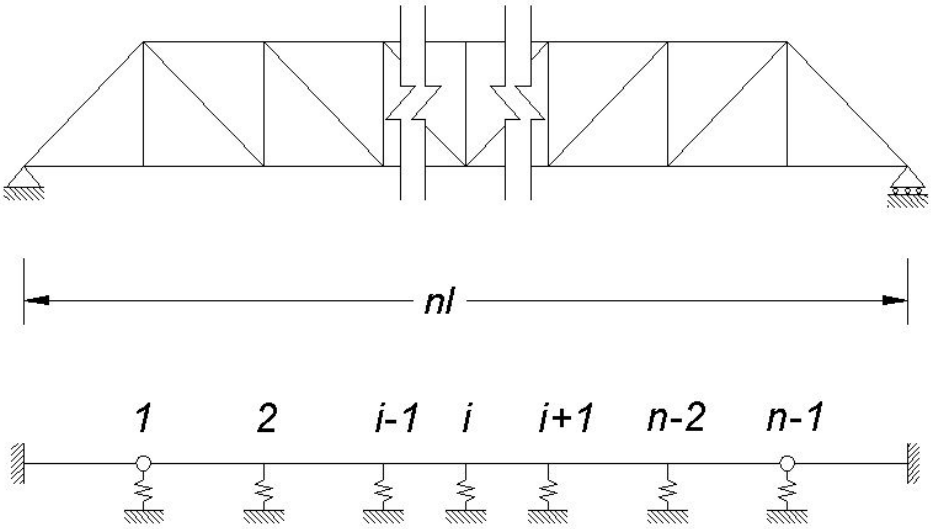

Figure 3.15 Pony truss and analogous top chord (Adapted from Ziemian 2010)

Most solutions used for the determination of the critical load of a pony truss bridge involve the procedure presented above without providing a direct approach for the critical load determination of the entire bridge as a whole.

Influence of Imperfections

It has been stated that the perfect or ideal column do not exist in real structures because actual columns and structures have inherent imperfections. These imperfections can be categorized as material imperfections and geometric imperfections which produce nonlinear behavior of a loaded structure.

Figure 3.16 illustrates the influence of geometric and material imperfections on the critical load of the column. In addition, Figure 3.16 includes the influence of a column with an initial curvature (geometric imperfection) only, residual stresses (material imperfection) only and the combined effects of both imperfections.

In stability design and analysis of framed structures, it is imperative to account for the effects of imperfections; out-of-plumbness of framing and out of-straightness of columns are referred to geometric imperfections while residual stresses are referred as to material imperfections. The development of the column strength curves that are used in design specifications was discussed in Chapter II, in which it was mentioned that only two types of imperfections have been considered in the development of such curves: residual stresses and member out of straightness.

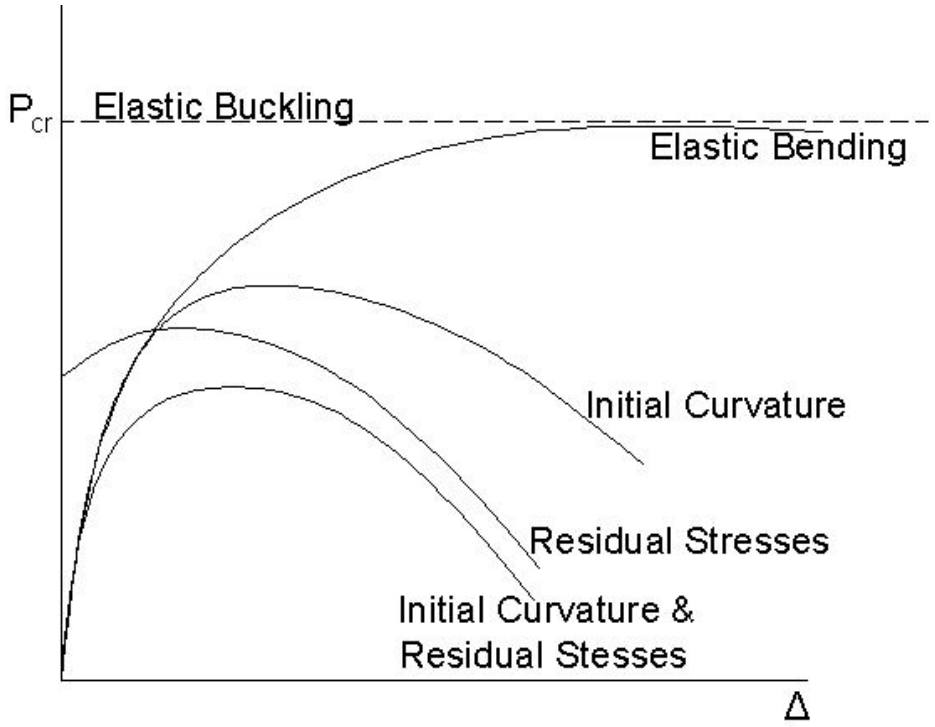

Figure 3.16 Influence of imperfections on column behavior (Adapted from ASCE Task Committee 1997)

Material Imperfections

Residual stresses, which are considered the main factors of material nonlinearity, are the direct result of the cooling process of hot rolled steel sections. During hot-rolling of steel, the cross section of the steel section is heated to a uniform temperature. Once the rolling is completed, the heat must dissipate. In this process the cooling is not uniform, therefore some of the individual fibers in the steel section cool at different rates, that is, some of the fibers reach room temperature faster than the rest (Geschwindner 1994).

The stress strain relations for structural steel is of elastic-perfectly plastic type shown in Figure 3.17(a) (Chen 1985) Using this stress strain curve and the Euler buckling load theory described in Chapter II, the column strength curve is shown in Figure 3.17(b). According to this curve, a column will fail as a result of elastic buckling if $\frac{KL}{r} > \pi\sqrt{E/\sigma_y}$ or will yield if $\frac{KL}{r} \leq \pi\sqrt{E/\sigma_y}$. However, a large number of tests have shown that columns of intermediate slenderness ratios tend to buckle at loads significantly below those given by Figure 3.17(b) (Chen 1985). An extensive investigation at Lehigh University in the 1950s demonstrated conclusively that residual stresses are responsible for a large portion of the discrepancy between the theoretical curve and the tests results. It is noted that residual stresses reduce the critical load of columns with intermediate length (Chen 1985).

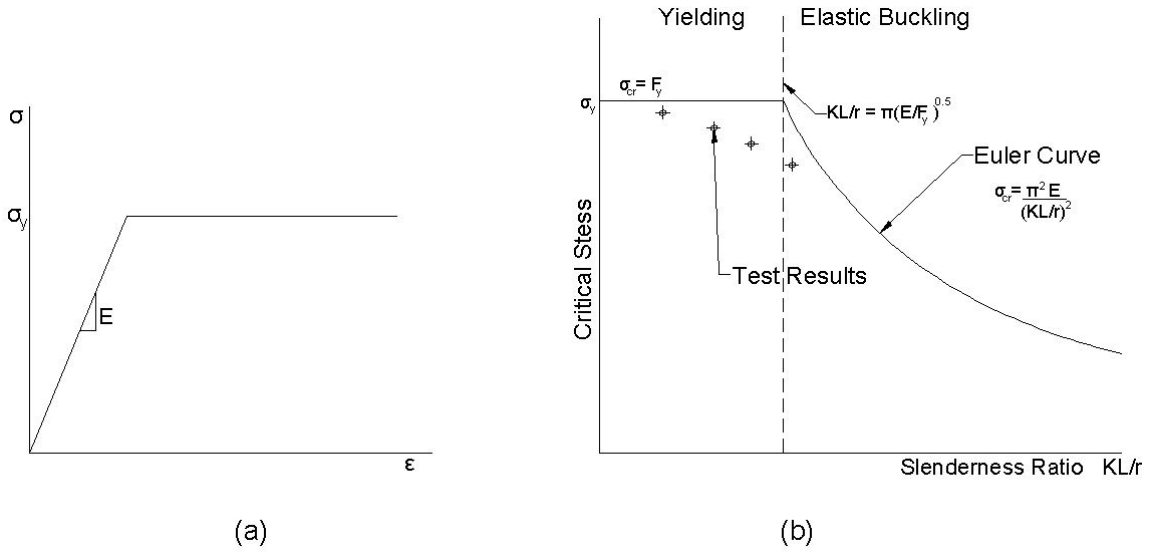

Figure 3.17 Column curve for structural steels. (a) elastic-perfectly plastic stress-strain relationship; (b) column curve (Adapted from Chen 1985)

For I-section members, the residual stresses are usually compressive at the flange tips. Compared to sections free of residual stress, the magnitude and distribution of these compressive residual stresses influences the strength of compression members because of the earlier initiation of yielding and subsequent lowering of flexural strength that occurs. The effects of residual stresses are more severe for I-section columns bent about the minor axis the major axis (ASCE Task Committee 1997). This causes a nonlinear behavior of the compression element since the fibers with residual compression will reach the proportional limit before the rest of the fibers.

The residual stress pattern employed by Galambos and Ketter (ASCE Task Committee 1997) in their studies of the strength of steel beam-columns is shown in Figure 3.18. Based on numerous measurements of residual stresses made by various researches over the years, analytical models have been recommended that follow the residual stress pattern shown in Figure 3.18. In addition, this stress distribution pattern is consistent with measured residual stresses in American wide-flange column-type sections resulting from cooling of the section during and after rolling (ASCE Task Committee 1997). Parabolic distributions, varying from 0.35*Fy* compression at the flange tips to 0.5*Fy* tension at the flange web, have been presented by various researches investigating the inelastic lateral buckling of beams and beam-columns (ASCE Task Committee 1997).

However, in order to achieve a better match to experimental distribution, the bi-linear flange distributions shown in Figure 3.18 has been employed widely in parametric studies of beam-column and frame strength in the context of calibration and development of the AISC LRFD interaction equations (ASCE Task Committee 1997).

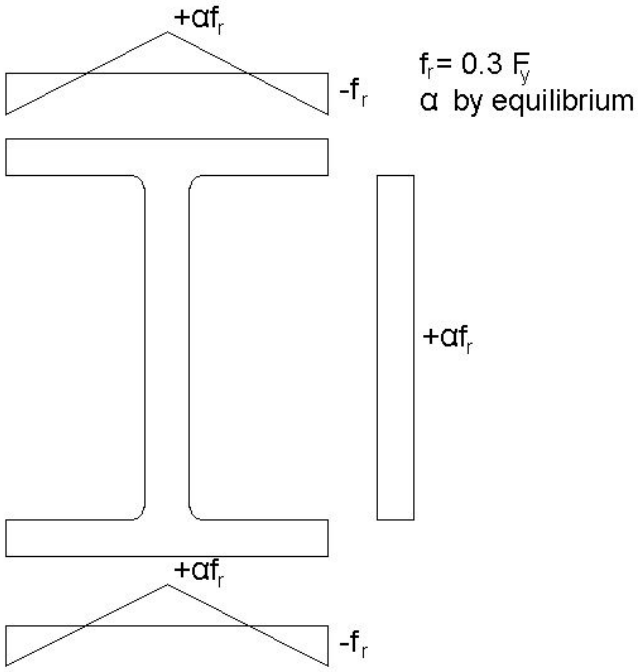

Figure 3.18 Lehigh residual stress pattern (Adapted from Surovek 2012)

Geometrical Imperfections

There are two types of geometrical imperfections considered for the assessment of lateral stability of a structure: out-of-straightness and out-of-plumbness.

Out-of-straightness refers to the amount of initial bow in a structural steel member. Initial out-of-straightness develops as a result of the cooling conditions for the shape, once it has been rolled to final dimensions. Once the structural shape has passed through the last set of rolls, is then left on the cooling bed to cool in air over a period of time. However, cooling is non-uniform since heat is typically retained longer in the mid length portion of the column. This non-uniform cooling not only causes residual stresses in the cross section as mentioned above, but tends to distort the structural shape to the point that ends up in a curved configuration along its length. Depending on how the shape has been placed on the cooling bed, the curvature may appear in both orthogonal directions of the cross section. Crookedness about the major axis is called camber and curvature about the minor axis is designated as sweep (Geschwindner 1994).

The maximum out-of-straightness is limited by material standards, for example ASTM A6 in the United States, and is typically based on length of the member. In the case of wide-flange shapes produced in the United States, this limit is approximately $L/1000$ (AISC 2010).

In past specifications, the effect of initial out-of-straightness or crookedness was covered through a factor of safety, and used the strength of the straight member as the actual criterion (AISC 1961). As mentioned earlier, in the limit states philosophy of the LRFD Specifications all the major parameters (residual stresses and an initial out-of-straightness) have to be accounted for. Therefore, the strength

equations in the AISC Specifications include the influence of initial crookedness (AISC 2005). The inclusion of out-of-plumbness in the design procedure for frames is much more complex. Out-of-plumbness refers to the amount of initial drift or tilt that an actual structure may have.

Prior to 2005, the load resistance and factor design (LRFD) AISC specifications did not provide requirements for inclusion of out of plumbness in the design of structures, except through the use of the effective length method described in chapter C of the AISC Specifications (AISC 1999). Eurocode 3 (ASCE Task Committee 1997) recommends that frame imperfections be included in the elastic global analysis of the frame. Although the influence of the number of columns in a plane and the number of stories is considered, only limited guidance is given with respect to the shape and distribution of imperfections (ASCE Task Committee, 1997).

The Australian and Canadian codes include the effect of frame imperfections through the use of an equivalent notional lateral load, a procedure also allowed in Eurocode 3 (ASCE Task Committee, 1997). The 2005 AISC Specifications introduced a new analysis method for the assessment of lateral stability of steel structures; this new method of analysis, known as the Direct Analysis Method, includes the notional load approach mentioned above. The notional load approach and Direct Analysis Method are discussed further in Chapter IV.

CHAPTER IV

METHODS AND PROCEDURES FOR ANALYSIS AND DESIGN OF STEEL STRUCTURES

Structural and Stability Analysis

One of the most important aspects during the design process of structures in civil engineering is structural and stability analysis of such structures. Structural analysis refers to the determination of forces and deformations of the structure due to applied loads. Structural design, on the other hand, involves the arrangement and proportioning of structures and their components in such a way that the assembled structure is capable of supporting the designed loads within the allowable limit states. An analytical model is an idealization of the actual structure. The structural model should relate the actual behavior to material properties, structural details, and loading and boundary conditions as accurately as is practicable before proceeding to design the members and connections of a structure (Hibbeler 2009).

Thus, when designing a structure, a structural analysis must be performed so that the internal forces and stresses are determined, and an equally important aspect of structural analysis and design, is a lateral stability analysis. This type of analysis requires that all structural members and connections of a structure have adequate strength to resist the applied loads with equilibrium satisfied on the deformed geometry of the structure (Ziemian 2010). In common design practice it is difficult to satisfy the above statement due to the fact that most practical methods of analysis are

limited to first order elastic analysis, that is, equilibrium is satisfied only on the original geometry of the structure and the material is assumed to behave elastically without consideration of material and/or geometry nonlinearities. Common methods of analysis for stability include, first-order elastic, second-order elastic, first-order elasto-plastic and second-order inelastic, to name some. These types of analyses can be differentiated by whether or not they include imperfections such as geometric and material nonlinearity. That is, is equilibrium is satisfied on the deformed or undeformed geometry of the structure? And, are residual stresses, spread of plasticity through the cross section, and yielding considered?

During the structural design process, the serviceability limit state and strength or ultimate limit state need to be considered. A serviceability limit state is one in which the structure would become unfit for normal service loads, for example, excessive deformations or vibrations, and problems with durability. On the other hand, a strength limit state is one in which the structure would become unsafe. With regard to the type of structural analysis, a linear elastic analysis will provide the engineer with a good representation of the actual response of the structure to service loads, that is, when a serviceability limit states is investigated. When a strength limit state is reached, it generally results in an increasing nonlinear elastic or inelastic response of the structure that, sometimes, culminates in structural instability. However, for the most part in common practice, the internal load distribution at a strength limit state is calculated by a linear method. During the design and sizing of

structural members, the analytical results obtained by the linear method are modified with empirical or curve fitting equations to account for the effects of nonlinearity. Figure 4.1 shows a comparison between several analyses approaches and load-displacements curves. These analyses are summarized below and range from the most basic first-order linear-elastic analysis to the rigorous second-order inelastic analysis.

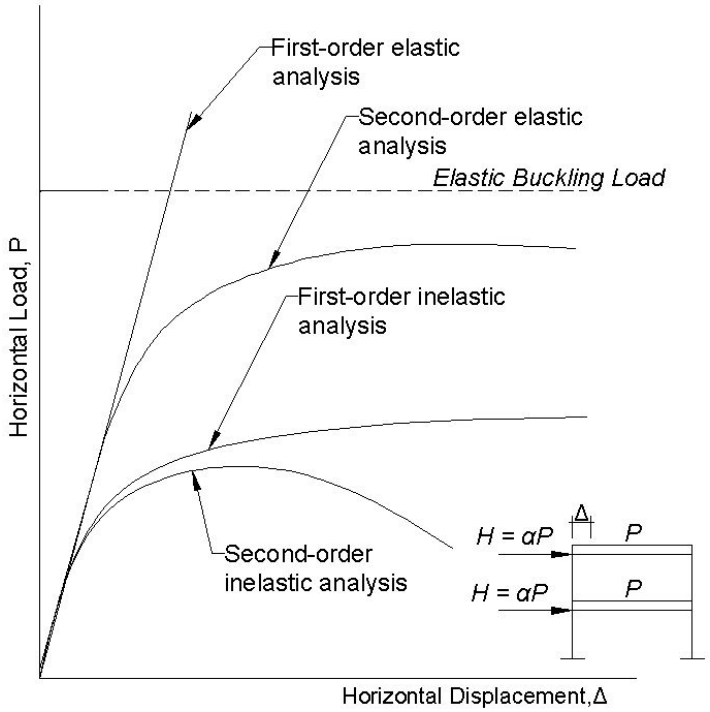

Figure 4.1 Comparison of load-deflection behavior for different analysis methods (Adapted from Geschwindner 2002)

First-Order Elastic Analysis

This is the most basic and common method of analysis in which the material is modeled as linear-elastic. This method is also called simply elastic analysis. Deformations are assumed to be small and equilibrium is satisfied on the undeformed

configuration of the structure. Because inelastic behavior of the material is ignored, superposition is valid. However, this method excludes nonlinearity, but it generally represents conditions at service loads very well. In addition, the load displacement curve shown in Figure 4.1 is linear. This is the approach used in the development of the common analysis tools of the profession, such as slope-deflection, moment distribution, and the matrix stiffness method that is found in most commercial computer software (Geschwindner 2002).

Elastic Buckling Load

The elastic buckling load (i.e. Euler buckling load) analysis provides the critical buckling load of the system without a load-deflection history. That is, the results of this analysis do not provide a load-displacement curve but rather the single value of load at which the structure buckles as shown in Figure 4.1. The critical buckling load may be determined through an eigenvalue solution or through the classical solution presented in Chapter III, where equilibrium equations are written with reference to the deformed configuration. This analysis can provide the critical buckling load of a single column and is the basis for the effective length factor, *K*. (Geschwindner 2002).

Second-Order Elastic Analysis

A second-order elastic analysis, also known as a *P-Δ* analysis, provides the load-displacement history of an imperfect column, typically through an iterative solution thus it is a bit more complex than the first-order elastic analysis. The

equations of equilibrium are written with reference to the deformed configuration of the structure and the deflections are determined as a function of that deformed configuration. The load-displacement history obtained through this analysis may approach the Euler buckling load as shown in Figure 4.1.

Two components of these second-order effects should be included in the analysis. The first effect is known as P-δ or as the member effect, this second-order effect is influenced by the member curvature or member imperfection. The second effect known as P-Δ or as the story effect is influenced by the story sidesway. Nonetheless, second order elastic analysis can produce an excellent representation of destabilizing influence of the P-Δ effect, but has no provisions for representing inelastic behavior due to spread of plasticity.

First-Order Inelastic Analysis

In the first order inelastic analysis the equations of equilibrium are written in terms of the geometry of the undeformed structure. Inelastic regions may develop gradually or as abrupt changes in the structure response. When the destabilizing effects of finite displacements are relative insignificant, first-order inelastic analysis can produce an excellent representation of simple elastic-plastic behavior and failure through hinge formation. However, this analysis has no provisions for detecting geometric nonlinearity and of principal concern, their influence on the stability of the system as a whole, (McGuire 2000).

Second-Order Inelastic Analysis

The second-order analysis, often referred to as “advanced analysis”, is the most complete analytical approach for stability assessment of structures in which combines the same principles of second-order analysis discussed previously with the inelastic analysis. Although this type of analysis is more complex than any of the other methods of analysis discussed so far, it provides a more complete and accurate picture of the behavior of the structure.

In the second order inelastic analysis the equations of equilibrium are written in terms of the geometry of the deformed system. This type of analysis has the ability for accommodating the geometric and material imperfections and elastic factors that influence the response of a structure and is capable of simulating actual behavior. Thus, the inelastic stability limit (i.e. the point at which as system’s continued deformation results in a decrease in load resisting capacity) can be calculated directly from this type of analysis, that is, this is the true strength of the structural system, (McGuire 2000).

Design of Compression Members

Most structures behave in a linear elastic manner under service loads. Under ultimate loads the behavior can be quite different, and in most cases, structures loaded close to their limit of resistance would most likely exhibit significant nonlinear response. Thus, if a linear elastic analysis is the highest level of analysis available for

design, the design engineer must find another way to account for the effects that the analysis is not able to simulate. That is, the results from an elastic analysis are used with code or material specifications formulas that make allowance for nonlinearity in some empirical or semi-empirical way or supplementary theoretical or experimental studies. (McGuire 2000).

It is very important that the approach taken for member design be consistent with the approach chosen for analysis, which is a requisite of the AISC Specifications. Chapter B of the 2010 AISC Specifications requires that:

> The design of members and *connections* shall be consistent with the intended behavior of the framing system and the assumptions made in the *structural analysis*. Unless restricted by the *applicable building code*, *lateral load* resistance and *stability* may be provided by any combination of members and connections.

Currently, three design approaches are acceptable for steel structures under U.S. building codes as they incorporate AISC specifications (AISC, 1999; AISC, 2005; AISC, 2010). The most up-to-date tool for steel design is the load and resistance factor design specification (LRFD). However, the plastic design (PD) approach, now called *Design by Inelastic Analysis* in the 2010 AISC Specifications, is also permitted and the allowable stress design specification (ASD) may still be used. The LRFD Specification stipulates, in Section C1, that "Second order effects shall be considered in the design of frames", (AISC 2010). Because the typical analysis method is first-order, satisfying deformation capacity requirements and assuring stability are left to the engineer.

When using the AISC Specifications, stability is usually addressed through an estimate of column buckling capacity using the effective length approach, and second-order effects may be addressed through a first-order analysis, together with an amplification factor for second-order effects, or through direct use of a second-order analysis (Geschwindner 2002). Another approach allowed by the AISC Specifications for structural stability, which is gaining more acceptance and popularity and is the basis of this research project is the Direct Analysis Method, which will be described in more detail later on in this chapter. However, if the plastic design approach is used, member design and stability are directly obtained from the analysis. Design by Inelastic Analysis is addressed in Appendix 1 of the AISC Specifications. Section B3 of the 2010 AISC Specifications says:

> **Required Strength**
>
> The required strength of structural members and connections shall be determined by structural analysis for the appropriate load combinations as stipulated in Section B2. Design by elastic, inelastic or plastic *analysis* is permitted. Provisions for inelastic and plastic analysis are as stipulated in Appendix 1, Inelastic Analysis and Design.

The general requirements of Appendix 1 of the 2010 AISC Specifications require that:

> Strength *limit states* detected by an inelastic analysis that incorporates all of the above requirements are not subject to the corresponding provisions of the Specification when a comparable or higher level of reliability is provided by the analysis. Strength limit states not detected by the inelastic analysis shall be evaluated

using the corresponding provisions of Chapters D, E, F, G, H, I, J and K.

Determining Required Strength

The ASCE task committee on effective length published a report in 1997 on two different types of approaches for assessing frame stability, the effective length method and the notional load approach (ASCE Task Committee 1997). This document mentions that both of these approaches are capable of accounting the effects of imperfections and nonlinearity on the strength of columns and beam-columns that must be considered in design. However, the effective length approach and the notional load approach differ in the way they approximate these effects.

Since 1961, the AISC Specifications has used an effective length concept to determine the axial resistance term of the beam-column interaction equation. Second order elastic analysis is performed on the structure assuming perfectly straight and perfectly plumb members. Out-of-straightness imperfections and residual stresses are accounted for through the column curve for an equivalent pin-ended member, while out-of-plumbness imperfections are accounted through the effective length of the column, KL, where K is the equivalent length factor and L is the actual member length (ASCE Task Committee 1997).

An alternative to computing effective length factors to take into account different end restraints in columns of unbraced frames, is to use the actual column length (i.e. K=1) and add artificial frame imperfections to the analysis of the

structural system through the use of notional lateral loads. A second-order elastic analysis is then conducted on the structure. This approach for the assessment of frame stability is termed the notional load approach (ASCE Task Committee 1997).

The Australian Standard, AS4100, the Canadian Standard CSA and the European specification Eurocode 3, since the early 1990's (ASCE Task Committee 1997), and now the AISC Specification since 2005 (AISC 2005), use notional lateral loads with second-order elastic analysis of the geometrically perfect structures to account for story out-of-plumbness under gravity loads and then use the actual member length in the beam-column interaction equations to account for member out-of-straightness and residual stresses, (ASCE Task Committee 1997).

Determining Available Strength

Beam-columns need to be designed for the combined effects of flexural moments and compression axial force. The determination of the compressive strength of a column and the flexural strength of a beam, are typically specified in standard design specifications. In the United States, the standard specification ANSI/AISC 360 governs the design of columns (AISC 2005), (AISC 2010). A brief summary is presented here. The AISC Specifications provide, for general use, a single interaction equation to determine both, in-plane and out of plane member strength. For in-plane instabilities, the AISC interaction equations either implicitly accounts for geometric imperfections, partial yielding and residual stresses effects by using a column strength curve that is based on effective column lengths or explicitly accounts for these effects

by use of the direct analysis method, presented below, with column strength calculated on actual member length (Ziemian 2010).

Figure 4.2 illustrates the two approaches mentioned above, (the effective length and notional load approach), when using the interaction equations specified in the AISC Specifications, with the purpose of checking the combined effects of bending and compression. In order to develop the interaction equation curve shown in Figure 4.2, two nominal strength points need to be determined first. These two points represent the nominal strength under pure compression, P_n, and the nominal strength in bending, M_n.

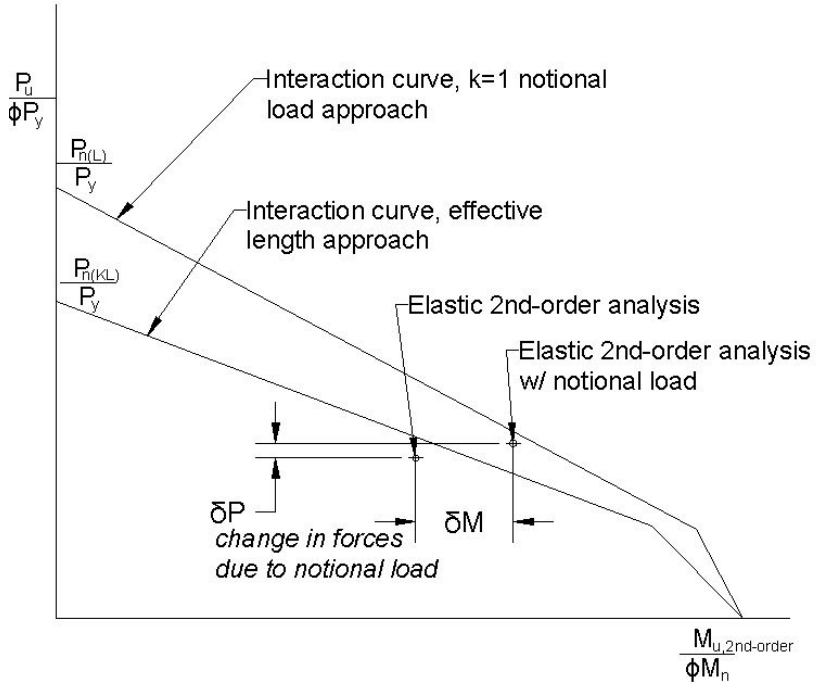

Figure 4.2 Distinction between effective length and notional load approaches (Adapted from Ziemian 2010).

The nominal compression strength, P_n, represents the nominal axial strength of the column as limited by the effects of lateral buckling either in or out of the plane of the frame. When the effective length method is employed, $P_{n(KL)}$, the nominal axial strength is determined considering the limit of stability of the framing system, or of a local subassembly within the framing system, where all the columns are concentrically loaded. The nominal resistance $P_{n(KL)}$ is calculated using a single column curve that is a function of the effective buckling length. When the direct analysis method is used, the nominal axial strength, $P_{n(L)}$, is based on the same curve but in this case is a function of the actual member length. This is the result of the analysis being modified to account for frame stability effects and in turn calculating larger moments and forces associated with column out-of-plumbness and reduction of stiffness due to inelastic deformations.

The nominal bending strength, M_n, is determined for bending in the plane of the frame considering the potential for elastic or inelastic lateral-torsional buckling out of the plane, (Ziemian 2010). The column strength equations that are presented below are calibrated from results of distributed plasticity analyses that include geometric imperfections and residual stresses (Ziemian 2010).

Compression Strength

For doubly symmetric compact and noncompact compression members, flexural buckling is normally the governing limit state (Williams 2011). This capacity is obtained by multiplying the critical stress, F_{cr}, by the cross sectional area of the

column, A_g. Thus, the nominal capacity of a compression member, which is given in chapter E of the AISC Specifications, can be calculated by the following formula (AISC 2005), (AISC 2010):

$$P_n = F_{cr} A_g \qquad (4.1)$$

The AISC Specification provides two empirical expressions for the determination of the critical compressive stress, F_{cr}, which is required in order to determine the maximum compressive strength of the column (AISC 2005), (AISC 2010). A historical discussion on the origin of these empirical expressions was presented in Chapter II.

For members with slenderness ratios, *KL/r*, of less than:

$$4.71\sqrt{\frac{E}{F_y}} \qquad (4.2)$$

The critical stress is given by the following expression:

$$F_{cr} = \left[0.658^{\frac{F_y}{F_e}} \right] F_y \qquad (4.3)$$

$$F_e = \frac{\pi^2 E}{\left(\frac{KL}{r} \right)^2} \qquad (4.4)$$

Where *KL* is the effective length of the column, *r* is the radius of gyration of the section in the direction being analyzed, *E* is the modulus of elasticity, F_y is the

yield strength of the material, and F_e is the elastic buckling stress and is given by Equation 4.4. For slenderness ratios of less than the limit determined in Equation 4.2, the outer fibers of the column cross-section yield before the critical load is reached and the Euler expression is no longer valid. Therefore, as shown in Figure 4.3, Equation 4.3 provides an empirical expression to model the behavior of the actual column in the inelastic range. The behavior of a compression member in this range was described in Chapter II.

For columns that behave in the elastic range, that is, columns in which the slenderness ratio, *KL/r*, exceeds the limit given in Equation 4.2, Equation 4.5 provides an empirical expression to model such behavior. In this case, such column will reach the critical buckling stress before yielding occurs within the cross section.

$$F_{cr} = 0.877F_e \qquad (4.5)$$

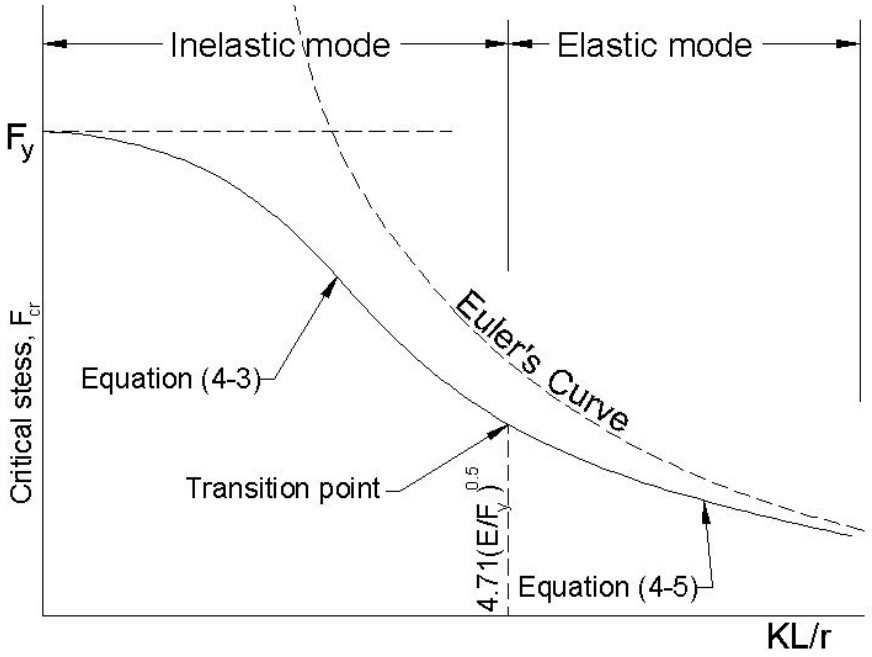

Figure 4.3 Standard column curve (Adapted from Williams 2011).

The effective length factor, *K*, in Equation 4.2, is required in order to account for the effects of different support conditions, other than pin-pin as in the basic column, and is illustrated in Chapter II. In addition, the effective length factor is used to account for the effects of frame out-of-plumbness. Therefore, if the effects of structure nonlinearity or geometrical imperfections are accounted for through the use of notional loads, as described in the previous section, the effective length factor is then equal to 1.0, thus an effective length factor "*K*" is no longer needed.

Combined Forces

Once the nominal compression and bending strengths of a beam-column element have been determined, the next step is to check the combined effects through

the use of an interaction equation. The AISC Specification (AISC 2005), (AISC 2010) provides the following interaction equations for design of steel beam-columns:

When the ratio of the required axial strength to the available strength is more than 20%, the interaction curve is given by the following equation:

$$\frac{P_r}{P_c} + \frac{8}{9}\left(\frac{M_{rx}}{M_{cx}} + \frac{M_{ry}}{M_{cy}}\right) \leq 1.0 \qquad (4.6)$$

When the ratio of the required axial strength to the available strength is less than 20%, the interaction curve is given by the following equation:

$$\frac{P_r}{2P_c} + \left(\frac{M_{rx}}{M_{cx}} + \frac{M_{ry}}{M_{cy}}\right) \leq 1.0 \qquad (4.7)$$

Where P_r is the required axial compressive strength or the axial load effect on the member being considered, P_c is the available or nominal compressive strength, M_{rx} and M_{ry} are the maximum second-order elastic moments about the strong and weak axis respectively, within the unsupported length of the member, and M_{cx} and M_{cy} are the corresponding nominal flexural strengths. The load effects P_r, M_{rx} and M_{ry} may be determined either directly from second-order elastic analysis or by use of first-order elastic analysis with approximate amplifiers applied to the first order forces. Equations 4.6 and 4.7 describe a single interaction curve that characterizes the strengths of steel frame members associated with all the possible beam-column limit states.

As shown in Figure 4.4, the two interaction expressions defined by Equations 4.6 and 4.7, are used to define the lower bound curve for the non-dimensional strengths. The AISC interaction equations were determined in part by curve fitting to strength curves obtained from "exact", two-dimensional, second-order-inelastic analyses. In these analyses, the spread of plasticity, including the effects of initial residual stresses, is explicitly modeled (ASCE Task Committee 1997).

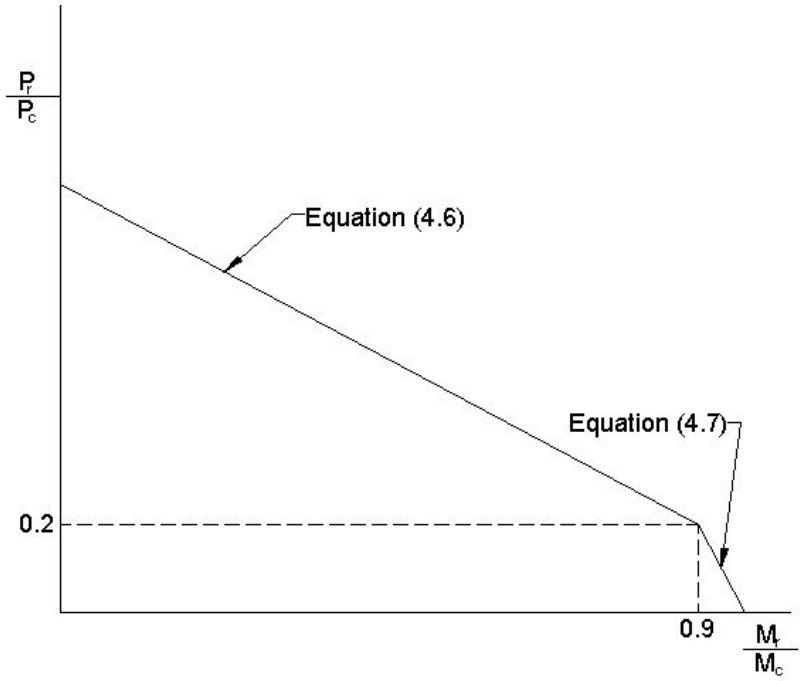

Figure 4.4 Interaction curve (Adapted from Williams 2011)

Current Stability Requirements (AISC Specifications)

The AISC Specifications require that structural stability must be provided for the entire structure and for each of its elements. The Specifications permit any rational method of design for stability that considers all of the effects listed below;

this includes the following methods: the effective length method (AISC 360-10 Specifications Appendix 7), the direct analysis method (AISC 360-10 Specifications Chapter C) and the first order elastic analysis method presented in Appendix 1 of the ASIC Specifications, (AISC 2010).

Both elastic methods, the direct analysis method and the effective length method, require a second-order analysis of the structure. This may be accomplished using a rigorous, second-order computer analysis or by an approximate second-order analysis. An Alternate approximate approach is presented in AISC Specifications in Appendix 8, this approach is known as the B_1-B_2 or amplification factors procedure (Williams 2011).

The AISC Specification Section C1 lists the effects that must be considered in the design of a structure for stability. These are:

1. Flexural, shear, and axial deformations of members
2. All other deformations that contribute to the displacements of the structure
3. P-Δ, second-order effects caused by structure displacements
4. P-δ, second-order effects caused by member deformations
5. Geometric imperfections caused by initial out-of-plumbness
6. Reduction in member stiffness due to inelasticity and residual stresses
7. Uncertainty in stiffness and strength

The first four of these items are covered within the method selected for the analysis of the structure. Geometric imperfections are caused by permitted tolerances

in the plumbness of columns, among others. As specified by AISC *Code of Standard Practice for Steel Buildings and Bridges* (AISC 303) Section 7.13.1.1, the maximum tolerance on out-of-plumbness is $L/500$ (AISC 2010). Residual stresses cause premature yielding in a member with a consequent post-yield loss of stiffness and increase in deformations. This effect may be taken into account by reducing the axial and flexural stiffness of members that contribute to the lateral stability of the structure prior to analysis (Williams 2011).

The Effective Length Method

When the effective length method is used, the required member strength must be determined by a second-order analysis, either by rigorous analysis using computer software or by the amplification factors in accordance with Appendix 8 of the AISC specifications (AISC 2010). In any case, the effective length method is not permitted when the ratio of the second-order to the first-order deflections exceeds 1.5. The AISC Specification allows the ratio of second-order drift to first-order drift in a story to be taken only as the B_2 amplification factor, calculated in accordance with Appendix 8.

To account for initial geometrical imperfections of the structure, notional lateral loads are applied at each story in accordance with Section C2.2b of the AISC Specifications, except that the stiffness reduction indicated in Section C2.3 is not required to be applied, thus, the nominal stiffness of all members is used. (AISC 2010). The available strength of the members is determined using the appropriate

effective length factor K as defined in Appendix 7 of the AISC Specification (AISC 2010). The empirical column curve then accounts for member geometrical imperfections and inelastic softening effects (Williams 2011).

Direct Analysis Method

The 2005 AISC specifications (AISC 2005), for the first time, permit a more direct assessment of steel framing systems with the inclusion of Appendix 1 (Design by Inelastic Analysis) and Appendix 7 (Direct Analysis Method). In the most recent AISC Specifications (AISC 2010), the direct analysis method has been moved into chapter C as the preferred method of frame stability assessment, and the traditionally used effective length approach has been moved to Appendix 7. By incorporating both, a nominal out-of-plumbness and a nominal stiffness reduction in the structural analysis, the direct design method and design by inelastic analysis provisions focus on obtaining more realistic analysis results for the stability of steel structures. In addition, both methods account, explicitly, for the effects of imperfections that affect the system and member strengths when checking the strength of steel structures. (Surovek 2012). Some of the major advantages of the direct analysis method are:

1. It eliminates the need for effective length factors
2. It provides an improved representation of the member frame forces throughout the structure at the ultimate strength limit state.
3. It applies in a logical and consistent fashion for all types of frames including braced frames, moment frames and combined framing systems.

Another advantage of the direct analysis method is that it can be applicable to all types of structures, including structures with compression members with elastic supports such as in the case of the compression chord of a pony truss bridge or a wind girt truss. When the direct analysis method is used, a second-order analysis is required that considers both *P-Δ* and *P-δ* effects. However, in accordance with Section C2.1 of the AISC Specifications (AISC 2010) when *P-δ* effects are negligible a *P-Δ* only analysis is permitted. This typically occurs when the ratio of second-order drift to first-order drift is less than 1.7 and no more than one-third of the total gravity load on the building is on columns that are part of the moment-resisting frames.

Nonetheless, in the direct analysis method the effects of inelasticity and frame imperfections are accounted for in the calculated forces required for the design of all the structural components. One of the benefits of this approach is that it provides a direct path from elastic analysis and design to advanced analysis and design (Surovek 2012).

Imperfections

To account for initial imperfections in the members, notional lateral loads are applied at each story in accordance with Section C2.2b of the AISC Specifications (AISC 2010) and are given by

$$N_i = 0.002Y_i \qquad (4.8)$$

Where N_i is the notional load applied at level i and Y_i is the gravity load applied at level i. The notional loads are additive to the applied lateral loads when the sidesway amplification factor is larger than 1.7 when using the reduced elastic stiffness or 1.5 when using the unreduced elastic stiffness. As an alternative to applying the notional loads at each level, the imperfections can be directly modeled in the analysis by including an initial displacement, at the points of intersection of members, which represents the out-of-plumbness permitted by the Specifications, (Williams 2011).

Reduced Flexural and Axial Stiffness

To account for residual stresses and inelastic softening effects, the flexural and axial stiffness of members that contribute to the lateral stability of the structure are reduced as specified in Section C2.3 of the AISC Specification (AISC 2010) and are given by

$$EI^* = 0.8\tau_b EI \qquad (4.9)$$

$$EA = 0.8EA \qquad (4.10)$$

Where τ_b is the stiffness reduction parameter and is given by

$$\tau_b = 1.0 \text{ when } \alpha P_r \le 0.5 P_y \qquad (4.11)$$

$$\tau_b = 4\left(\alpha P_r / P_y\right)\left(1 - \alpha P_r / P_y\right) \text{ when } \alpha P_r > 0.5 P_y \qquad (4.12)$$

Where α is an adjustment factor when ASD load combinations are used and is equal to 1.6. When LRFD combinations are used the adjustment factor is equal to 1.0. P_r is the required second-order axial strength and P_y is the member yield strength (AF_y). Because of the allowance for initial geometric and material imperfections and inelastic softening effects in the analysis, stability effects are incorporated in the calculated required member strengths. Thus, the available strength of members can be determined using as effective length factor of K=1.0 for all members, in other words, the K factor is not necessary (Williams 2011).

Advanced Analysis

In traditional design, the load capacity of the system is assessed on a member-by-member basis, limiting the load carrying capacity of the system to the strength of the weakest member. Alternatively, the use of a nonlinear-inelastic analysis to directly determine the strength and stability of a steel framing system as a whole rather than limiting the strength of the structural system at design load levels by the first member failure is the subject of Appendix 1 of the AISC Specifications. This type of analysis is commonly referred to in the literature as "Advanced Analysis".

Appendix 1 of the 2010 AISC Specifications states that (AISC 2010):

> Strength limit states detected by an inelastic analysis that incorporates flexural, shear and axial member deformations and all other component and connection deformations that contribute to the displacements of the structure, second-order effects (including P-Δ and P-δ effects), geometric imperfections, stiffness reductions due to inelasticity, including the effect of residual stresses and partial yielding of the cross-section, are not subject to the

> corresponding provisions of the Specification when a comparable or higher level of reliability is provided in the analysis (AISC 2010).

However, Appendix 1 is not prescriptive in how these attributes are to be included in an inelastic analysis. A report prepared by the American Society of Civil Engineers (ASCE) and edited by Andrea Surovek called "Advanced Analysis in Steel Frame Design: Guidelines for Direct Second-Order Inelastic Analysis", presents recommendations for the use of second-order inelastic analysis in the design and assessment of steel framing systems. One of the objectives of this document is to provide guidelines for how the requirements of Appendix 1 might be met while also providing the necessary background to understand the rationale for the recommendations. In addition, the guidelines were developed to provide an understanding of the baseline requirements for directly capturing member and system strength limit states when using a second-order inelastic analysis (Surovek 2012).

The guidelines include analysis and modeling requirements as well as design considerations (i.e. suggested resistance factors) using the advanced analysis approach in Appendix 1 of the AISC Specifications, such that the behavior and strength of the overall system and the limit states of individual members are checked concurrently (Surovek 2012).

Below are summarized these requirements (Surovek 2012):

1. The analysis model must be able to represent the reduction in member stiffness due to spread of plasticity through the member cross-sections and

along the member lengths, and due to in-plane stability effects of axial forces acting on the inelastic member deflected geometry. The report recommends two types of analysis approaches for advance analysis: Distributed plasticity analysis and refined plastic hinge analysis.

2. The analysis and design procedure must account for the attributes that significantly influence member and system strength. Inelastic material behavior must be included, by using one of the analysis approaches recommended above, that accounts for residual stresses. The residual stress pattern chosen should be appropriate for the type of cross-section being considered.
3. Effects of geometric imperfections should be included, and they include out-of-plumbness (i.e. frame nonverticality) and out-of-straightness (i.e. member sweep). The report recommends to model out-of-plumbness by modifying the frame geometry. For orthogonal frames, imperfections may be modeled through the use of equivalent horizontal notional loads. The frame nonverticality should be modeled to a degree that accurately captures the potential out-of-plumbness that can occur during construction. Member out-of-straightness should be modeled in such a way that it represents the potential deformed shape due to production tolerances.
4. Limit states, (i.e. column strength flexural buckling, beam yielding, and beam-column in-plane flexural buckling) that can be demonstrated being directly

captured within the analysis are not required to be verified with a separate limit state check using the corresponding strength resistance equations.

5. Resistance factors must be incorporated in the analysis/design process if advanced analysis methods are to be used in the context of AISC Specifications.

Pony Truss Bridges

Design of pedestrian bridges is addressed in AASHTO "LRFD Guide Specifications for the Design of Pedestrian Bridges" (AASHTO 2009). Section 7.1.2 provides the requirements for stability of the compression chord. The Specifications require that the compression chord (top chord) must be considered as a column with elastic supports at panel points, in other words, at the location of the vertical members. Thus, lateral support of the top chord is provided by a transverse U-frame consisting of the floor beams and truss verticals. The stiffness of the elastic supports is determined from the bending of this U-frame, shown in Figure 4.5, and it can be found from Equation 4.13.

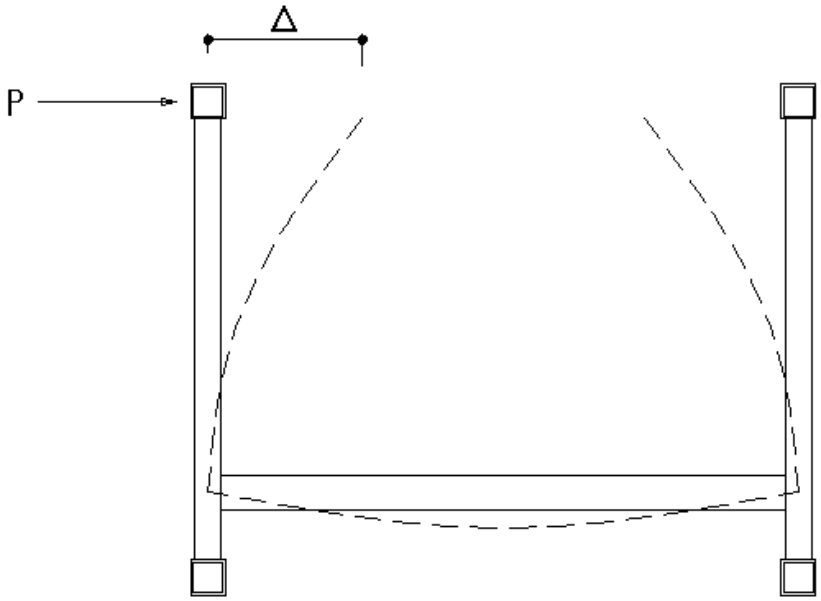

Figure 4.5 Lateral U-Frame (Adapted from AASHTO 2009)

$$C = \frac{E}{h^2\left[\left(h/3I_c\right)+\left(b/2I_b\right)\right]} \qquad (4.13)$$

Where C is the transverse frame stiffness, E is the modulus of elasticity, h is the height of the vertical, b is the width of the transverse frame, I_c and I_b are the moment of inertias of the vertical and the beam, respectively, of the transverse frame.

The general procedure for lateral stability of the pony truss bridge is as follows:

1. Design loads are obtained from the LRFD load combinations in *AASHTO LRFD Bridge Design Specifications*.
2. A first order elastic analysis of the 2D truss is performed and the axial forces, P, on the top chord are determined from such analysis.

3. A factor of 1.33 is applied to the compression chord to account for the probability that the maximum compression force would occur simultaneously in adjacent truss panels, thus the design compression chord force, P_c, is equal to 1.33P.
4. The transverse frame stiffness, C, is determined from Equation 4.13
5. The parameter, CL/P_c, is then determined, where C, the transverse frame stiffness, L is the length of the compression chord between panels and P_c is design compression chord force.
6. The effective length factor, K, is found from Table 7.1.2-1 of the Specifications (AASHTO 2009), based on the number of panels, n, and the parameter CL/P_c.
7. The capacity of the compression chord is then found from empirical equations given in the AASHTO Bridge Design Specifications, section 6.9.4 (AASHTO 2012) similar to AISC design of compression members.

CHAPTER V

STABILITY ANALYSIS USING NONLINEAR MATRIX ANALYSIS WITH COMPUTER SOFTWARE

Matrix Structural Analysis

Basically, the behavior of all types of structures can be described by means of differential equations. In practice, the writing of differential equations for framed structures is rarely necessary because exact or approximate solutions to the ordinary differential equations for each member, which can be treated as assemblages of one dimension, are well-known. These solutions can be set in the form of relationships between the forces and displacements at the end of each member. Proper combinations of these relationships with the equation of equilibrium and compatibility at the joints and supports, yields a system of algebraic equations that describes the behavior of the structure (McGuire 2000). On the other hand, structures consisting of three dimensional components are more complicated, thus, exact solutions are very difficult to obtain and practical solutions seldom exist for the applicable partial differential equations.

In the past years, significant changes have taken place in the way structures are analyzed in common engineering practice. These changes have primarily occurred because of the great developments made in high-speed digital computers and the increasing use of very complex structures. Matrix methods of analysis provide a convenient mathematical language for describing complex structures and because the

necessary matrix manipulations can easily be handled with computers, matrix analysis using computers has almost completely replaced the classical methods of analysis in engineering offices (McCormac 2007).

Matrix algebra is a mathematical notation that simplifies the presentation and solution of simultaneous equations. A key feature of matrix analysis methods is that it can be use to analyze practically all kind of structures, whether they are statically determinate or indeterminate. Additionally, due to the systematic nature of the matrix concepts and techniques, matrix analysis forms the basis of the computer programs used today for the analysis and design of structures. Thus, matrix analysis is used to obtain a concise description of a structural problem and to create a mathematical model of the structure.

The ability of application of matrix methods in structural engineering is very important because all linearly elastic, statically determinate and indeterminate structures are governed by systems of linear equations. And therefore, any method of analysis involving linear algebraic equations can be put into matrix notation and matrix operations can be used to obtain their solution. Basically there are two general approaches to the matrix analysis of structures: the flexibility matrix method and the stiffness matrix method.

The flexibility matrix method is also known as the force or compatibility method. It obtains the solution of a structure by determining the redundant forces. Thus, the number of equations involved is equal to the degree of indeterminacy of the

structure. The redundant forces may be selected in an arbitrary manner, and their choice is not an automatic procedure. The primary consideration in the selection of the redundant forces is that the resulting equations are well conditioned (Williams 2009).

The stiffness method is also known as the displacement or equilibrium method, in which the displacement of joints (rotations and translations) necessary to describe fully the deformed shape of the structure are used in the equations instead of the redundant forces used in the force methods. When the simultaneous equations that result are solved, these displacements are determined and then substituted into the original equations to determine the various internal forces, thus, the solution of a structure is obtained by determining the displacements at its joints. The stiffness matrix method is the most common method utilized in computer programs for the solution of building structures (McCormac 2007).

Direct Stiffness Method

When a structure is being analyzed with the stiffness method, it is subdivided into a series of discrete finite elements and identifying their end points as nodes and the joint displacements (translations and rotations) are treated as unknowns. Equilibrium equations are written for each joint of the structure in terms of:

1. The applied loads
2. The properties of the members framing into the joint
3. The unknown joint displacements

These relationships, for the entire structure, are then grouped together into what is called the structure stiffness matrix, **K.** This results in a set of linear, algebraic equations that can be solved simultaneously for the joint displacements. These displacements are then used to determine the internal member forces and support reactions.

The general stiffness equation is written symbolically as follows:

$$\{\mathbf{P}\} = [\mathbf{K}]\{\mathbf{\Delta}\} \qquad (5.1)$$

The order of listing the nodal forces in the matrix [**K**] should be the same as the order of listing of the corresponding displacements of the matrix {**Δ**}. Thus if the first listed nodal force in {**P**} is X_1 , then the first listed displacement in the matrix {**Δ**} should be u_1, and so on.

Nonlinear Analysis using Matrix Methods

In nonlinear analysis the aim is to trace the load displacement history of all material points in a structure as it undergoes progressive loading. The only practical way to do this is by approximating their nonlinearity with a piecewise or step-by-step series of linear analyses that employ one or more of the most common equation solution methods to calculate nonlinear structural behavior. These methods are known as the incremental analysis method and the iterative (multi-step) procedures.

Behavior can be traced incrementally and each method can be stated symbolically as a variant of the global stiffness Equation, 5.1, shown below as Equation 5.2.

$$[\mathbf{K_t}]\{\mathbf{d\Delta}\} = \{\mathbf{dP}\} \qquad (5.2)$$

Where $\mathbf{[K_t]}$ is the tangent stiffness matrix, $\mathbf{\{d\Delta\}}$ is a vector of incremental nodal point displacements, and **{dP}** is a vector of incremental nodal point loads and reactions. The computational problem can be addressed as the conventional one of solving for unknown displacements and back substitution of the results in element stiffness equations to determine element forces, but doing so in a stepwise fashion in which the total response is determined through summation of increments.

In second-order elastic analysis the effects of finite deformations and displacements are accounted for in formulating the equations of equilibrium and Equation 5.2 becomes Equation 5.3:

$$[\mathbf{K_e} + \mathbf{K_g}]\{\mathbf{d\Delta}\} = \{\mathbf{dP}\} \qquad (5.3)$$

Where $\mathbf{[K_g]}$ is the geometric stiffness matrix and represents the change in stiffness that results from the effects mentioned above, and $\mathbf{[K_e]}$ is the elastic stiffness matrix.

In first order inelastic analysis the equations of equilibrium are written in terms of the geometry of the undeformed structure, thus, Equation 5.2 becomes Equation 5.4:

$$[\mathbf{K_e} + \mathbf{K_m}]\{\mathbf{d\Delta}\} = \{\mathbf{dP}\} \qquad (5.4)$$

Where $\mathbf{[K_m]}$ is called the plastic reduction matrix and represents the change in stiffness that results from inelastic behavior of the system.

In second-order inelastic analysis both geometric and material nonlinearity are accounted for. The equations of equilibrium are written in terms of the geometry of the deformed system and Equation 5.2 becomes Equation 5.5:

$$[\mathbf{K_e} + \mathbf{K_g} + \mathbf{K_m}]\{\mathbf{d\Delta}\} = \{\mathbf{dP}\} \qquad (5.5)$$

In nonlinear analysis the response of the elements is a continuously or intermittently changing function of the applied loads. It is often impossible to solve the underlying equations in any direct analytical way. Thus is necessary to deal with them in some piecewise linear way.

The basic objective of the methods mentioned above is the establishment of equilibrium at the end of the load increment. They do so by analyzing the imbalance between the applied loads at the end of a linear step and the internal (element-end) forces calculated from the results of that step. Each method is intended to correct, in an iterative fashion, the imbalance between the linear approximation and the actual nonlinear response, or in other words, to reduce it to a tolerable level.

In the iterative methods a single representative stiffness is not used for each load increment, instead, increments are subdivided into a number of steps, each of

which is a cycle in an iterative process aimed at satisfying the requirements of equilibrium to within a specified tolerance.

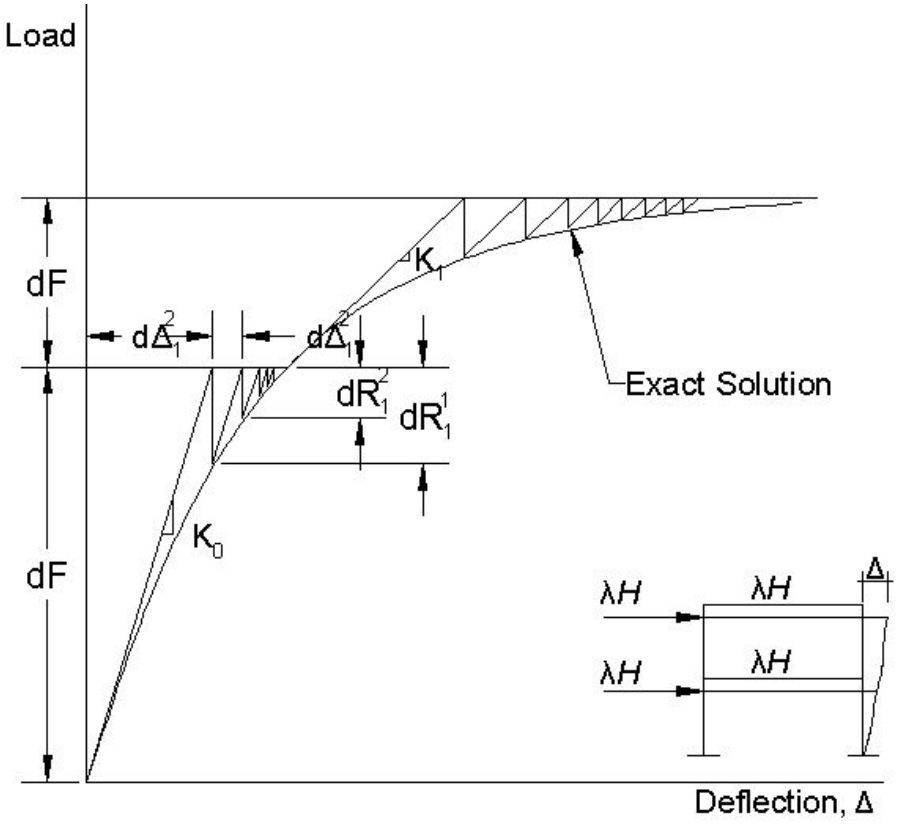

Figure 5.1 Schematic representation of incremental-iterative solution procedure. (Adapted from Ziemian 2011)

Computer Software Used

Given that the proposed method is targeted to the practicing engineer, the computer program selected for this research project is a commercially available structural analysis software and is commonly used in structural engineering firms. The computer program is not an academic or advanced finite element analysis

software. As in a practicing office, the models in this research project were created with simplified assumptions (i.e. pinned end or fixed end members) as commonly performed by practicing engineers, that is, without modeling the actual rotational properties of the connections. The computer program used throughout this research project is commercially known as RISA-3D v11 (RISA-3D 2012).

Key characteristics of the software as they relate to stability analysis:

- The software has the ability to perform a rigorous second-order analysis (e.i. *P-Δ* analysis).
- The software allows the user to select a stiffness reduction in accordance with AISC 360-10 chapter C.

P-Δ and P-δ

RISA-3D can perform a *P-Δ* analysis and determine the secondary moments of a column in a frame, for example. *P-Δ* effects are accounted for whenever the user requests it in the Load Combinations spreadsheet. The actual modeling of these secondary moments is done through the calculation of secondary shears (Figure 5.2). These shear forces are applied at the member ends. For a 3D model, this *P-Δ* calculation is done for the member's local x and local z directions. In other words, the secondary effects are calculated simultaneously for in plane and out of plane directions (RISA-3D 2012).

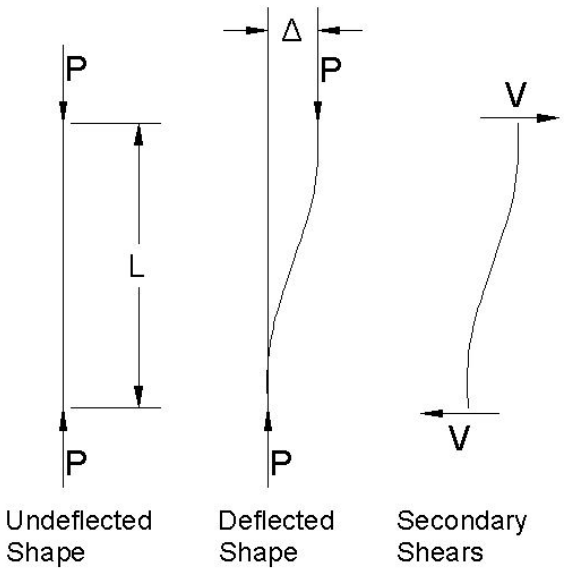

Figure 5.2 RISA second-order effects process (Adapted from RISA-3D 2012)

The program's *P-Δ* solution sequence is as follows (RISA-3D 2012), Figure 5.2:

1. The model is solved with the original applied loads
2. Calculate the secondary shears (V) for every member in the model, Equation 5.6.

$$P(\Delta) = V(L) \quad \text{Thus, } V = \frac{P(\Delta)}{L} \qquad (5.6)$$

3. Add these the shears (V) to the original loads and re-solve.
4. Compare the displacements for this new solution to those obtained from the previous solution. If they fall within the convergence tolerance the solution has converged. If not, return to step 2 and repeat.

When the *P-Δ* process, described above, is diverging dramatically, this process will be stopped before numerical problems develop and an error will be

displayed. When this error is displayed, the *P-Δ* displacements have reached a level where they are more than 1000 times greater than the maximum original displacements. When this happens the model is considered to be unstable under the given loads (RISA-3D 2012).

RISA's second order analysis method is based entirely on nodal deflections; the effect of *P-δ* is not directly accounted for. Thus, addition of nodes at discrete locations along the column, where member displacement effects are at their maximum, will account for the effects of *P-δ*. There are a number of "benchmark" problems, which are discussed below, given in various publications to determine if a program is capable of properly considering this effect. These comparisons can be used as a basis for when the *P-Δ* effect is significant enough to consider in the analysis. They can also be used to determine how many intermediate nodes are required to adequately account for the effect at a given load level (RISA-3D 2012).

Modeling Geometrical Imperfections

Geometrical imperfections can be modeled in RISA-3D by either, applying notional loads or directly modeling the imperfection. This can be done by adding an initial displacement to the members at node locations that represents the out-of-plumbness required by code. As it was mentioned above, the program determines second order effects at joint (node) locations only, thus, it is recommended that the notional loads or modeled initial displacements to be applied at the joints.

Assessment of the Computer Software with Benchmark Problems from Established Theory

Underlying contemporary nonlinear matrix analysis are established classical methods of structural mechanics. These methods are applied to elementary systems in the following benchmark problems for the purpose to illustrate types of physical behavior and in appraising the matrix methods used in the computer software.

To provide perspective and a basis for comparison with the computer program selected herein, established classical solutions of some elementary problems are given in the commentary to Appendix 7 of the AISC Specifications (AISC 2005).

The benchmark problems presented in the commentary to Appendix 7 of the 2005 AISC Specifications (AISC 2005) are recommended as a first-level check to determine whether an analysis procedure meets the requirements of a rigorous second-order analysis that is adequate for use in the direct analysis method. As discussed earlier, second-order analysis procedures in some software packages may not include the effects of P-δ on the overall response of the structure. Where P-δ effects are significant, errors arise in approximate methods that do not accurately account for the effect of P-δ moments on amplification of both local (δ) and global (Δ) displacements and corresponding internal moments. These errors can occur with second-order computer analysis programs if additional nodes are not included along the members.

The benchmark problems are intended to assess the ability of the computer program to perform a rigorous second order analysis and to reveal whether or not *P-δ* effects are included in the analysis. The benchmark problems used to assess the correctness of the computer program are shown in Figures 5.3 and 5.4. A brief description is presented here; however, full descriptions and solutions will be presented later in Chapter VII.

Benchmark problem 1, shown in Figure 5.3, is a simply supported beam-column subjected to an axial load and a uniformly distributed transverse load between supports. This problem contains only *P-δ* effects because there is no relative translation between the ends of the column.

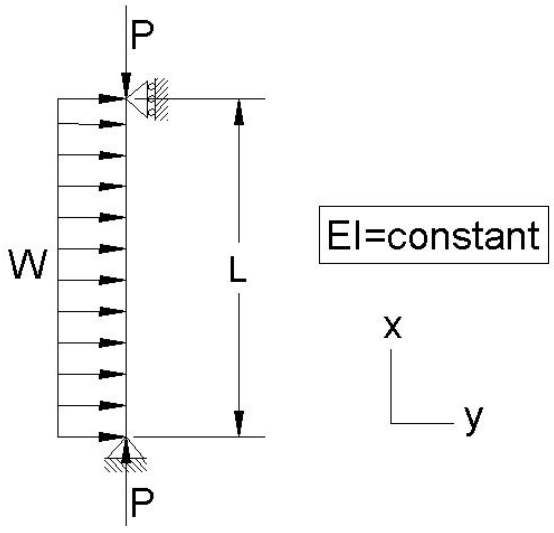

Figure 5.3 Benchmark Problem 1 (AISC 2005)

Benchmark problem 2, shown in Figure 5.4, is a fixed-base cantilevered beam-column loaded simultaneously with an axial load and a lateral load at its top. This problem contains both *P-Δ* and *P-δ* effects.

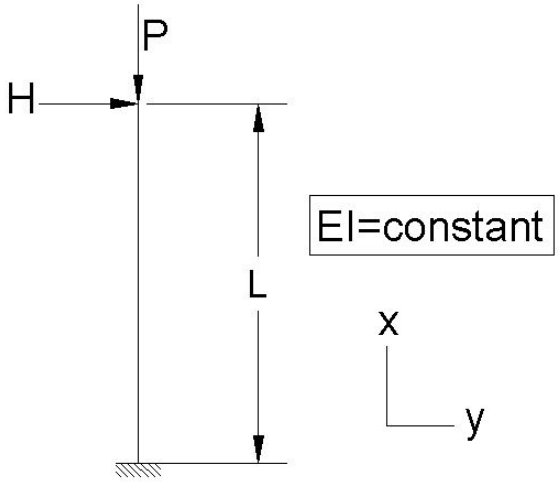

Figure 5.4 Benchmark Problem 2 (AISC 2005)

AISC points out that, when the correctness of a proposed second-order analysis method is evaluated, through these two benchmark problems, both, moments and deflections should be checked at various levels of axial load on the member and in all cases the results should agree within 3% and 5%, respectively (AISC 2010).

CHAPTER VI

A PRACTICAL METHOD FOR CRITICAL LOAD DETERMINATION OF STRUCTURES

The goal of this research project is to propose a practical method for stability evaluation and critical load determination of structures that are difficult to analyze with conventional hand calculation methods, (e.g. the compression chord of a pony truss bridge or a wind girt). The proposed methodology relies on a commercially available computer program in which a second order analysis can be readily accomplished by taking into consideration end-restraints, reduced flexural stiffness and initial geometrical imperfections or out-of-plumbness. The method can also be used for any 3D structure.

The proposed procedure incorporates an iterative process to determine the critical load at which the structure becomes unstable, by systematically increasing the load until the computer program does not converge on a solution. The two key factors in this procedure are the introduction of an initial imperfection combined with the ability of the program to perform a *P-Δ* analysis. The methodology is based on combining the direct design method and utilizing readily available 3D commercial computer software that allows the user to incorporate the two key factors mentioned above. A step-by step process for the implementation of the methodology is presented below.

Proposed methodology: Step-by-step process

Step 1: Software Selection. For the methodology proposed here, it is essential to select a 3D computer program for structural analysis that can perform a rigorous second-order analysis, *P-Δ* including *P-δ*. The software package selected for this research project was RISA-3D v 11 (RISA-3D 2012). An introduction to the software was presented in Chapter V.

The following steps (2-5) were implemented in Chapters VII through IX.

Step 2: P-Δ Capability Assessment. Not all analysis computer software packages are capable of performing a rigorous second-order analysis. A crucial part of the software selection process is the need to verify the software's ability to perform a rigorous second-order analysis. This can be done with the analysis of benchmark problems. AISC 360-05 and 360-10 both give two benchmark problems to determine if the analysis procedure meets the requirements of a rigorous second order analysis. AISC requires that the results from the computer program should fall within 3% of the moment amplification values and 5% of the deflection amplification values, given by the benchmark solutions (AISC 2010).

Step 3: Structure Modeling. Once the computer program has been verified to be performing rigorous second-order analyses correctly, the next step is to build a representation of the structure within the program. It is recommended to model the structure in the same manner a similar structure would be modeled (i.e. same restraint assumptions and boundary conditions). However, for members that are subjected to

second-order effects, additional nodes may be needed for the determination of *P-δ* effects if the software's second-order analysis method is based entirely on nodal deformations, as is in the case of RISA-3D.

Step 4: Geometrical Imperfections. One of the key elements of the methodology is to account for the destabilizing effects of second-order forces, moments and deformations due geometrical imperfections. Hence, it is necessary to include initial imperfections in the model to initiate these secondary effects on axially loaded members. The initial imperfections can be modeled directly in to the structure by applying initial displacements to the nodes or by modeling the nodes in a displaced configuration. A second alternative is to apply notional loads to the nodes in the direction of the imperfection. As mentioned in step 3, additional nodes may be needed to account for the effects of *P-δ* in some software packages.

Step 5: Critical Load Determination. The determination of the critical load is the final step and goal; this is accomplished through an iterative process in which the gravity load is systematically increased. One way to go about this process is to increase the load factor in the load combinations tab. This way, the gravity loads in the structure do not need to be changed, thus, saving significant time in the analysis. Throughout the process, if the structure is stable, the *P-Δ* feature of the program will lead to successively smaller displacements until a convergence is reached. The analysis is repeated with larger loads until the analytical model no longer converges, shown in Figure 6.1, and that is the load that causes instability (i.e. buckling).

Figure 6.1 Error message from RISA-3D that *P-Δ* is no longer converging

CHAPTER VII

COMPUTER SOFTWARE EVALUATION WITH BENCHMARK PROBLEMS

In order to verify that the *P-Δ* capability of the program meets the requirements of a rigorous second-order analysis, the computer program used in this research project was evaluated by analyzing the two problems that were described in Chapter V and by following the proposed methodology illustrated in Chapter VI

In addition, the effects of *P-δ* on the benchmark problems were evaluated by varying the number of nodes along the beam-column. According to the software developer, additional nodes along the member provide a more accurate representation of the *P-δ* effects on a structure. Therefore, different intermediate node configurations were evaluated and compared to the benchmark solutions presented in the commentary to the AISC Specification. The intermediate node configurations for benchmark problems 1 and 2 are described below.

It is important to note that for problem 1, Figure 7.1; at least one intermediate node needs to be included along the member. That is, because there is no translation of the supports, this is a case of *P-δ* only; in other words, *P-Δ* does not exist for this case. If no intermediate nodes were added to problem 1, the computer program will not perform a second-order analysis and the results will be based on a first-order analysis regardless of the compressive force.

The general procedure consisted on applying a constant the lateral load (*W* shown in Figure 7.1 and *H* shown in Figure 7.2), that would simulate the inherent geometrical imperfections in real structures, while increasing the axial load, *P*, from zero to the point where the program did not converge anymore. This procedure was followed for each case.

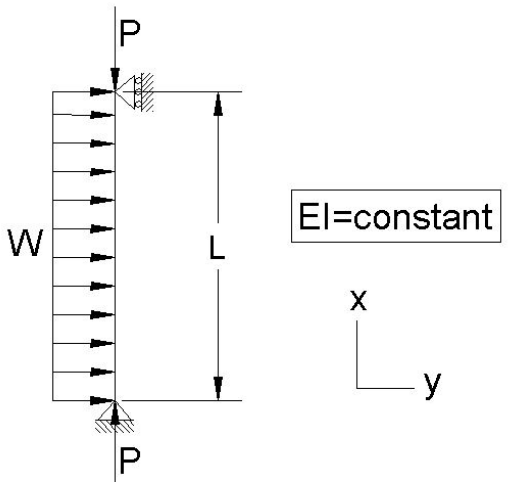

Figure 7.1 Benchmark Problem 1 (AISC 2005)

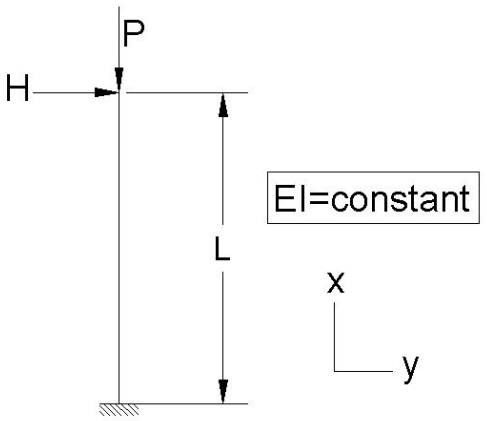

Figure 7.2 Benchmark Problem 2 (AISC 2005)

The results of problem 1 and problem 2 are presented below and are plotted as the load ratio, P/P_{eL}, versus the moment amplification factor, M_{max}/M_0, and the load ratio, P/P_{eL}, versus the deflection amplification factor, Y_{max}/Y_0. Where P is the incremental compressive load and P_{eL} is the Euler buckling load given by Equation 7.1.

$$P_{eL} = \frac{\pi^2 (EI)}{L^2} \qquad (7.1)$$

The moment amplification factor and deflection amplification factor are the ratios of any given moment to the initial moment and any given deflection to the initial deflection respectively. According to the commentary to the AISC Specifications, the results from the computer program should fall within 3% and 5% of the moment amplification values and deflection amplification values, respectively, given by the benchmark solutions (AISC 2010).

Benchmark Problem 1

The first problem used to evaluate the ability of the computer software to perform a rigorous second-order elastic analysis is a simply supported beam-column subjected to a uniform transverse load between the supports and an applied compressive load at its ends. The beam-column used in the analysis is a W14x48 I-Section, 28ft long and pin-supported at its top and bottom. The initial deformation, Y_0, was created by applying a horizontal uniform distributed load along the column

equating to 0.20 kip/ft. This initial displacement represents an initial imperfection of $L/1700$.

The problem contains only the P-δ effect because there is no translation of one end of the member relative to the other. Problem 1 is the same as the benchmark problem *Case 1* presented in the commentary to the AISC Specifications (AISC 2005) and is shown in Figure 7.3. The classical solution is presented by Timoshenko (1961), McGuire (2000) and by Chen (1985) which is summarized in the commentary to the AISC Specification and is presented below (AISC 2005).

The maximum moment of problem 1 is given by

$$M = \frac{wL^2}{8}\left[\frac{2\left(\sec u - 1\right)}{u^2}\right] \tag{7.2}$$

And the maximum deflection is given by

$$Y = \frac{5wL^4}{384EI}\left[\frac{12\left(2\sec u - u^2 - 2\right)}{5u^4}\right] \tag{7.3}$$

Where the parameter u is given by

$$u = \sqrt{\frac{PL^2}{4EI}} \tag{7.4}$$

P represents the axial load which is increased from 0.0 kip until the program no longer converges. L is the distance between supports; also known as the length of the beam-column. E is the modulus of elasticity of steel and I is the moment of inertia

of the beam-column in the direction of bending. The above moment and deflection rigorous solutions (M_{max} and Y_{max}), are plotted in Figures 7.4 and 7.5 as functions of the applied load ratio P/P_{eL}.

As discussed earlier, RISA's second order analysis method is based entirely on nodal deflections, thus, for the evaluation of the computer software, three cases of intermediate nodes were evaluated and are shown in Figure 7.6. For the first case, one intermediate node at mid height was included. As mentioned above, at least one node needs to be included in this case so that the computer program can calculate second-order effects due to P-δ effects. For cases 2 and 3, two and three intermediate nodes, respectively, were added to the beam-column as shown in Figure 7.6. The load-moment history and the load-deflection history of all three different node configuration cases are presented in Figures 7.7 and 7.8 respectively, along with the rigorous solution from the classical solution.

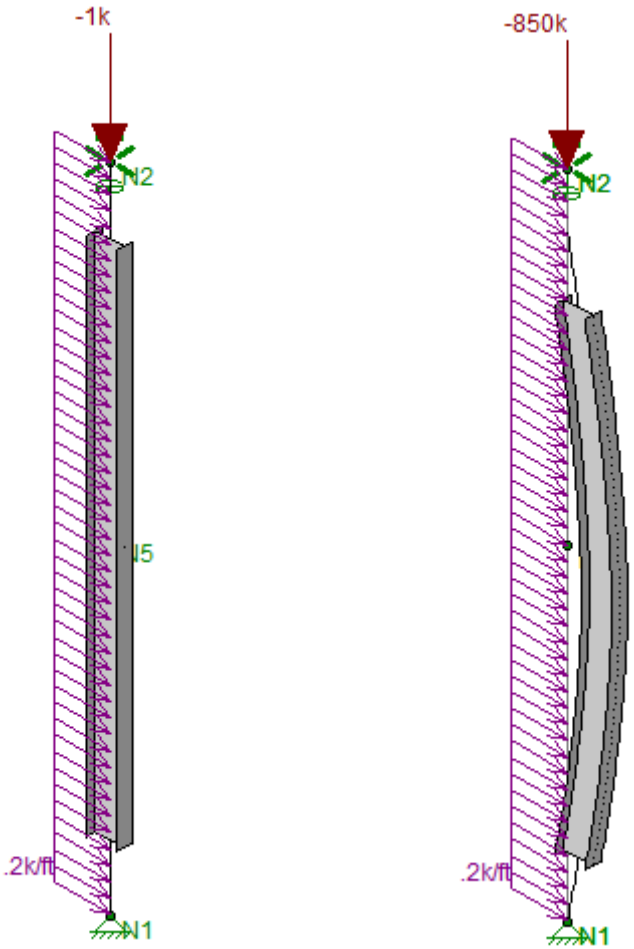

a) **b)**

Figure 7.3 Benchmark problem 1: a) undeflected shape b) deflected shape

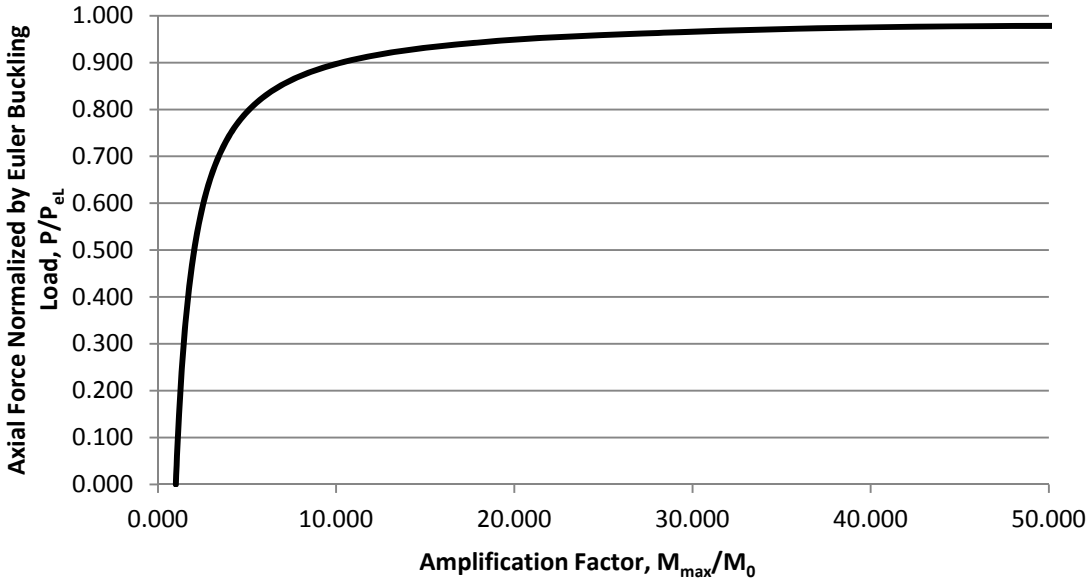

Figure 7.4 Maximum moment values as a function of axial force for benchmark problem 1 (classical solution, Equation 7.2)

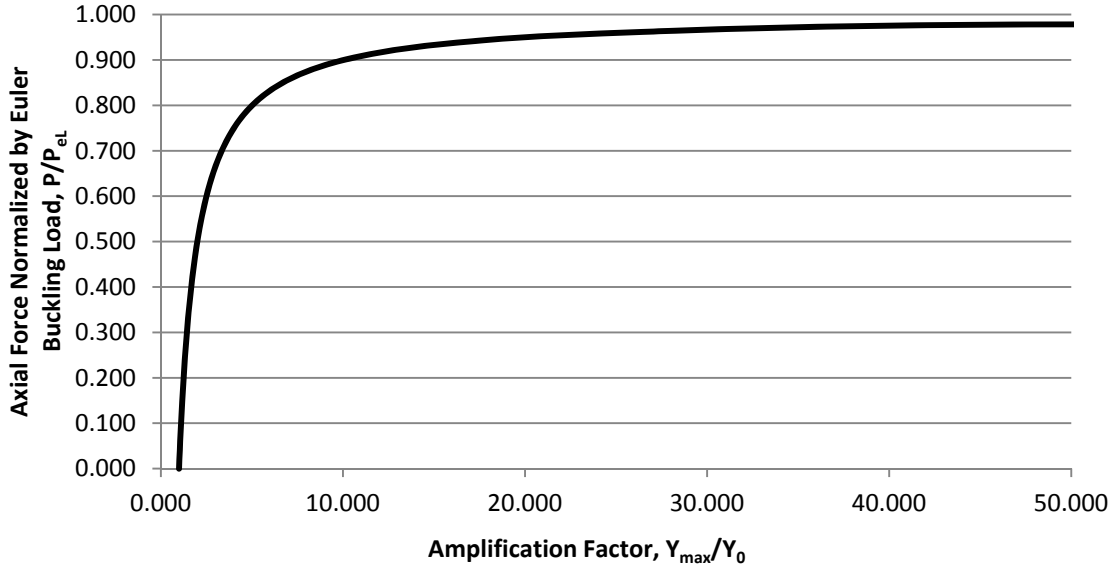

Figure 7.5 Maximum deflection values as a function of axial force for benchmark problem 1 (classical solution, Equation 7.3)

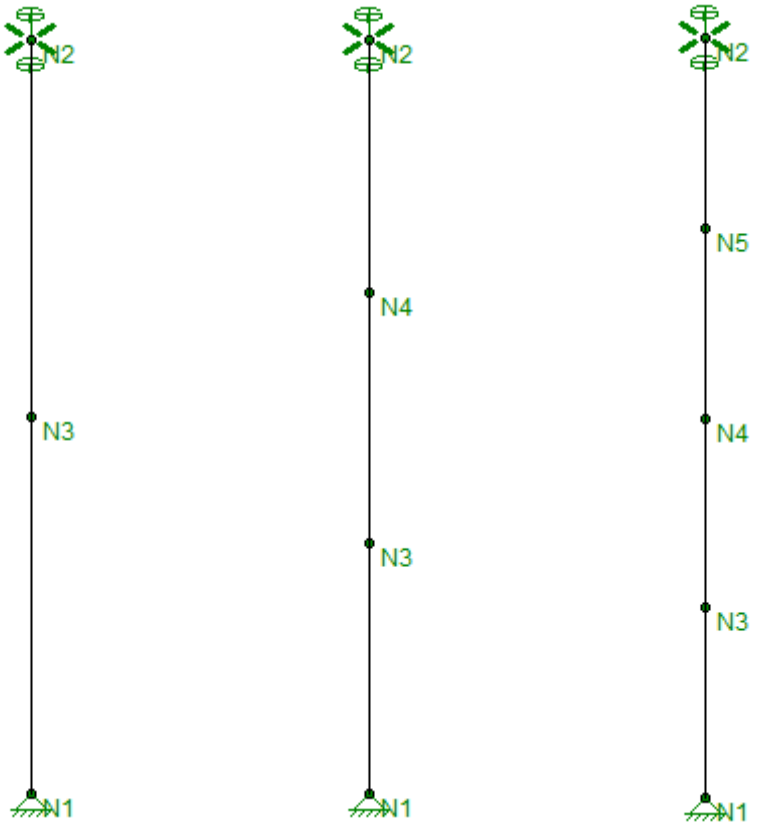

a) **b)** **c)**

Figure 7.6 Benchmark problem 1 node arraignments a) Case 1, one additional node at mid height of the beam-column b) Case 2, two additional nodes at equal distance c) Case 3, three additional nodes at equal distance

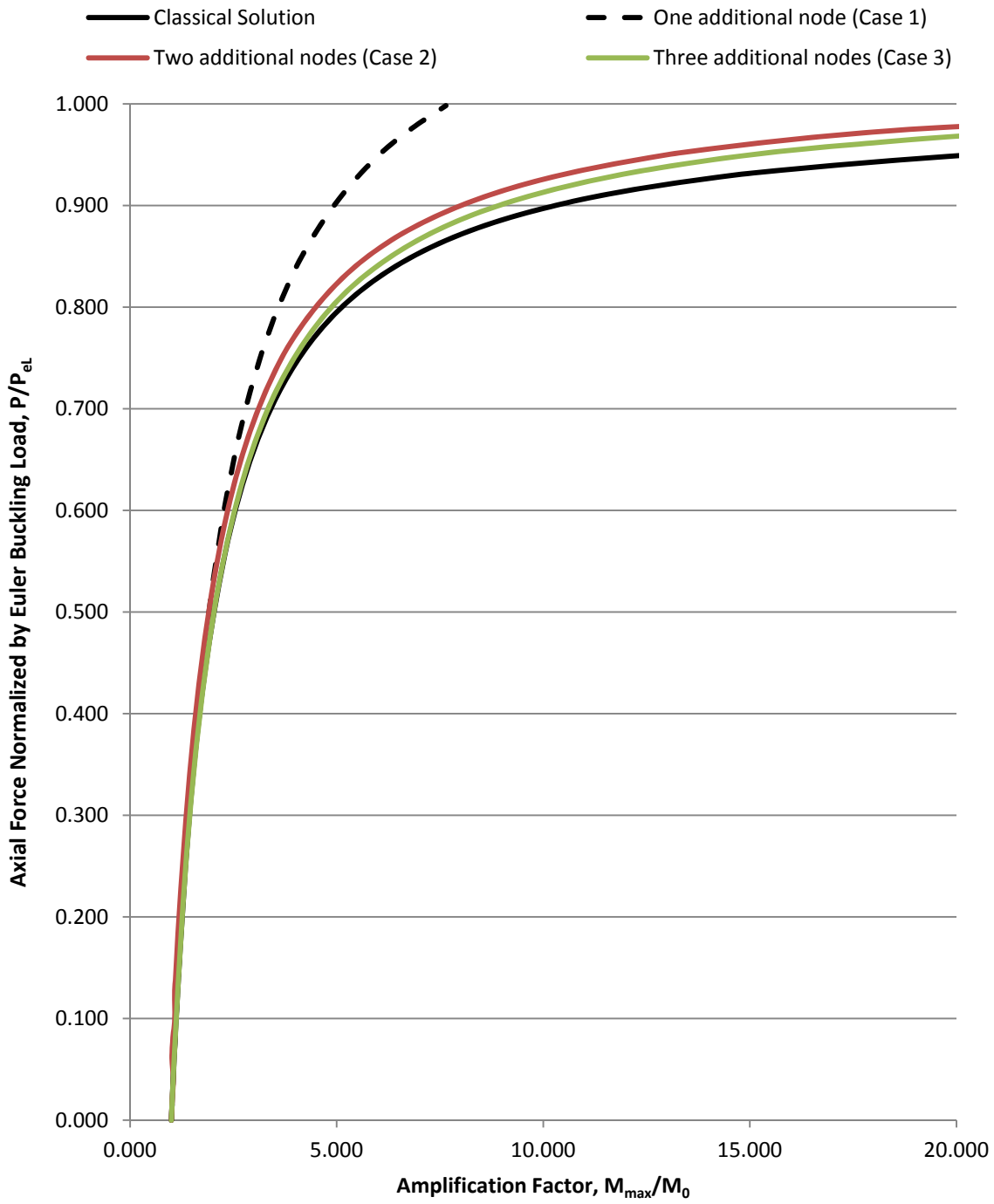

Figure 7.7 Maximum moment values as a function of axial force for benchmark problem 1 (classical solution, with one, two and three additional nodes)

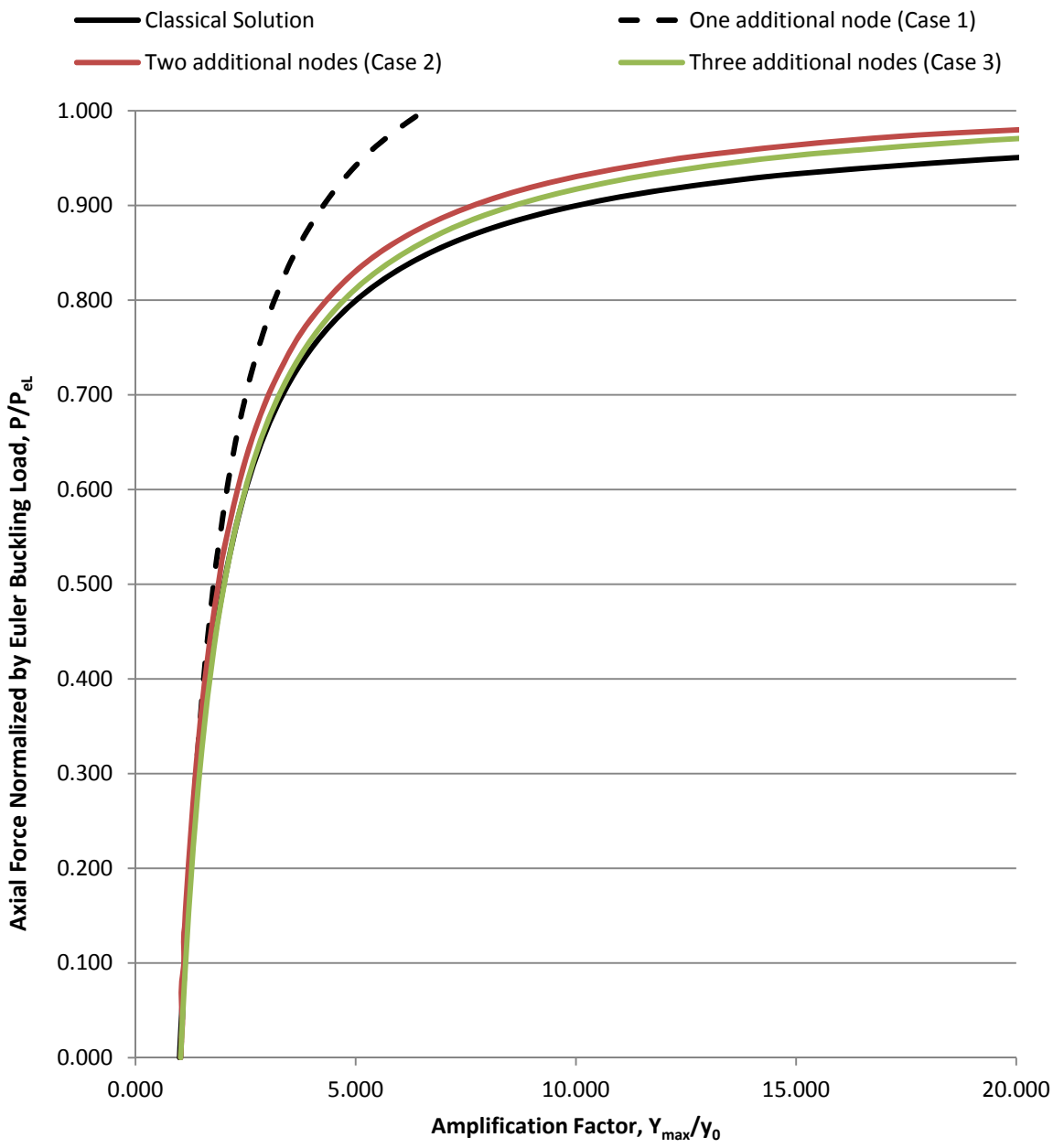

Figure 7.8 Maximum deflection values as a function of axial force for benchmark problem 1 classical solution, with one, two and three additional nodes)

Benchmark Problem 2

The second problem is a cantilever beam-column, fixed at the bottom and free at the top with lateral and vertical loads applied at its top. The beam-column used is a W14x48 I-Section with a length of 28ft. The initial deformation, Y_0, is created by applying a horizontal point load at the top of the column equating to 1.0 kip. This initial displacement represents an initial imperfection of $L/350$. Problem 2 contains both P-Δ and P-δ effects since the top node is free to translate. Problem 2 is the same as the benchmark problem Case 2 presented in the commentary to the AISC Specifications (AISC 2005) and is shown in Figure 7.9. The rigorous classical solution is presented by Timoshenko (1961) and McGuire (2000). The solution is summarized in the commentary to the AISC Specification and presented below (AISC, 2005). The solutions presented below are plotted in Figures 7.10 and 7.11.

The maximum moment of problem 2 is given by

$$M = HL\left[\frac{tan\,\alpha}{\alpha}\right] \tag{7.5}$$

And the maximum deflection is given by

$$Y = \frac{HL^3}{3EI}\left[\frac{3\left(tan\,\alpha - \alpha\right)}{\alpha^3}\right] \tag{7.6}$$

Where the parameter α is given by

$$\alpha = \sqrt{\frac{PL^2}{EI}} \tag{7.7}$$

P represents the axial load which was increased from 0.0 kip until the program no longer converged. *L* is the distance between supports; also known as the length of the beam-column. *E* is the modulus of elasticity of steel and *I* is the moment of inertia of the beam-column in the direction of bending.

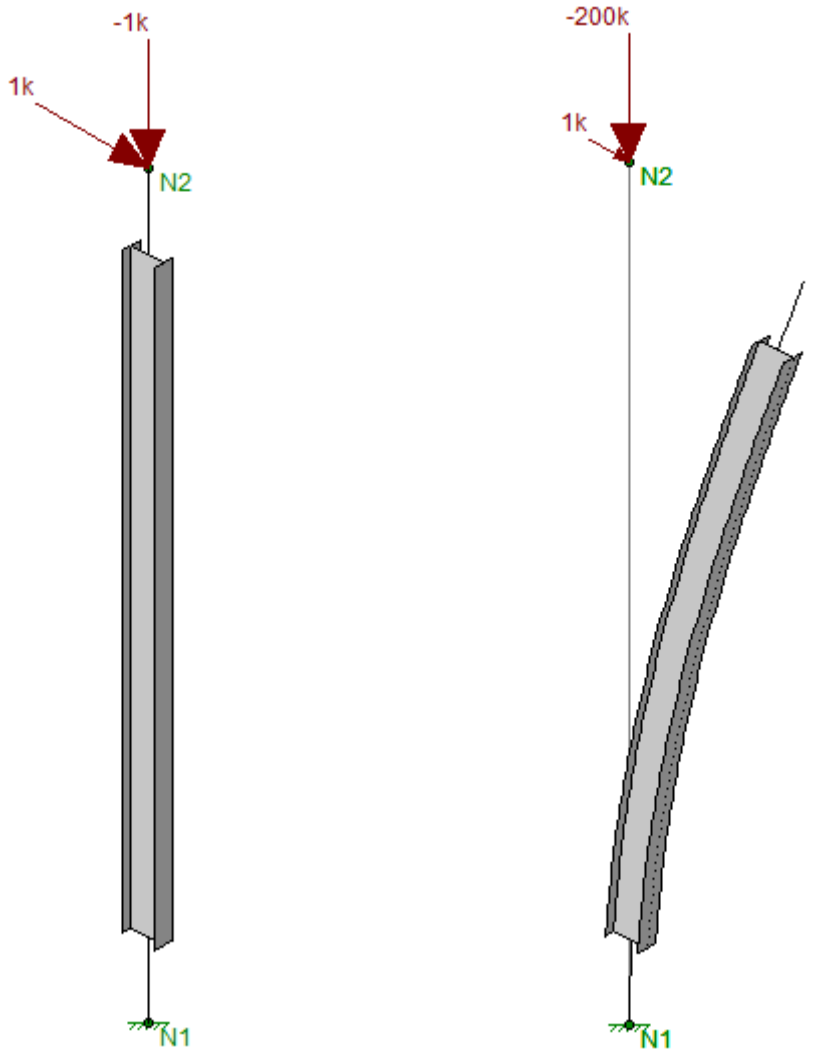

a) **b)**

Figure 7.9 Benchmark problem 2, a) undeflected shape b) deflected shape

As discussed above, this problem contains both, *P-Δ* and *P-δ*, thus it is necessary to add additional nodes along the length of the member to account for the effects of *P-δ*. Three different node configurations were evaluated and are shown in Figure 7.12. However, as opposed to problem 1, the first case consisted of no intermediate nodes at mid height. The results from this case are mainly due to *P-Δ*.

For cases 2 and 3, one and two intermediate nodes, respectively, were added to the beam-column as shown in Figure 7.11. The load-moment history of all cases and the load-deflection history are presented in Figures 7.13 and 7.14 respectively, along with the rigorous solution from the classical solution. It is important to note that the maximum load ratio for problem 2 is equal to 0.25(P/P_{el}), this is due to the fact that for cantilever columns, the effective unsupported length is twice the length of an equivalent pin-ended column, thus the Euler buckling load is given by:

For a pin-ended column, $P_{eL} = \frac{\pi^2 (EI)}{(L)^2}$ and (7.1)

For a cantilever column, $P_{eL\_cant} = \frac{\pi^2 (EI)}{(L_{cantilever})^2}$ (7.8)

Because $L_{cantilever}=2L$, then

$$P_{eL\_cant} = \frac{\pi^2 (EI)}{(2L)^2} = \frac{1}{4}\frac{\pi^2 (EI)}{(L)^2} = \frac{1}{4}P_{eL} = 0.25P_{eL} \quad (7.9)$$

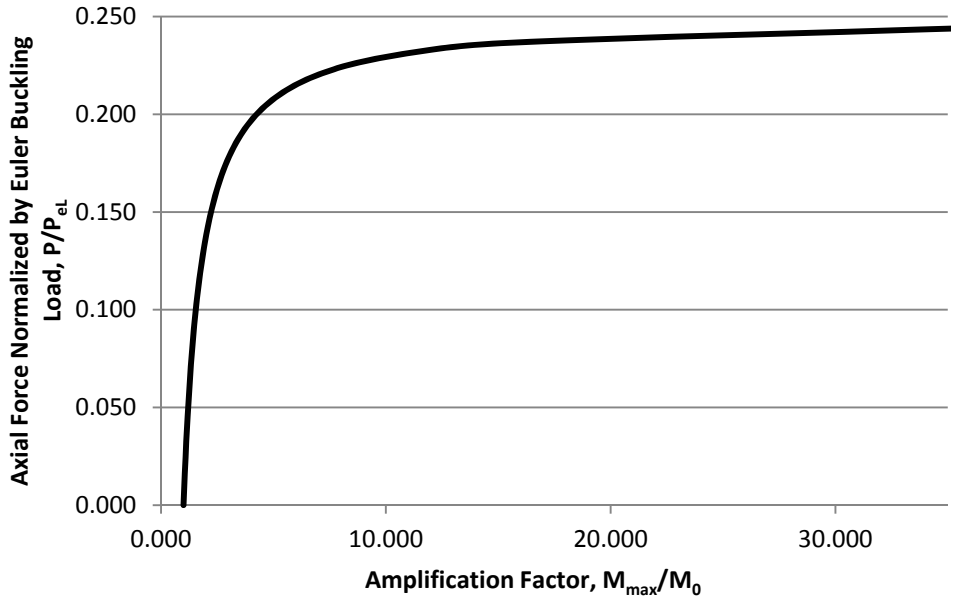

Figure 7.10 Maximum moment values as a function of axial force for benchmark problem 1 (classical solution, Equation 7.5)

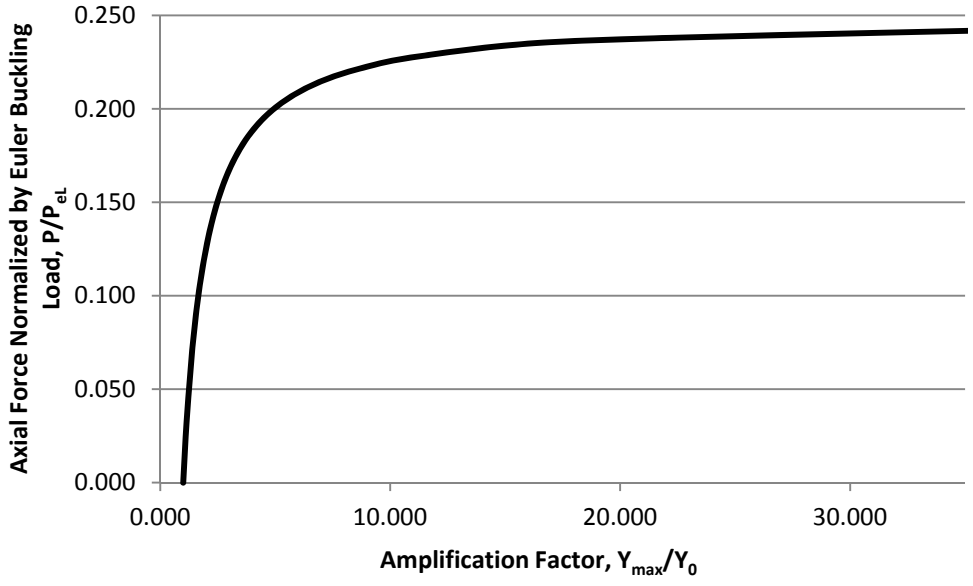

Figure 7.11 Maximum deflection values as a function of axial force for benchmark problem 1 (classical solution, Equation 7.6)

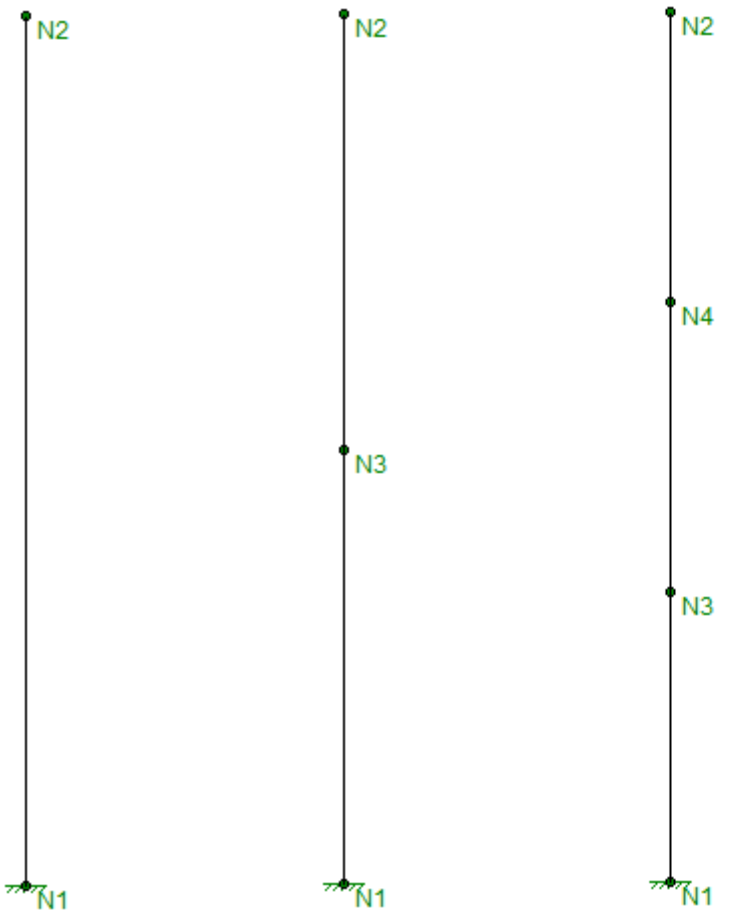

a) **b)** **c)**

Figure 7.12 Benchmark problem 2 node arraignments a) Case 1, no additional node along the height of the beam-column b) Case 2, one additional node at mid height of the beam-column c) Case 3, two additional nodes at equal distance

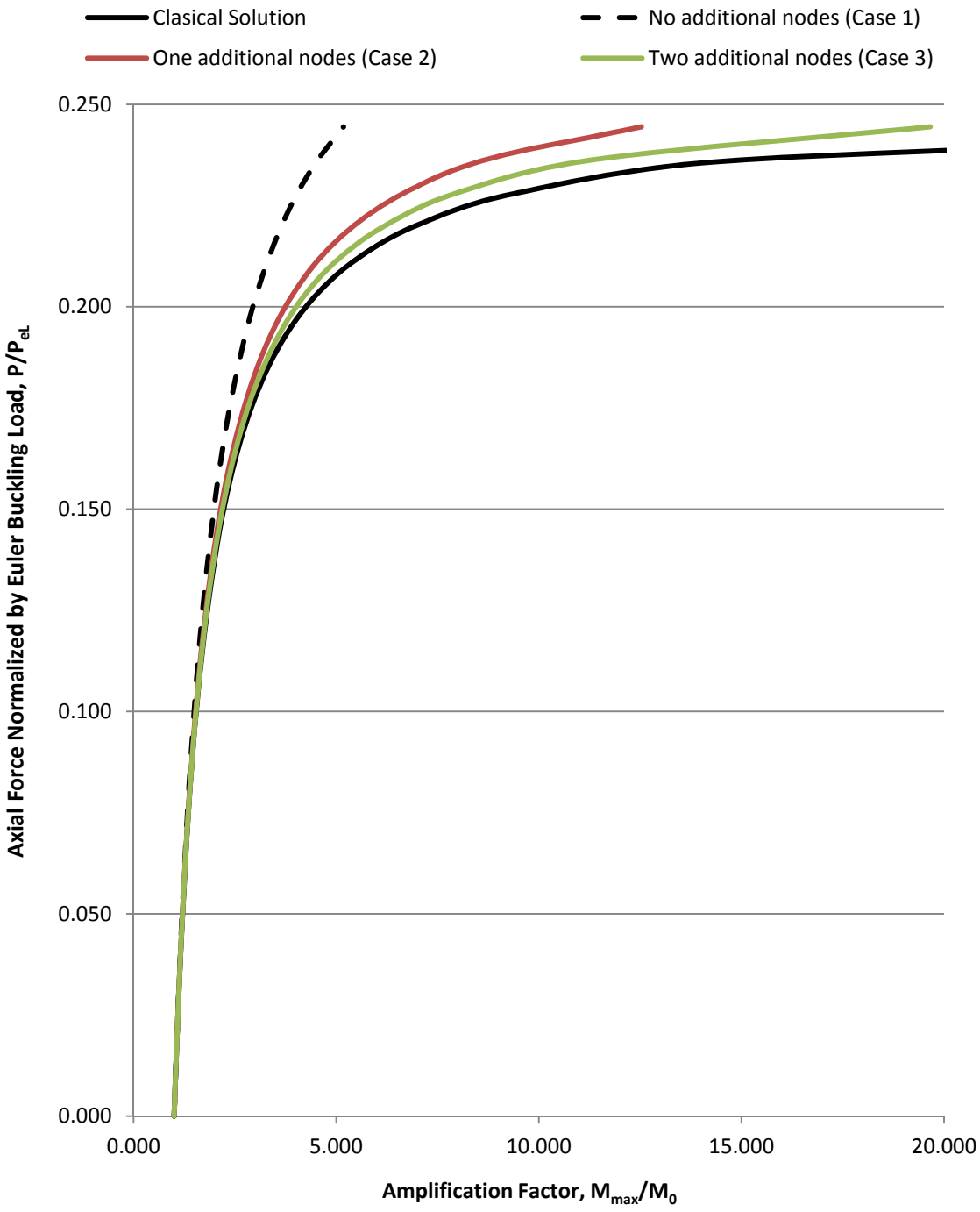

Figure 7.13 Maximum moment values as a function of axial force for benchmark problem 2 (classical solution, with zero, one and two additional nodes)

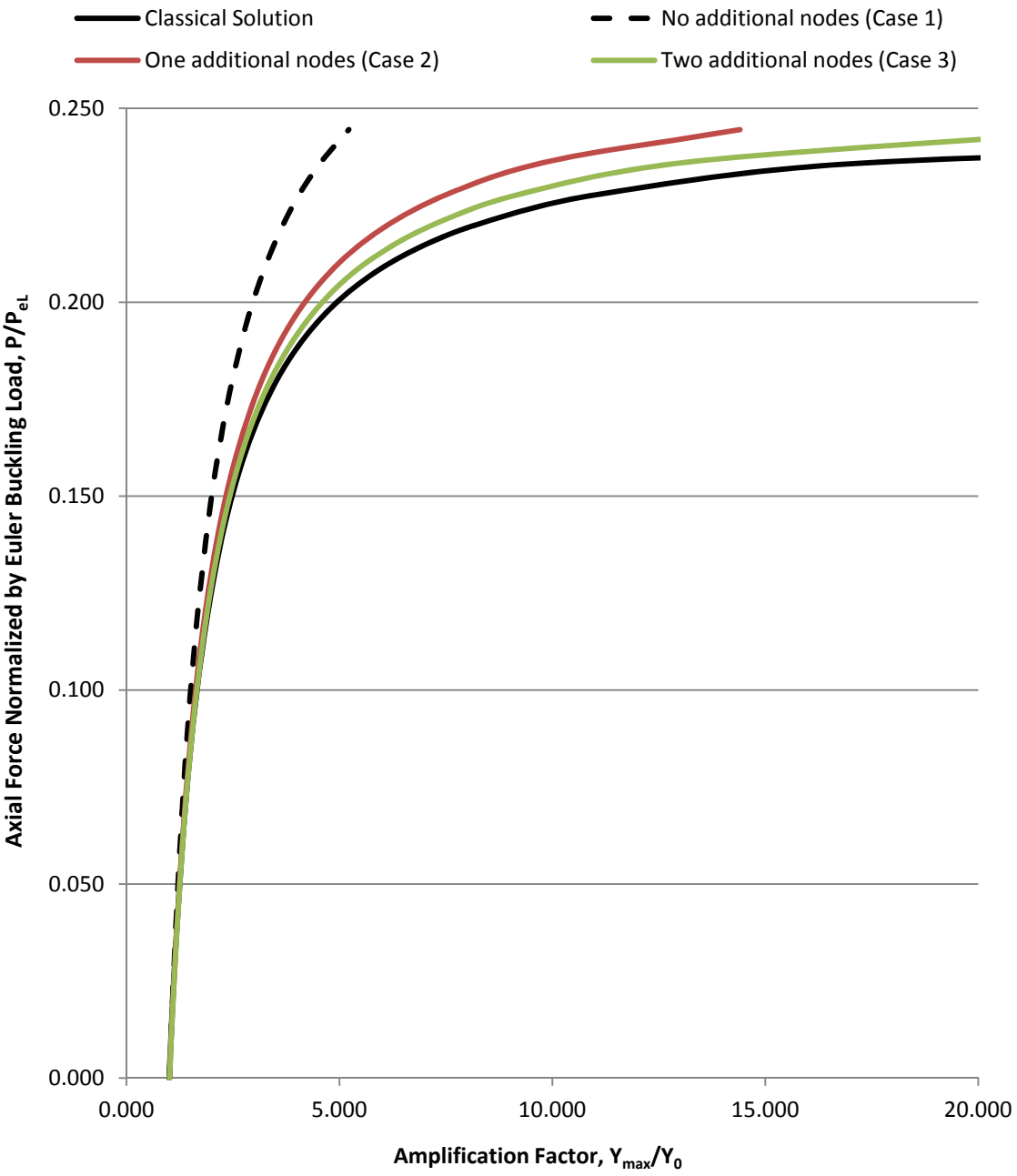

Figure 7.14 Maximum deflection values as a function of axial force for benchmark problem 2 (solution, with zero, one and two additional nodes)

Discussion of Results from Benchmark Problems

From the results presented above it can be seen that the computer program used in this research project meets the requirements of a rigorous second-order analysis, as defined by AISC (AISC 2005). Therefore, the computer program, RISA-3D, can be used with the proposed analytical method. However, because the computer program calculates secondary effects at node locations, it is necessary to add intermediate nodes between joints, along the length of compression members, when effects due to P-δ are significant. Thus, it is necessary to investigate the influence of P-δ on the structure on a case by case basis.

CHAPTER VIII

MODEL DEVELOPMENT

As discussed earlier in Chapter I, the aim of this research project is to propose a practical method for stability analysis of structures that are difficult to analyze with conventional methods. Examples of this type include, but are not limited to, the compression chord of a pony truss bridge or the compression chord of a wind girt truss in which the buckling mechanism takes place out of the plane of the truss. Nontheless, this method can also be used for any other 3D structure. Given the author's interest in bridges, it was decided, for this study, to work with pony truss bridges that can be load tested to validate the proposed methodology.

Currently, the design of pedestrian bridges including pony truss like structures is based on the requirements of AASHTO "LRFD Guide Specifications for the Design of Pedestrian Bridges" (AASHTO 2009). As discussed in Chapter III, the methodology for the design of the top chord used in this document is based on research that was done in the 1950's.

As illustrated earlier, the computer program used throughout this research project was evaluated using two benchmark problems to assess its ability to carry out a rigorous second-order analysis. The outcome of this evaluation was presented in Chapter VII with satisfactory results. Once it was determined that the computer program met the requirements for a rigorous second-order analysis, as required by AISC (AISC 2005), the next step was to develop two physical scaled-down test

models that can be load tested using available load testing equipment to verify the analytical method. Consequently, an analytical study was developed to determine the parameters that would affect the load-displacement behavior of the top chord and stability of the pony truss bridges. This analytical study started with a parametric scheme in which computer models, that simulated a full-size pony truss bridge, were developed with the purpose of targeting some specific parameters to understand the stiffening effects that the transverse frames have on the stability and overall behavior of the bridge.

These computer models of full-size bridges were labeled the *analytical models*. The results from the parametric study were used to develop an experimental study of scaled computer models for which the critical load was determined by following the methodology presented in Chapter VI. The ultimate goal of these scaled computer models was to fabricate and load a set of scaled models to validate the results from the computer models. However, it was also necessary to determine, approximately, the total load at which the scaled models will fail so that hydraulic jack and load cell capacities could be determined.

Full-Size Analytical Study

The analytical evaluation of pony truss bridge models, using RISA-3D, started with a parametric study, in order to assess the stiffening effects of the lateral restrains, in which a full size pony truss bridge model was set up using the computer program. The model, herein referred as the full size model, is a 40 feet long pony truss bridge

similar to the actual pony truss bridge shown in Figure 8.1. The full size computer model was modeled with the following dimensions: The span was set at 40 ft, and the deck width was set at 12 ft. The transverse frame consisted of hollow steel sections (HSS) 8 in x 4 in x ¼ in stringer beams and 4 in x 4 in x ¼ in verticals and diagonals. The 6 in concrete deck was modeled composite with the frames; refer to Figure 8.2. With the purpose of evaluating the influence of the transverse frame stiffness, and flexural stiffness of the top compression cord, a factorial process was developed such that, systematically, all of the variables described below were considered and the critical load was determined for each case. In total, the parametric study, shown in Figure 8.3 included 21 analyses.

This study included varying the compression chord size by using seven different sections and changing the height of the truss while keeping the length of the bridge constant. The analyses included varying the top chord cross-section form a HSS section of 2 in x 1 in x 1/8 in to a section of 6 in x 6 in x ¼ in. At the same time, three different truss heights were investigated, 4 feet, 6 feet and 8 feet which correspond to an aspect ratio, AR, of 0.10, 0.15 and 0.20 respectively. The combination of different aspect ratios, AR, and compression chord sizes yielded a variety of different out of plane stiffness parameters, ξ, for the bridge truss. In total, 21 different stiffness parameters, ξ, were generated and are presented in table 8-1. The stiffness parameter correlates the stiffness of the compression chord and

transverse frame to the deformational behavior (i.e. deformed shape) and critical load of the compression chord. A description of the parametric study is presented below.

Figure 8.1 Actual 40 foot long pony truss bridge

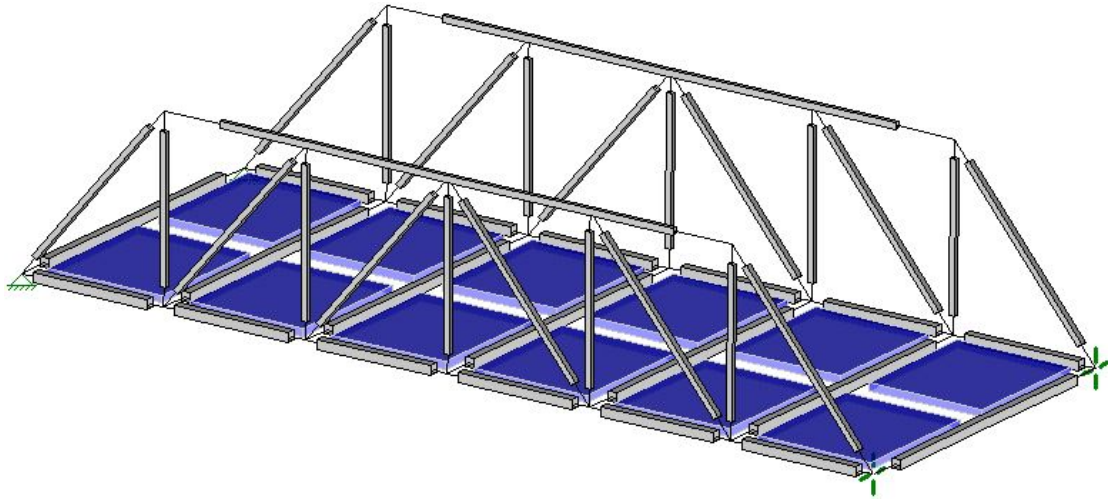

Figure 8.2 Computer model of the 40 foot long bridge (*analytical model*)

The aspect ratio, AR, refers to the ratio of the height of the truss, h, to the length of the bridge, L, and is given by equation 8.1. The stiffness parameter, ξ, refers to the transverse rigidity of the frame (elastic restraint), C, times the length of the chord, L_{chord}, divided by the cross sectional area of the chord, A_{chord}, given by equation 8.2.

$$AR = \frac{h}{L} \qquad (8.1)$$

$$\xi = C\frac{L_{chord}}{A_{chord}} \qquad (8.2)$$

Where C is the transverse rigidity of elastic restraints for the compression chord (AASHTO 2009) is given by equation 8.3

$$C = \frac{E}{h^2\left[\left(h/3I_c\right)+\left(b/2I_b\right)\right]} \qquad (8.3)$$

And h is the height of the truss and verticals, b is the width of the cross-frame, I_c is the moment of inertia of the vertical and I_b is the moment of inertia of the beam between the verticals.

Once the model was completed and the gravity loads were applied to the deck surface, the first step was to add a geometrical imperfection. This imperfection was entered as a notional load that simulated an initial imperfection, of the top chord of $L/500$, in the out of plane direction of the truss, and is shown in Figure 8.4.

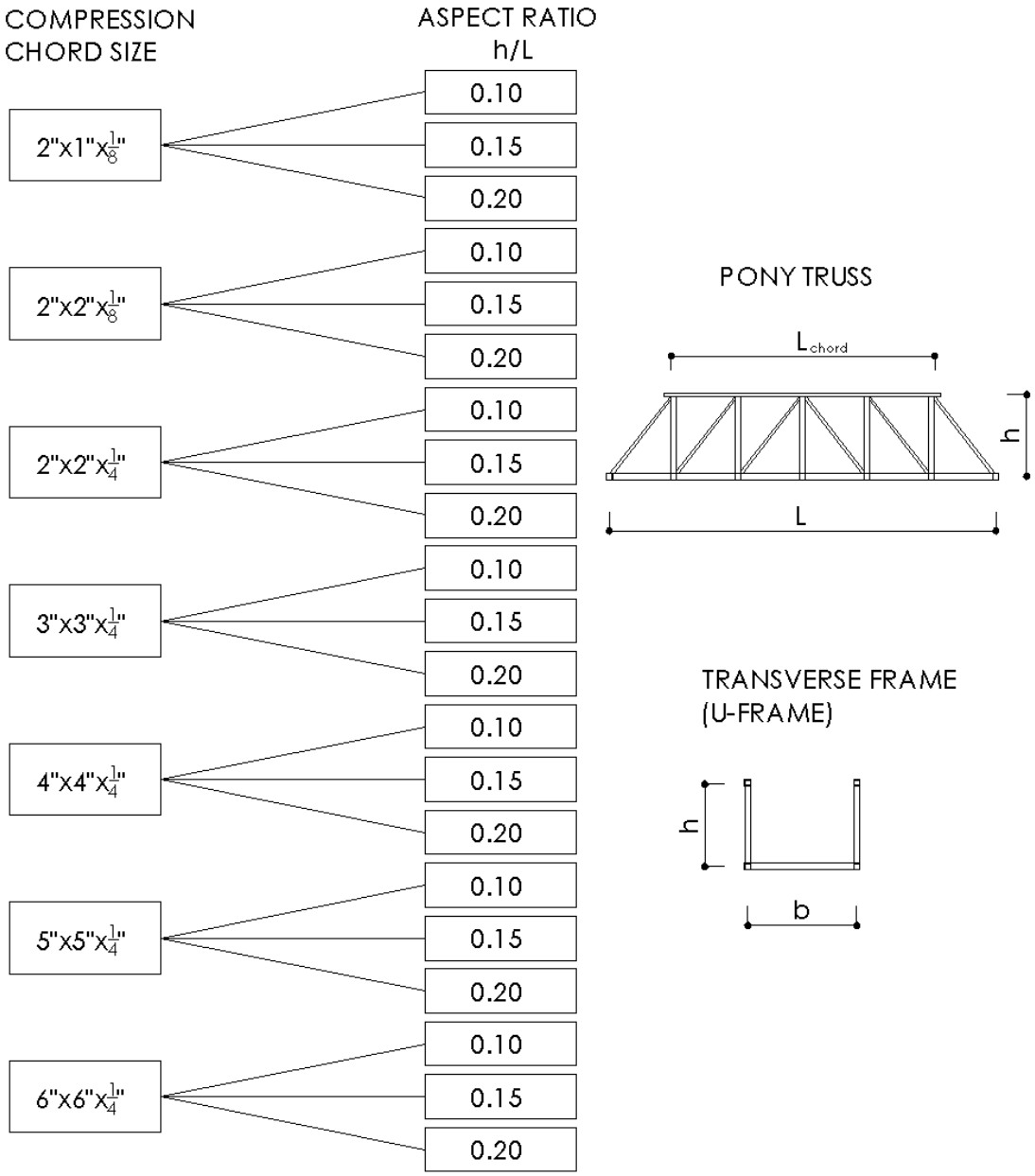

Figure 8.3 Parametric study

The next step was to systematically increase the gravity load, following the methodology presented in Chapter VI, until the critical load was found. In this case, the gravity load was maintained constant while incrementally changing the load factor until the program did not converge to a solution. Hence, for each case, the gravity load was increased until the *P-Δ* feature of the program no longer converged to a solution, in which, at this point the maximum load in the compression chord was recorded as the ratio of such maximum load to the yield load of the chord.

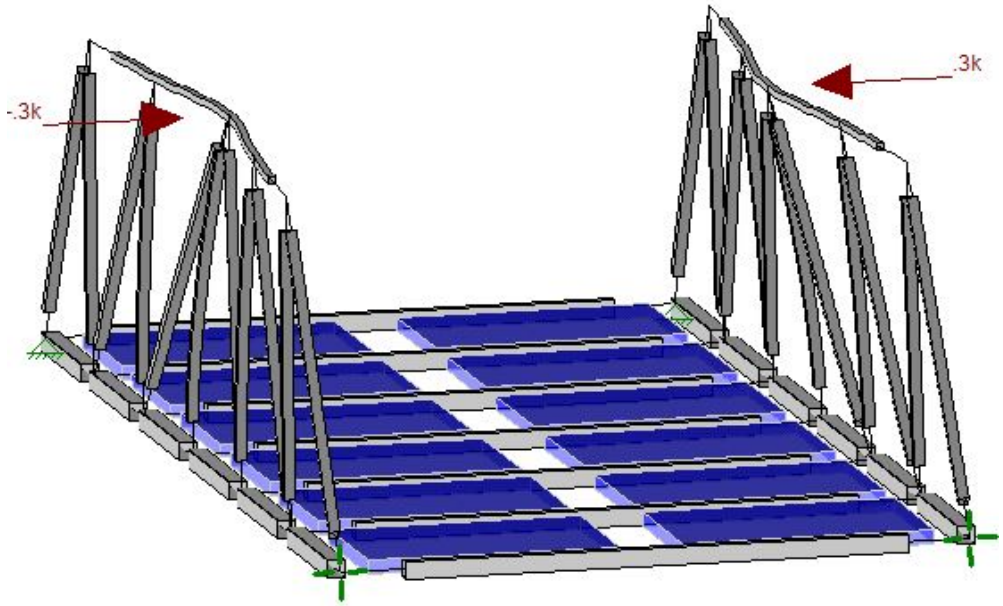

Figure 8.4 Geometric imperfection

The stiffening effects of the chord size and aspect ratio are evident in Figures 8.5 and 8.6. Figure 8.6 shows the deformed shape of the model at the critical load for the case when the top chord is slender with compared to the verticals of the truss. In comparison, Figure 8.6 shows the same model's deformed shape for the case when

the top chord is much stiffer compared to the verticals of the truss. The results of this parametric study are shown in Table 8.1. These results present a correlation between the stiffness parameter of the top chord and the critical load of that same top chord.

By looking at the results in Table 8.1, it is evident that for pony truss bridges with large stiffness parameters and low aspect ratios, in other words, bridges with stiffer cross-frames, the critical load in the top chord is close, and in some cases, larger than the yield strength of the chord. This means that it is likely that the top chord would fail in yielding before instability due to buckling occurs. Thus, for the experimental study, which includes the *theoretical models* and the *test models* mentioned above, it was decided to select parameters that would ensure that the top chord would fail due to elastic buckling before yielding.

An aspect ratio of 0.20 and stiffness parameters between 55 and 98 were selected to be used in the experimental study presented below. Based on the results shown in Table 8-1 and the selected parameters, it is expected that the critical load of the top chord is on the order of half the yield strength, thus, ensuring that the failure of the top chords is due to buckling. Based on the proposed test setup, described below, and for practical reasons it was decided to test two scaled down truss bridges. The first bridge was determined to be 5 feet long and the second bridge was determined to be 3.333 feet long. The corresponding truss heights, for an aspect ratio of 0.20, are 12 inches and 8 inches respectively. A full description of the experimental models is provided below.

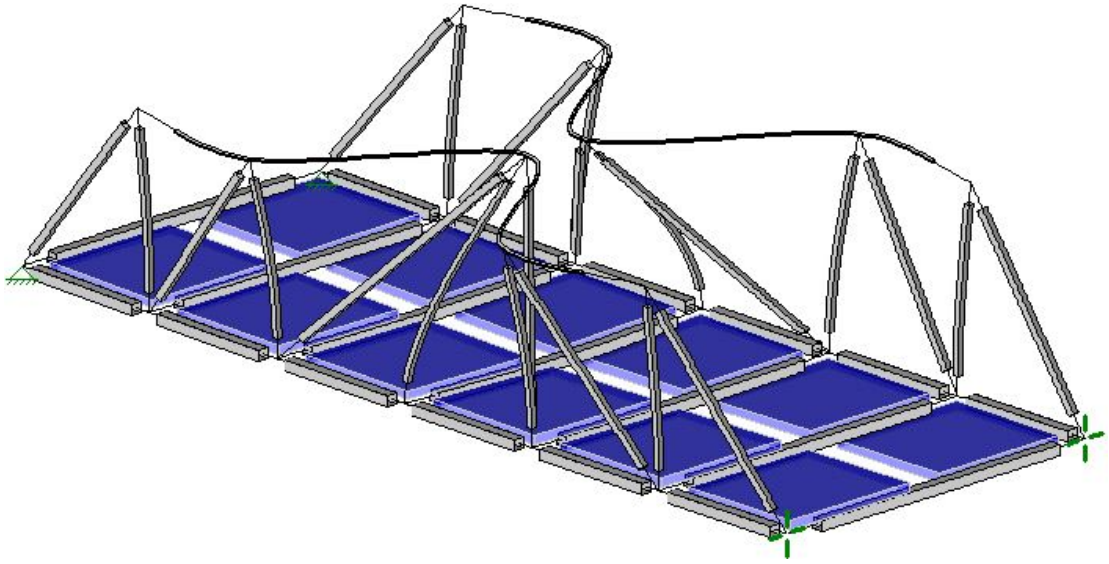

Figure 8.5 Deformed shape at critical load. Slender top chord

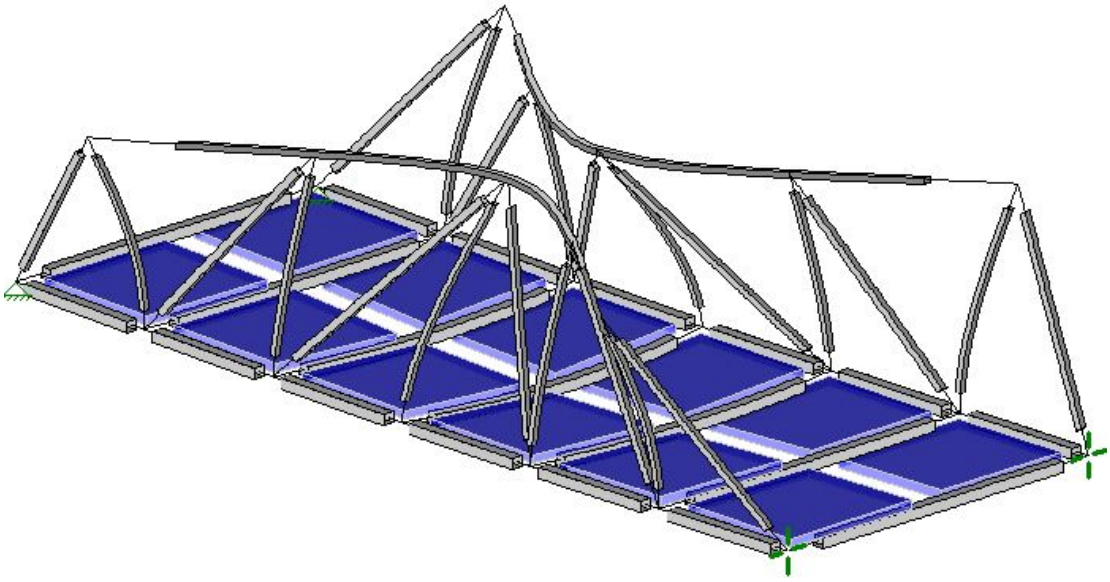

Figure 8.6 Deformed shape at critical load. Stiffer compression chord

Table 8.1Parametric Study of Analytical Models

Aspect Ratio (*AR*)	Top Chord Size	Stiffness Parameter (ξ)	Top chord Load Ratio P_{cr}/P_y
	2x1x1/8	**1989.83**	**2.39**
	2x2x1/8	**1440.26**	**1.74**
	2x2x1/4	**801.20**	**0.97**
0.10	3x3x1/4	**495.83**	**0.65**
	4x4x1/4	**359.00**	**0.63**
	5x5x1/4	**281.35**	**0.62**
	6x6x1/4	**230.88**	**0.60**
	2x1x1/8	**694.25**	**0.73**
	2x2x1/8	**502.51**	**0.61**
	2x2x1/4	**279.54**	**0.52**
0.15	3x3x1/4	**172.99**	**0.53**
	4x4x1/4	**125.25**	**0.55**
	5x5x1/4	**98.16**	**0.56**
	6x6x1/4	**80.55**	**0.54**
	2x1x1/8	**390.52**	**0.54**
	2x2x1/8	**282.66**	**0.54**
	2x2x1/4	**157.24**	**0.46**
0.20	3x3x1/4	**97.31**	**0.51**
	4x4x1/4	**70.46**	**0.51**
	5x5x1/4	**55.22**	**0.50**
	6x6x1/4	**45.31**	**0.49**

Experimental Study

Once the aspect ratio and stiffness parameters were selected from the analytical computer trials, such that buckling of the compression chord occurs before yielding, the next step was to define the member cross-section properties, for the 5.0 foot and 3.333 foot long pony truss bridges, that would result in the same parameters as those selected earlier. For reference purposes, the pony truss bridges were labeled *Bridge 1* and *Bridge 2*. *Bridge 1* refers to the smaller bridge, that is, the 3.333 foot long pony truss bridge, while *Bridge 2* refers to the bigger bridge, that is, the 5.0 foot long pony truss bridge. A description for each bridge will be presented below.

Following the selection of the cross-section properties of both pony truss bridges, an experimental study was developed and divided into two phases. The first phase consisted on modeling the pony truss bridges in the computer program in order to determine the critical load and load-deformation history. As mentioned earlier, these computer models were labeled *theoretical models*. The *theoretical models* are scaled down pony truss bridges that were modeled within the computer program to determine the critical load at which the bridge would fail due to instability of the compression chord.

The second phase consisted on fabricating two scaled pony truss bridges with the same cross-sections and properties as the *theoretical models* (i.e. physically represent the *theoretical models*) in order to validate, through load testing, the results from the *theoretical models*. These testing models were labeled *test models*.

Theoretical Models

The full-size analytical study provided the frame work for the development of the scaled models that eventually would be load tested for validation of the proposed methodology. Based on the test setup selected, which is described below, and with the purpose of having a baseline for comparison between the results of the load tests and the results of the computer analyses, two computer models were developed such that they would replicate all the properties and the loading condition at which the test models would be subjected to. The computer models, referred as to the *theoretical models*, were modeled in RISA-3D as close as practical possible, with consideration of common engineering practice in a design firm by practicing engineers, to simulate how the *test models* would be fabricated and load tested. A full description of each model, loading, inclusion of geometric imperfections and procedure, for the first phase (*theoretical models*), is presented below.

Bridge 1

The first model, shown in Figures 8.7, 8.8 and 8.9, consisted of a pony truss bridge of 3.33 feet in length and 8.0 inches in height. The trusses were set 12 inches apart, in other words, the width of the bridge was set to 12 inches. For this model, the aspect ratio, AR, and stiffness parameter, ξ, were determined to be 0.20 and 97 respectively. The pony truss bridge was modeled with four panels spaced at 10 inches apart. The top two chords, as well as the vertical and diagonal elements of the truss, were modeled as square tube sections of 0.5 in x 0.5 in x 1/6 in. The bottom chords,

as well as the transverse beams that form the transverse frames (U-frame), were modeled as square tube sections of 1 in x 1 in x 1/6 in. The floor slab was modeled as a 0.75 inch thick shell element with a modulus of elasticity, E, of 1,000 ksi and fully composite with the floor beams to simulate the wood plank that will be used in the test models. The vertical elements were modeled as pin-ended at the connection with the top chord and fix-ended at the connection with the bottom chord. On the other hand, the diagonal elements were modeled as pin connected at both ends.

Bridge 2

The second model, shown in Figures 8.10, 8.11 and 8.12, consisted of a pony truss bridge of 5.0 feet in length and 12.0 inches in height. The width of the deck was set to 12 inches. For this model, the aspect ratio, AR, and stiffness parameter, ξ, were determined to be 0.20 and 63 respectively. The pony truss bridge was modeled with six panels spaced at 10 inches apart. The top two chords, as well as the vertical and diagonal elements of the truss, were modeled as square tube sections of 0.5 in x 0.5 in x 1/6 in. The bottom chords, as well as the transverse beams that form the transverse frames (U-frame), were modeled as square tube sections of 1 in x 1 in x 1/6 in. The floor slab was modeled as a 0.75 inch thick shell element with a modulus of elasticity, E, of 1,000 ksi and fully composite with the floor beams to simulate the wood plank that will be used in the test models. Similar to *Bridge 1*, the vertical elements were modeled as pin-ended at the top chord and fix-ended at the bottom chord, and the diagonal elements were modeled as pin connected at both ends.

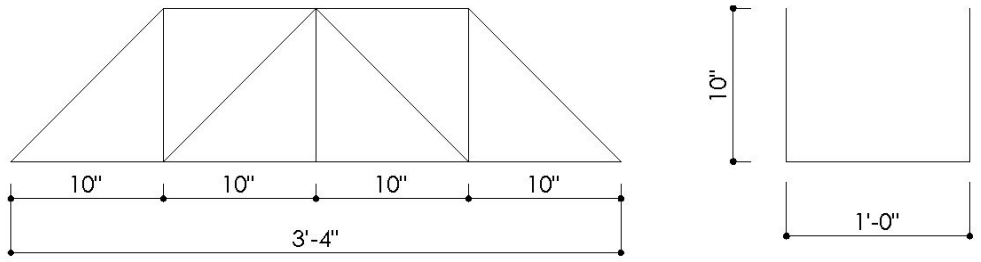

Figure 8.7 *Bridge 1* truss geometry

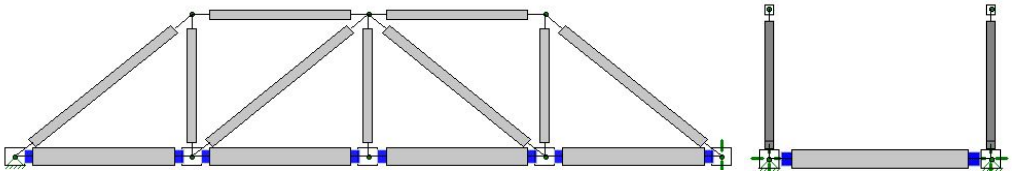

Figure 8.8 *Bridge 1* computer model of truss

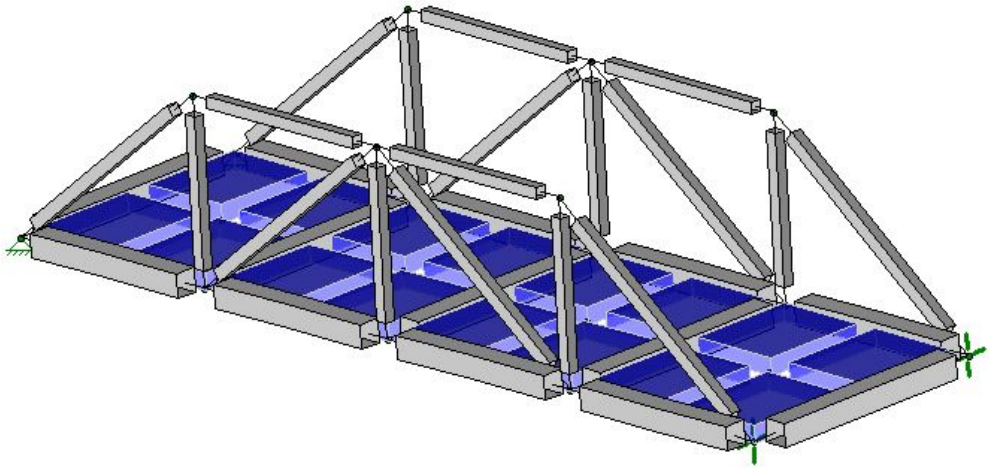

Figure 8.9 3D Model of *Bridge 1*

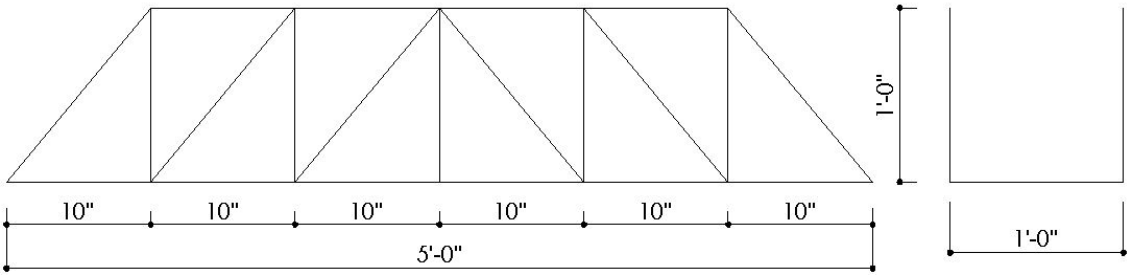

Figure 8.10 *Bridge 2* truss geometry

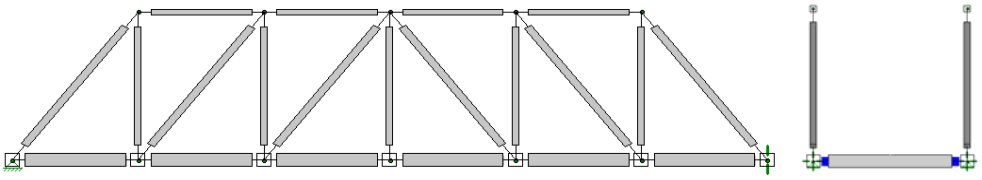

Figure 8.11 *Bridge 2* computer model of truss

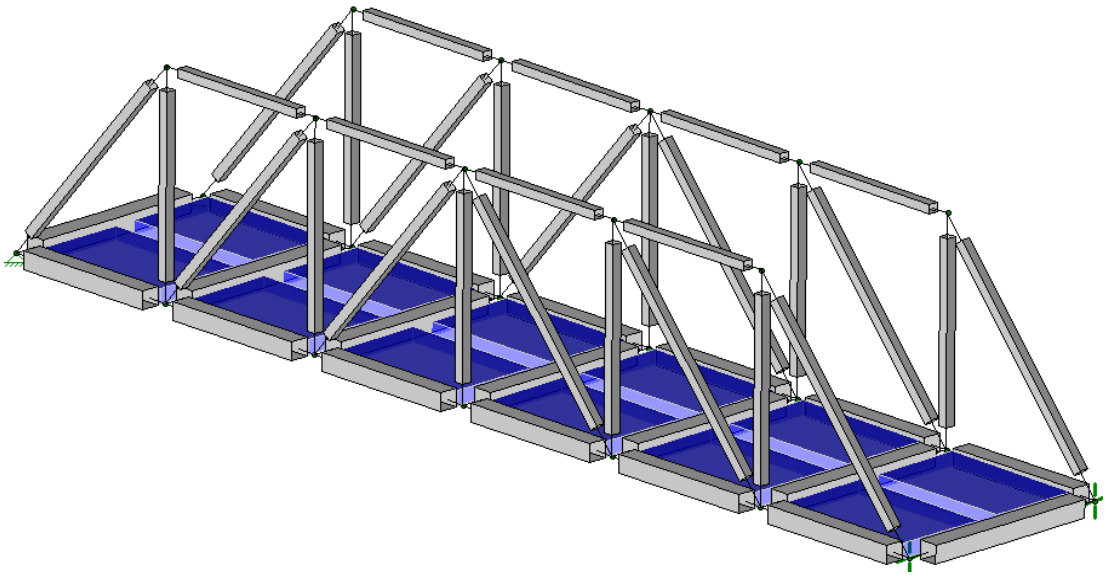

Figure 8.12 3D model of *Bridge 2*

Loading

It was anticipated that the *test models* would be loaded using a hydraulic jack and a reaction frame, shown in Figure 8.13. Furthermore, a spreader beam and two spreader plates would be used to distribute the load onto the two middle panels adjacent to the bridge center line. Thus, in order to simulate this loading condition, the *theoretical models* were loaded with a uniform distributed load on the two panels adjacent to the center line of the bridge, shown in Figures 8.14 and 8.15. An initial uniform distributed area load of 60 psf was selected. The gravity load was increased by changing the load factor in the load combinations tab of the computer software, as described in Chapter VI.

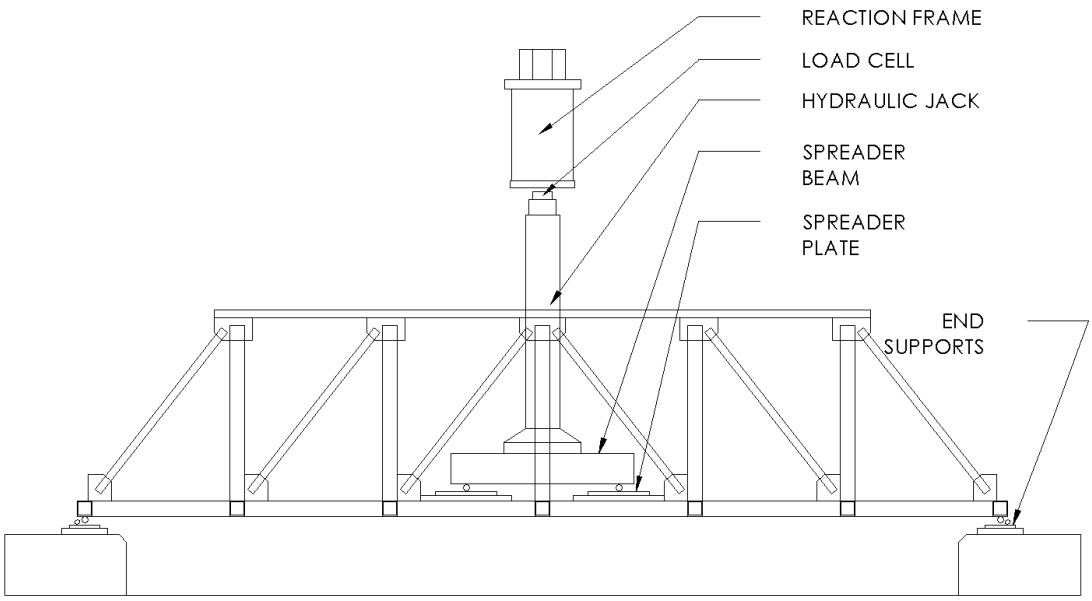

Figure 8.13 Load test setup diagram

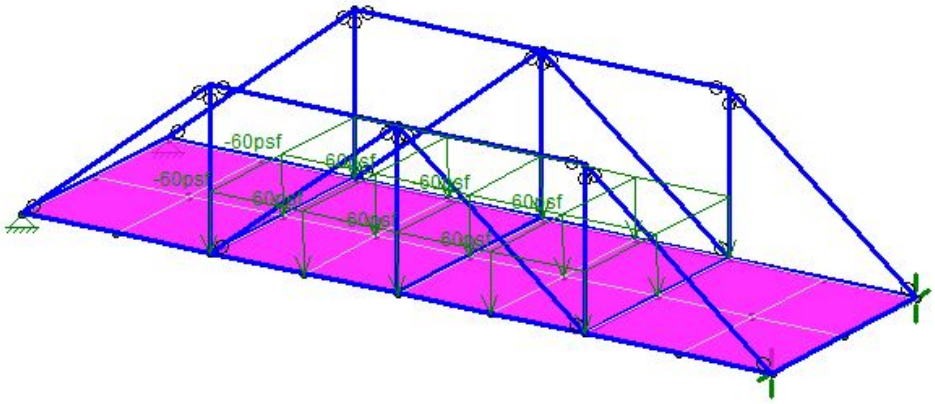

Figure 8.14 *Bridge 1* computer model loading configuration

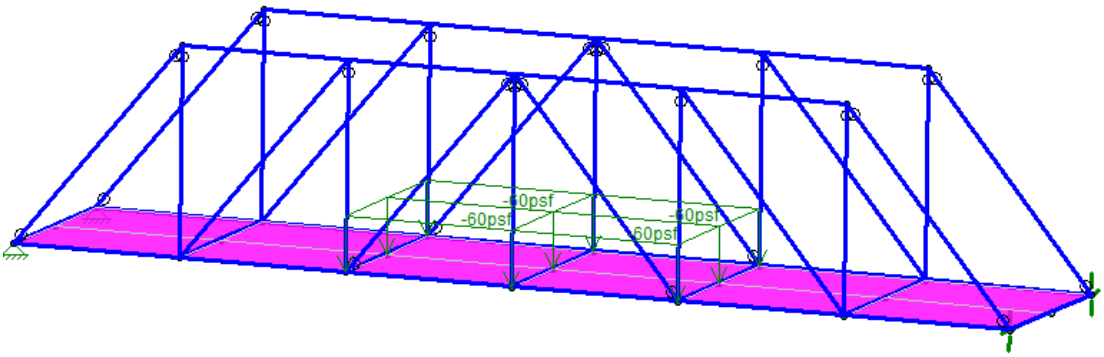

Figure 8.15 *Bridge 2*, computer model loading configuration

Geometric Imperfections

Three different geometric imperfections were incorporated into the computer model study. These three imperfections were modeled as initial imperfections of the top chord (out of plane) of, *L*/300, *L*/450 and *L*/700. As described in Chapter VI the geometric imperfections can be modeled by adding notional loads to the structure or

by physically modeling the compression chord in a deformed shape. For this study the initial imperfections were modeled in both ways, by adding notional loads to the top chord, as shown in Figure 8.16, and by displacing the chord nodes to a determined distance that would simulate such imperfection.

Procedure

The procedure used to determine the critical load and the load-deformation history of *Bridge 1* and *Bridge 2*, follows the same procedure presented in Chapter VI. The investigation included *P-Δ* only, that is, without stiffness reduction as described in AISC 360-10 (AISC 2010). In addition to determining the load-displacement history, the results from the *theoretical models*, confirmed that the critical load of the top chords was less than the yield strength of the chord and the total gravity load on the bridge was below the capacity of the hydraulic jack and load cell. The results from the *theoretical models* are presented in Chapter IX.

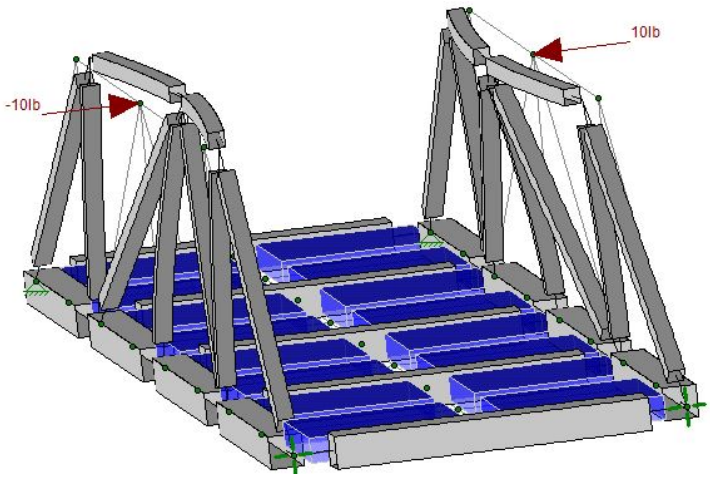

Figure 8.16 Modeling of geometric imperfections

Test Models

As mentioned earlier, the goal of the *test models* was validate the results obtained from the *theoretical models*, thus, the *test models* were built with the same dimensions, member cross-sections and material properties as the *theoretical models*. Figures 8.17 and 8.18 show the computer model and the actual test model respectively for *Bridge 1*. Figures 8.19 and 8.20 show the computer model and the actual test model respectively for *Bridge 2*. The truss members were connected with welded connections. Plans are presented in Appendix 1.

Prior to fabrication of the *test models*, a welding procedure specification, WPS, was developed and qualified, in accordance with AWS D1.1 (AWS 2002), in order to verify the quality of the welds. The connections that were modeled as fixed, within the computer program, were fabricated as "all-around" welded connections with a weld size of 3/16 in. The weld capacity was checked to ensure that the connection developed the full moment capacity of the member. On the other hand, for connections that were modeled as pinned connections, they were fabricated with gusset plates, so that rotation can occur without developing significant moment capacity. The gusset plate used was 1/8 in thick and the weld size used was 3/16 in. The length of the welds was checked to verify that it could develop the axial capacity of the members. The gusset plate geometry was developed based on the minimum weld length.

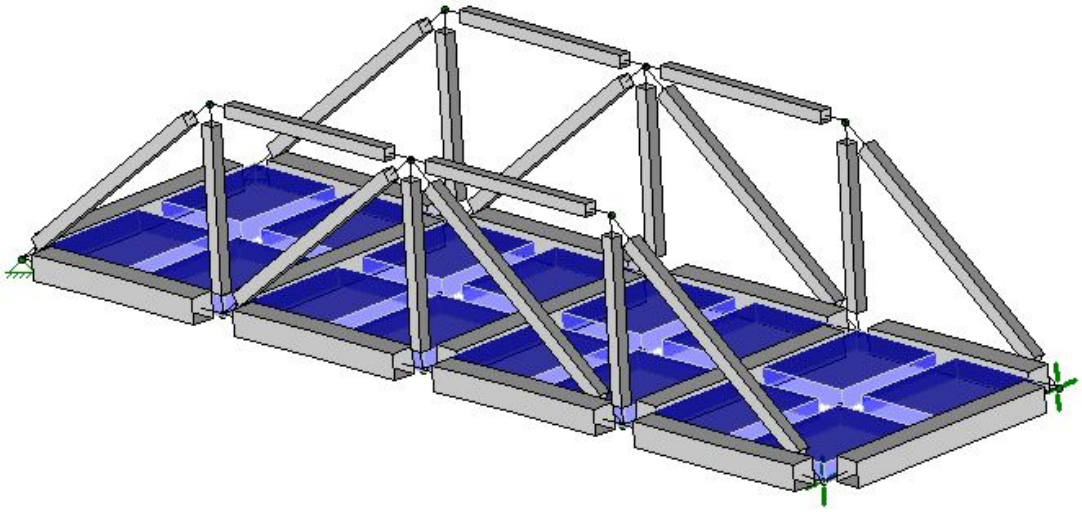

Figure 8.17 *Bridge 1* Computer Model

Figure 8.18 *Bridge 1* Test model

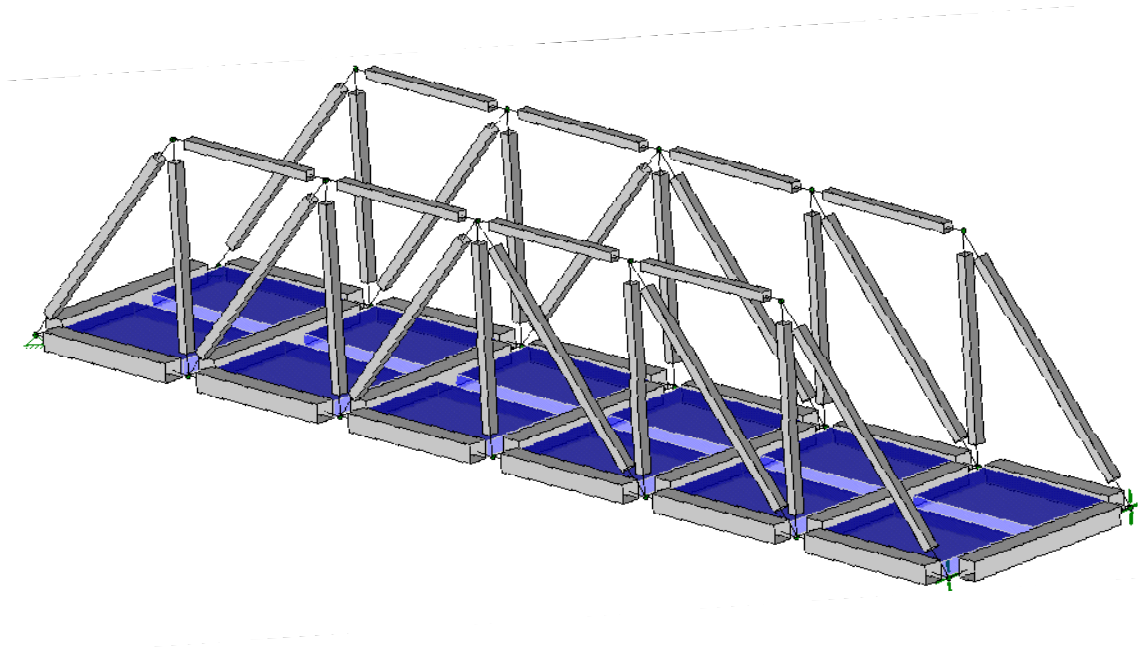

Figure 8.19 *Bridge 2* Computer Model

Figure 8.20 *Bridge 2* Test Model

Test Setup

A diagram of the test setup and the actual setup are shown in Figures 8.21 and 8.22 respectively. The load test setup was designed such that a hydraulic jack, shown in Figure 8.22, would load the bridge by applying a thrust force when the jack pushed against a reaction frame. The reaction frame was built with a header beam (HSS steel tube section 6in x 4 in x 3/8 in) held down at the ends by two 1-½ in dia. tiedown rods attached to the concrete reaction floor. The hydraulic jack, was supported on a transfer beam consisting on four 1 in x 1 in x 1/6 in steel tube section welded together to a ¼ in x 4 in flat plate, shown in Figure 8.23.

The load from the hydraulic jack was then transferred from the transfer beam onto two spreader plates. Each spreader plate consisted of a ½ in dia. solid steel bar welded to a ¼ in x 4 in flat plate shown in Figure 8.23. The purpose of the solid steel bar was to maintain the same load distribution to the bridge deck at all times, even when the bridge deflected downwards. Attached to each spreader plate was 3/8 in neoprene pad, that distributed the load onto the deck, thus simulating the uniform distributed load assumed in the *theoretical models*. The bridge end supports were designed and built so that the bridge would deflect downwards without any horizontal restraint along the center line of the bridge. This was accomplished by welding a ½ in dia. solid bar at each corner of the bridge, and then bearing on ¼ in steel plate attached to each abutment. The abutments were built with concrete-filled CMU blocks resting on a ½ in neoprene pad to distribute the load evenly onto the floor.

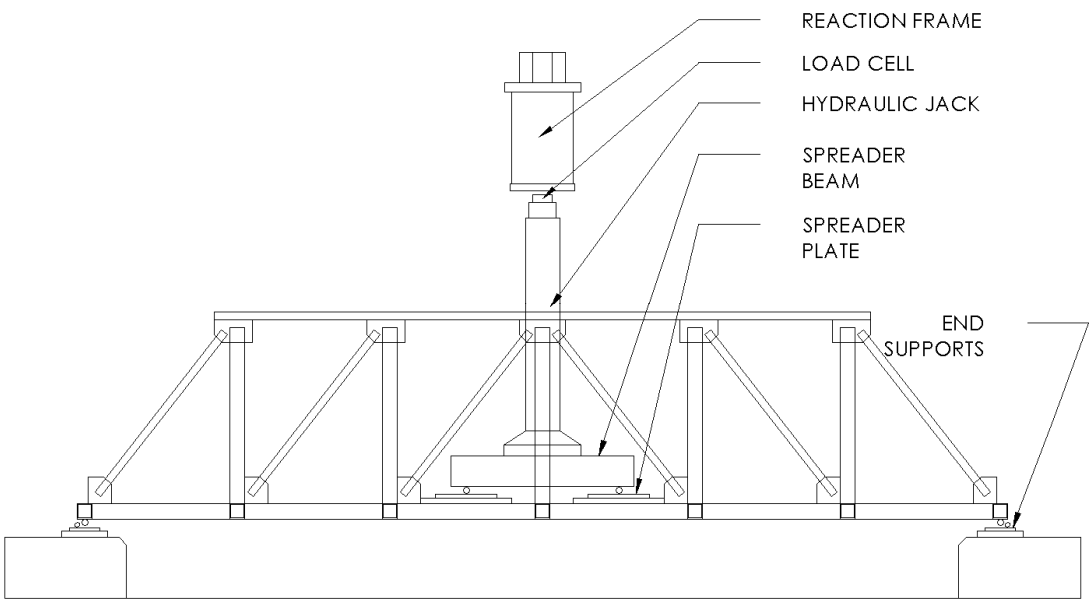

Figure 8.21 Load test setup diagram

Figure 8.22 Load test setup

Figure 8.23 Spreader beam and plates used to uniformly distribute the load on the bridge deck

Figure 8.24 Typical end support configuration and abutments

The load on the bridge was recorded by using a low-profile load cell and a meter, shown in Figures 8.25 and 8.26. The load cell was set between the hydraulic

jack and the reaction frame which was fitted with a smooth plate to distribute evenly the load across the load cell and prevent punching deformation of the tube wall. At each load interval, the load on the bridge was read directly from the meter. The working (allowable) capacity of the load cell and hydraulic jack were 25,000 lbs and 20,000 lbs respectively.

In order to measure the displacement of the compression chord as it deforms during the load test, three dial indicators were placed along each top chord, for a total of six. The dial indicators placement is shown in Figure 8.26, where it can be seen that the indicators were placed at each end of the top chords and at the center. In addition, the dial indicators, with a total displacement of 2 inches, were placed half way so that the displacement of the compression chord can be measured regardless of which way it displaced.

Figure 8.25 Load cell

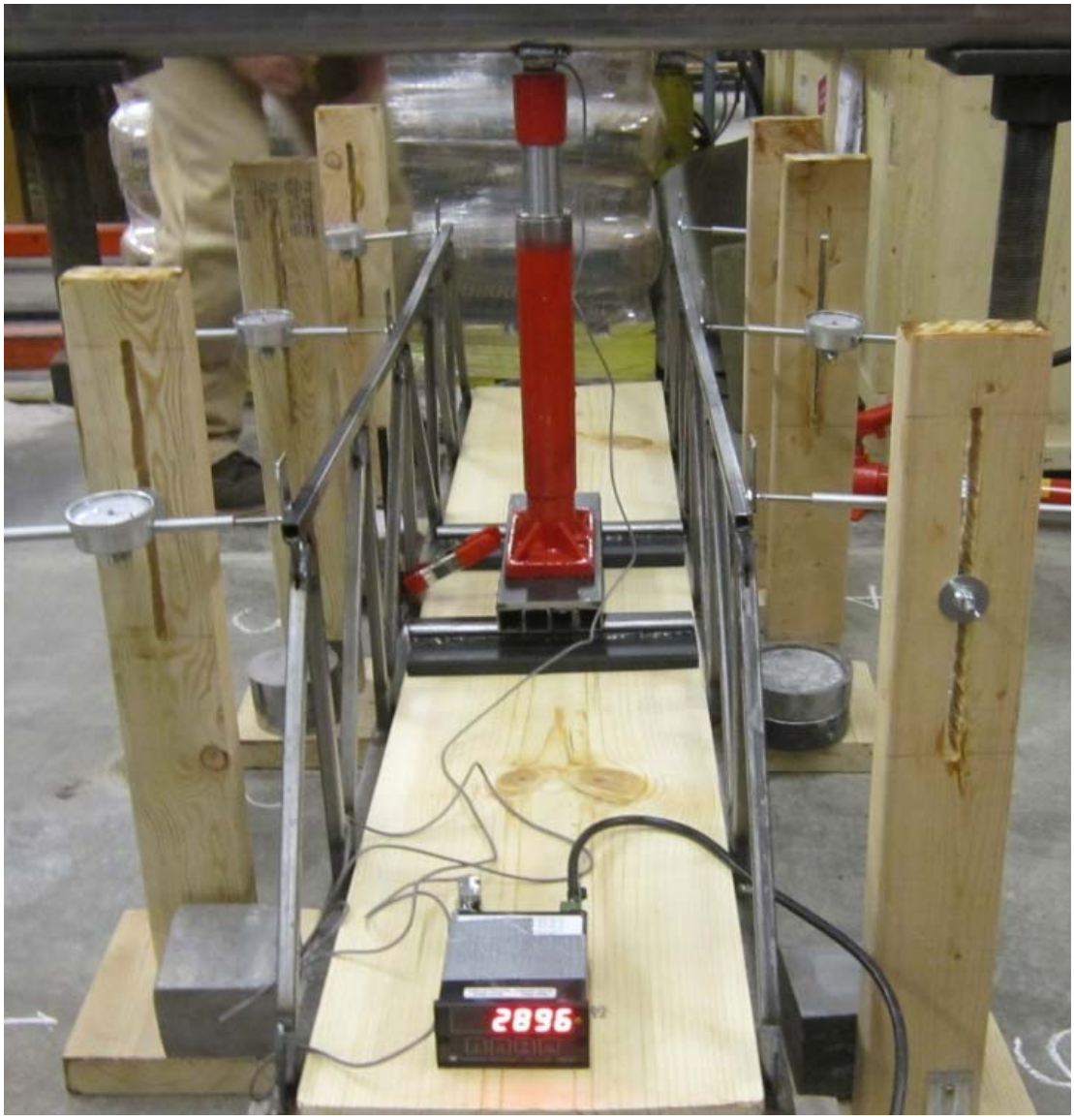

Figure 8.26 Data collection setup

Load Testing Procedure

The load testing procedure consisted on loading the bridge in 1,000 lbs increments, by manually pumping the hydraulic jack. When the target load was reached, the load test was stopped and the measurements from all instruments were

taken. The recordings included: load reading from the load cell meter, out of plane displacement of the truss at the end of each compression chord and out of plane displacement at the center of each compression chord from the dial indicators. Loading continued until each bridge was not able to maintain the load without excessive deformation of the top chords.

Figure 8.27 Test setup top view

CHAPTER IX

EXPERIMENTAL RESULTS

A discussion of the different experiments, the load testing setup and loading sequence was presented earlier in Chapter VIII, where it was mentioned that the *theoretical modes* were analyzed with three different initial imperfections, namely Δ_o: *L*/300, *L*/450 and *L/*700. In addition, two different approaches for modeling the initial imperfection were used. To facilitate the presentation of results in this chapter, the two approaches were labeled: Notional Load (NL) and Direct Modeling (DM); a description of these two approaches was presented in Chapter VI.

With the purpose of tracking the load-displacement history for both top chords of each bridge, the naming convention shown in Figures 9.1 and 9.2 was adopted. Prior to loading the bridges, the top chords of each bridge were measured for out of plane straightness (i.e. to determine the initial out of plane imperfection), illustrated in Figure 9.3. It was determined that the measured initial imperfection, Δ_o, for Chord 1 (C1) and Chord 2 (C2) of *Bridge 1* were 0.042 inches or *L/*475 and 0.050 inches or *L*/400, respectively. The measured initial imperfection, Δ_o, for Chord 1 (C1) and Chord 2 (C2) of *Bridge 2* were 0.090 inches or *L*/445 and 0.105 inches or *L*/377, respectively. These results are shown in Table 9.1. The results for *Bridge 1* are presented below followed by the results of *Bridge 2*. For reference purposes, the critical load of the theoretical models is defined as the load immediately obtained at the termination of the convergence to a solution of the *P-Δ* feature.

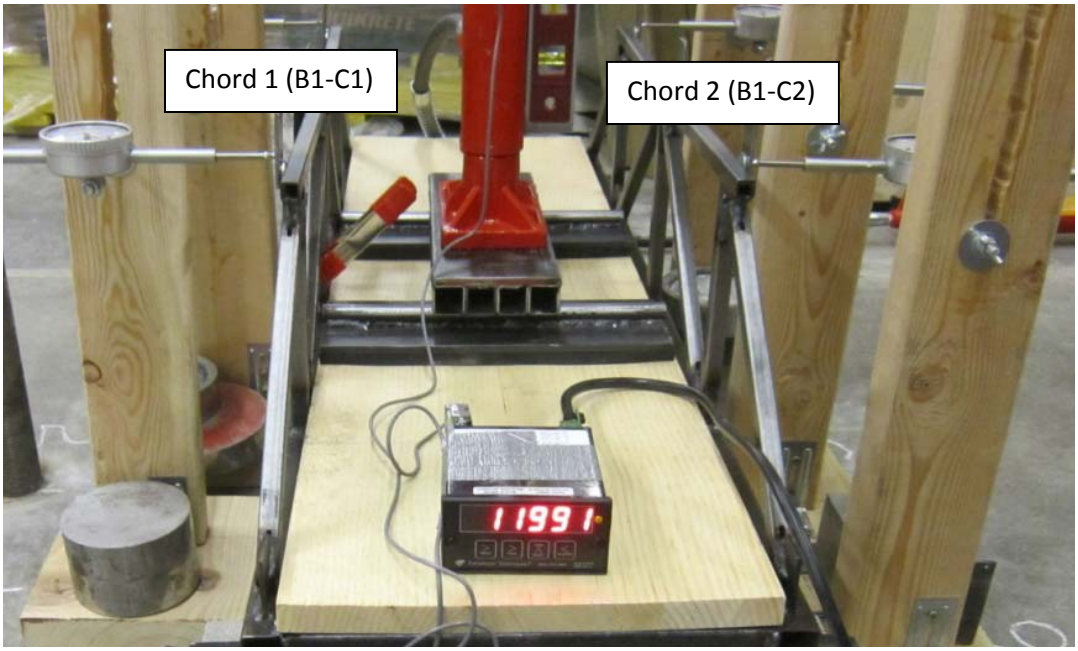

Figure 9.1 *Bridge 1* Naming convention for top chords

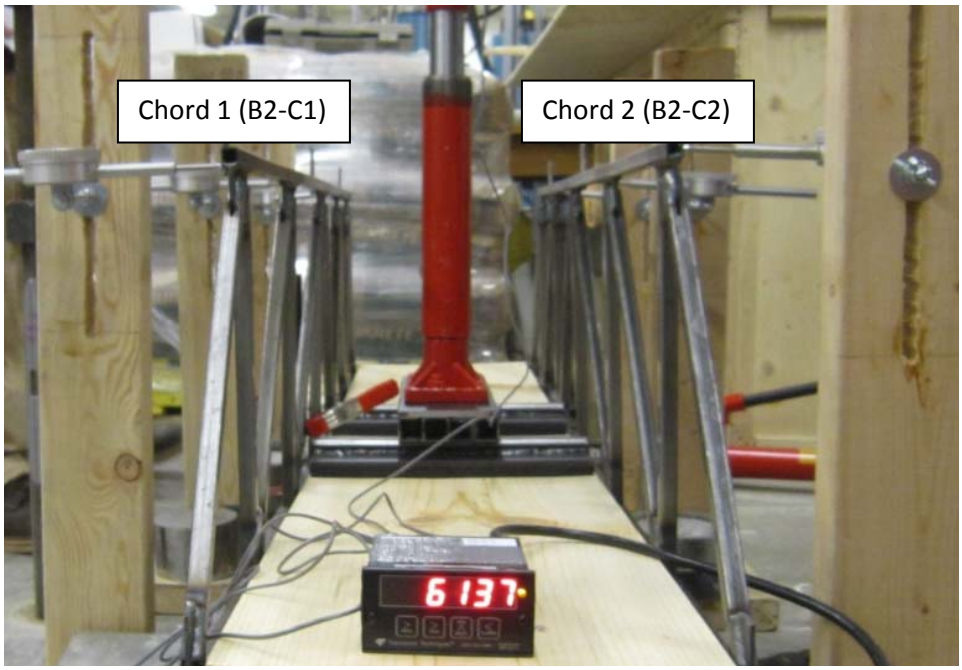

Figure 9.2 *Bridge 2* Naming convention for the top chords

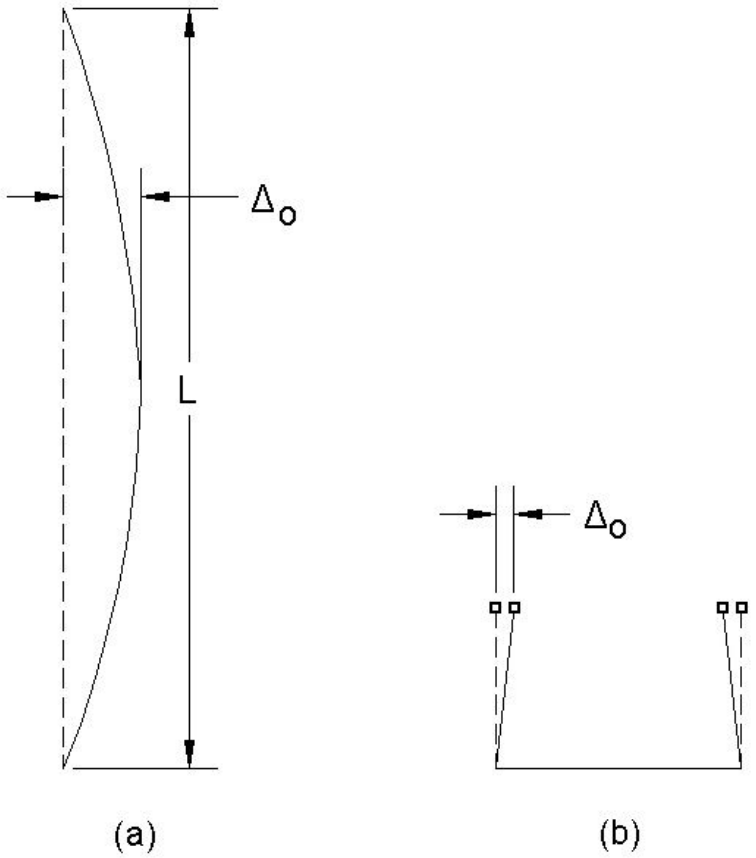

Figure 9.3 Top chord initial imperfection, Δ_o (a) Top view of compression chord (b) Cross-section view

Table 9.1 Measured initial imperfections, Δ_o, of top chords

Bridge	Chord 1 (C1) (in)	Chord 2 (C2) (in)
Bridge 1	0.042 (*L*/475)	0.050 (*L*/400)
Bridge 2	0.090 (*L*/445)	0.106 (*L*/377)

Bridge 1 Results

Theoretical Results

The *theoretical models* were analyzed in accordance with the proposed method described in Chapter VI, and the results are compared in Table 9.2 and plotted in Figure 9.4. These results are presented as the ratio of the second-order displacement, to the initial imperfection (Δ/Δ_o), of the top cord, for a corresponding gravity load. The critical loads for the theoretical models are summarized in Table 9.3.

From the results presented in Table 9.2, it can be seen that there is good correlation between the results from the notional load (NL) approach and the direct modeling (DM) approach. For example, at a load of 3,000 lb, and for an initial imperfection of *L*/300, the top chord amplifications were 1.515 and 1.530 for the notional load and the modeled imperfection methods respectively, compared to amplifications of 1.738 and 1.714 when an initial imperfection of *L*/450 is applied to the top chord. And for *L*/700, the top chord amplifications were 2.000 and 2.000 for the notional load (NL) and the direct modeling (DM) approach respectively. At 6,000 lbs the top chord amplifications were 2.439 (NL) and 2.439 (DM) for *L*/300, 2.929 (NL) and 2.881 (DM) for L/450 and 3.536 and 3.500 (DM) for *L*/700. At 8,000 lbs the top chord amplifications were 4.333 (NL) and 4.561 (DM) for *L*/300, 5.262 (NL) and 5.095 (DM) for *L*/450 and 6.214 and 6.179 (DM) for *L*/700.

The maximum difference in amplification values between the notional load approach and the modeled imperfection approach correspond to 5%, and occur when the applied load reached 8,000 lbs and for a initial imperfection of $L/300$. For the remaining applied load levels the difference is less than 3%.

Similarly, the critical loads correlate well between approaches. The maximum difference between methods was 1.97% and corresponds to an imperfection of $L/300$. However, for the other two initial imperfection analysis, the difference was less than 1%. Based on these results, the critical load of *Bridge 1* is expected to be approximately 9,400 lbs.

Figure 9.4 provides a good representation of the load-deformation history of the top chord and the destabilizing effects of P-Δ. For example, at load levels up to and less than 74% of the critical load, the structure remains reasonably stable, this correlates to a load of approximately 7,000 lbs. However, beyond this point, and as shown in Figure 9.4, it can be seen that significant instability starts to take place. At load levels of about 83% of the critical load, approximately 8,000 lbs, the secondary effects due to P-Δ lead to large amplifications of the top chord out-of-plane deflection, demonstrating that significant instability occurs when the applied load approaches the critical load.

Table 9.2 *Bridge 1* Theoretical Results: Top chord ratio Δ/Δ_o

Load (lbs)	NL	DM	NL	DM	NL	DM
	$\Delta_o = L/300$		$\Delta_o = L/450$		$\Delta_o = L/700$	
0	1.0	1.0	1.0	1.0	1.0	1.0
1000	1.152	1.152	1.214	1.214	1.321	1.321
2000	1.318	1.333	1.452	1.452	1.643	1.643
3000	1.515	1.530	1.738	1.714	2.000	2.000
4000	1.742	1.758	2.048	2.024	2.393	2.393
5000	2.030	2.045	2.429	2.405	2.893	2.857
6000	2.439	2.439	2.929	2.881	3.536	3.500
7000	3.061	3.076	3.690	3.643	4.464	4.429
8000	4.333	4.561	5.262	5.095	6.214	6.179
9000	11.258	10.924	12.786	12.524	14.643	14.571

NL=Notional load DM=Direct Modeling

Table 9.3 *Bridge 1* Theoretical Results: Critical load

Critical Load (lbs)	NL	DM	NL	DM	NL	DM
	$\Delta_o = L/300$		$\Delta_o = L/450$		$\Delta_o = L/700$	
	9365	9550	9422	9500	9460	9500

NL=Notional load DM=Direct Modeling

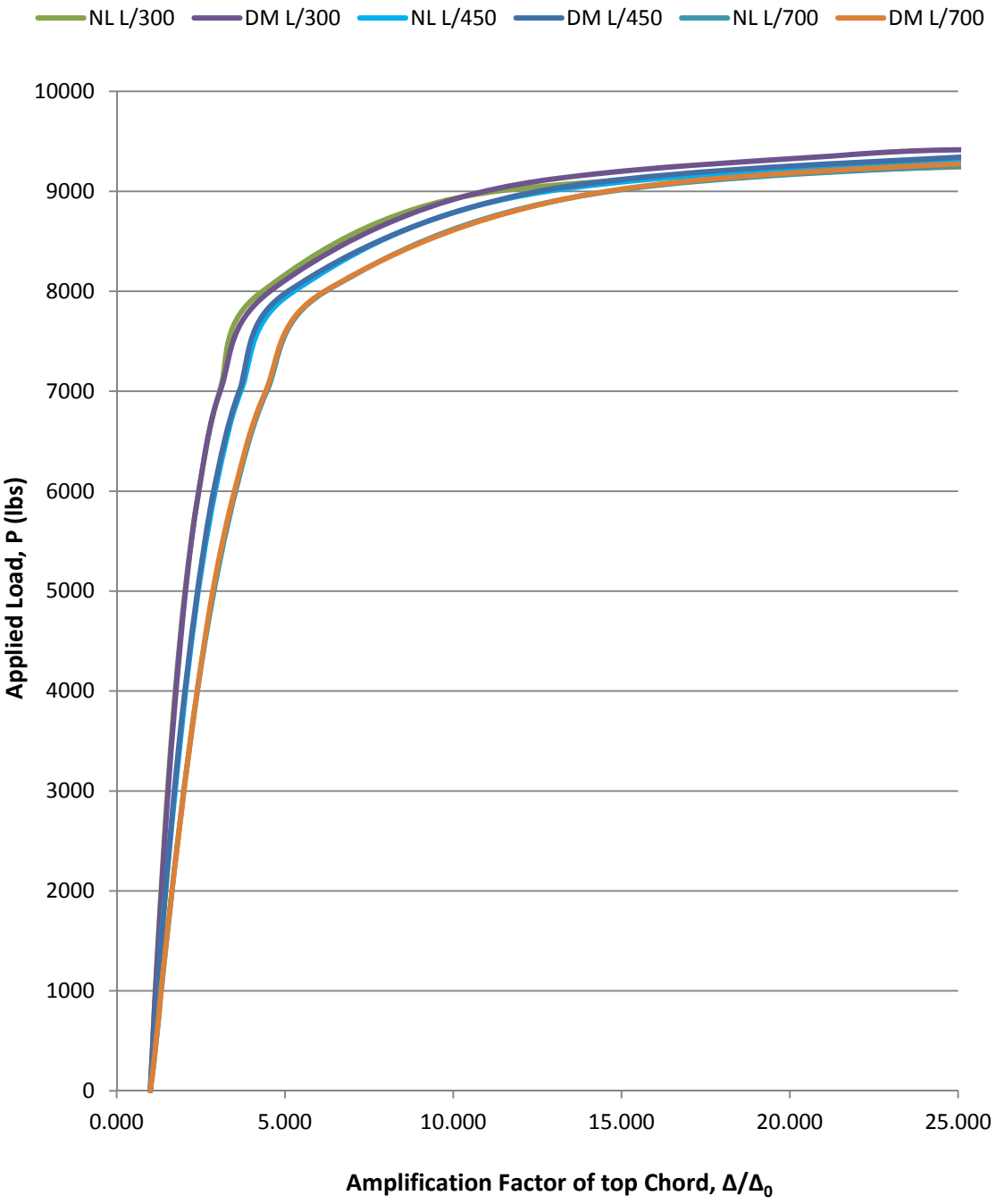

NL = Notional Load DM = Direct Modeling

Figure 9.4 *Bridge 1* Theoretical results

Load Test Results

The *test model* for *Bridge 1* was load tested in accordance with the procedure presented in Chapter VIII. As mentioned above, the expected critical load for *Bridge 1* was calculated to be approximately 9,400 lbs. The results from the *test model* for both top chords (C1 and C2) are presented in Table 9.4. These results are compared to the theoretical results that were obtained by using the notional load (NL) approach only. The results presented in Table 9.4 are also plotted in Figure 9.5. It can be observed from table 9.4 that up to a load level of 6,000 lbs, the ratios Δ/Δ_o for both, the theoretical models and the test models, correlate well. It is, however, from that point and for higher load levels that the results do not correlate well. This is due to the fact that the *test model* exhibited significant deformation capacity. At about the critical load of the *theoretical models,* the Δ/Δ_o ratio for the *test model* was less than 4.0, and it wasn't until a load level of 16,000 lbs, that the *test model* showed significant loss of stiffness. The critical loads are presented in Table 9.5 where it can be seen that the actual critical load from the *test model*, 18,200 lbs, was almost twice as much as the *theoretical model*.

From the deformed shape, shown in Figure 9.6, it was concluded that the joint connections at the diagonals were considerably stiff, hence, increasing the lateral stiffness of the top chord. Thus, by modeling the ends of the diagonals as pin-pin connections the computer model underestimated the additional stiffening effects of the connection. Therefore, re-modeling the theoretical model with diagonals with

partially fixed-ends would be more appropriate. However, for simplicity, it was decided to re-model and re-run the *Bridge 1 theoretical model* with fix-ended diagonals and using the notional load approach only. The first attempt at re-running the theoretical model yielded a critical load of 21,000 lbs, significantly higher that the test model. In addition, a review of the member's forces results from the computer program revealed that the axial load in the end diagonals had exceeded the yield strength of the members. Therefore, from the deformed shape at failure, Figure 9.6, which shows the end-diagonals buckling first, and the fact that the program calculates second-order effects at nodes only, it was decided to add an additional node at the midpoint of each end-diagonal and re-run the model for a second time.

This change proved to correlate better with the *test model* as it is shown by the chord amplification-factor results presented in Table 9.6. At the same time, the critical load of the *theoretical model* turned out to be very close to the critical load of the *test model* as seen in Table 9.7, this difference correlates to only 9%. The results of Table 9.6 are plotted in Figure 9.7 where it can be seen that the *theoretical model* and the *test model* correlate well. As with previous results, considerable destabilization starts to occur at loads higher than 80% of the critical load. Figures 9.8 through 9.11 show the sequence of the failure mode of one of the end-diagonals, for both, the *theoretical model* and the t*est model*, where it can be seen that there was significant deformation of the end-diagonal before buckling. In addition, one can observe that the deformed shapes are consistent between both models.

Table 9.4 *Bridge 1* Theoretical and Load Test Results: Top chord ratio Δ / Δ_o

Load (lbs)	NL *L*/300	NL *L*/450	NL *L*/700	B1-C1 *L*/475	B1-C2 *L*/400
0	1.000	1.000	1.000	1.000	1.000
1000	1.152	1.214	1.321	1.238	1.357
2000	1.318	1.452	1.643	1.357	1.607
3000	1.515	1.738	2.000	1.714	1.952
4000	1.742	2.048	2.393	1.952	2.190
5000	2.030	2.429	2.893	2.143	2.500
6000	2.439	2.929	3.536	2.310	2.667
7000	3.061	3.690	4.464	2.571	3.024
8000	4.333	5.262	6.214	2.810	3.381
9000	11.258	12.786	14.643	3.143	3.857
10000	N/A	N/A	N/A	3.500	4.238
11000	N/A	N/A	N/A	3.976	4.643
12000	N/A	N/A	N/A	4.452	4.976
13000	N/A	N/A	N/A	5.024	5.381
14000	N/A	N/A	N/A	5.167	6.000
15000	N/A	N/A	N/A	5.762	6.476
16000	N/A	N/A	N/A	6.476	6.976
17000	N/A	N/A	N/A	7.714	7.905
18000	N/A	N/A	N/A	9.619	10.048

NL=Notional Load

Table 9.5 *Bridge 1* Theoretical and Load Test Results: Critical load

	NL *L*/300	NL *L*/450	NL *L*/700	B1-C1 *L*/475	B1-C2 *L*/400
Critical Load (lbs)	9365	9422	9460	18200	18200

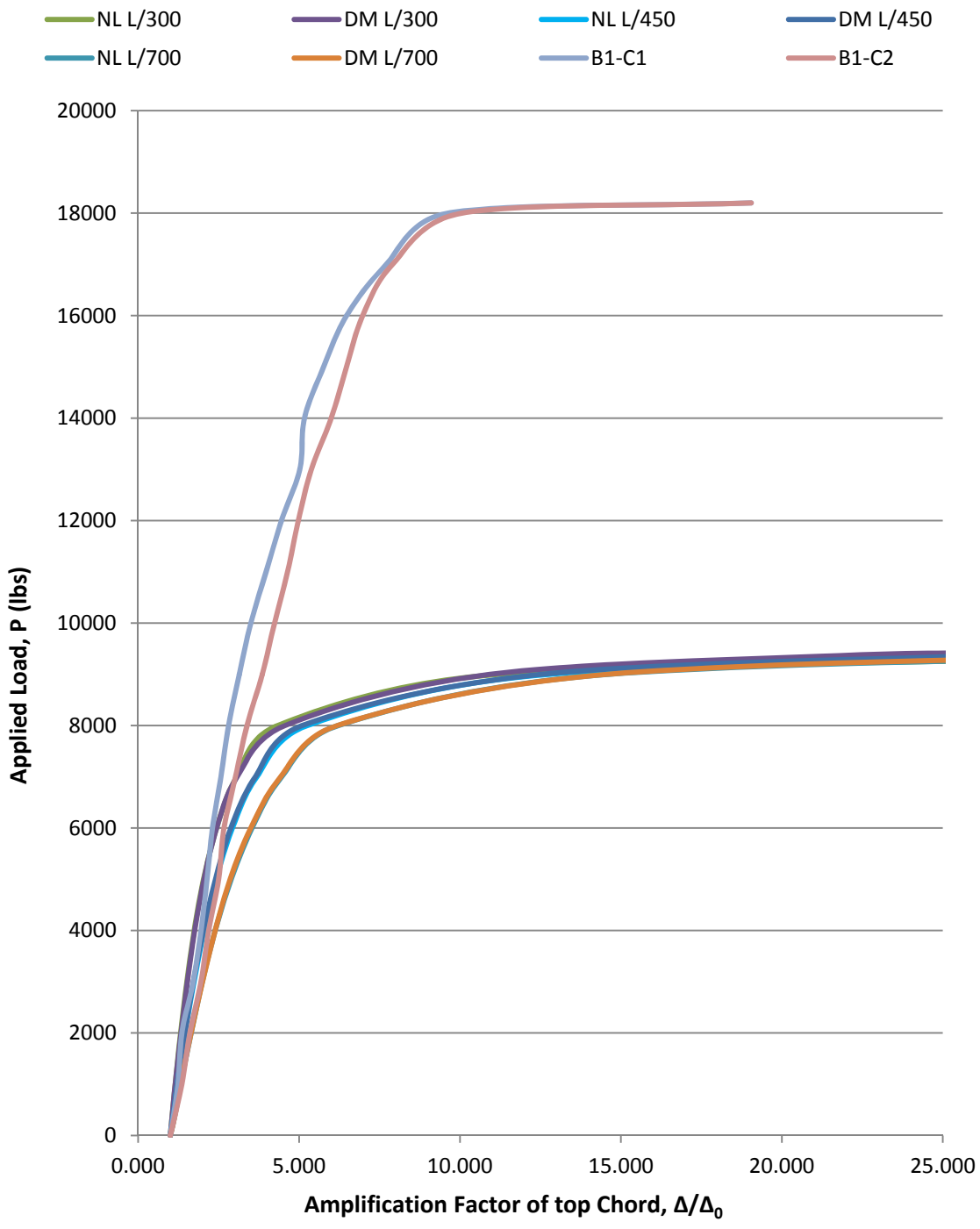

NL = Notional Load DM = Direct Modeling

Figure 9.5 *Bridge 1* Theoretical (pin-ended diagonals) and load test results

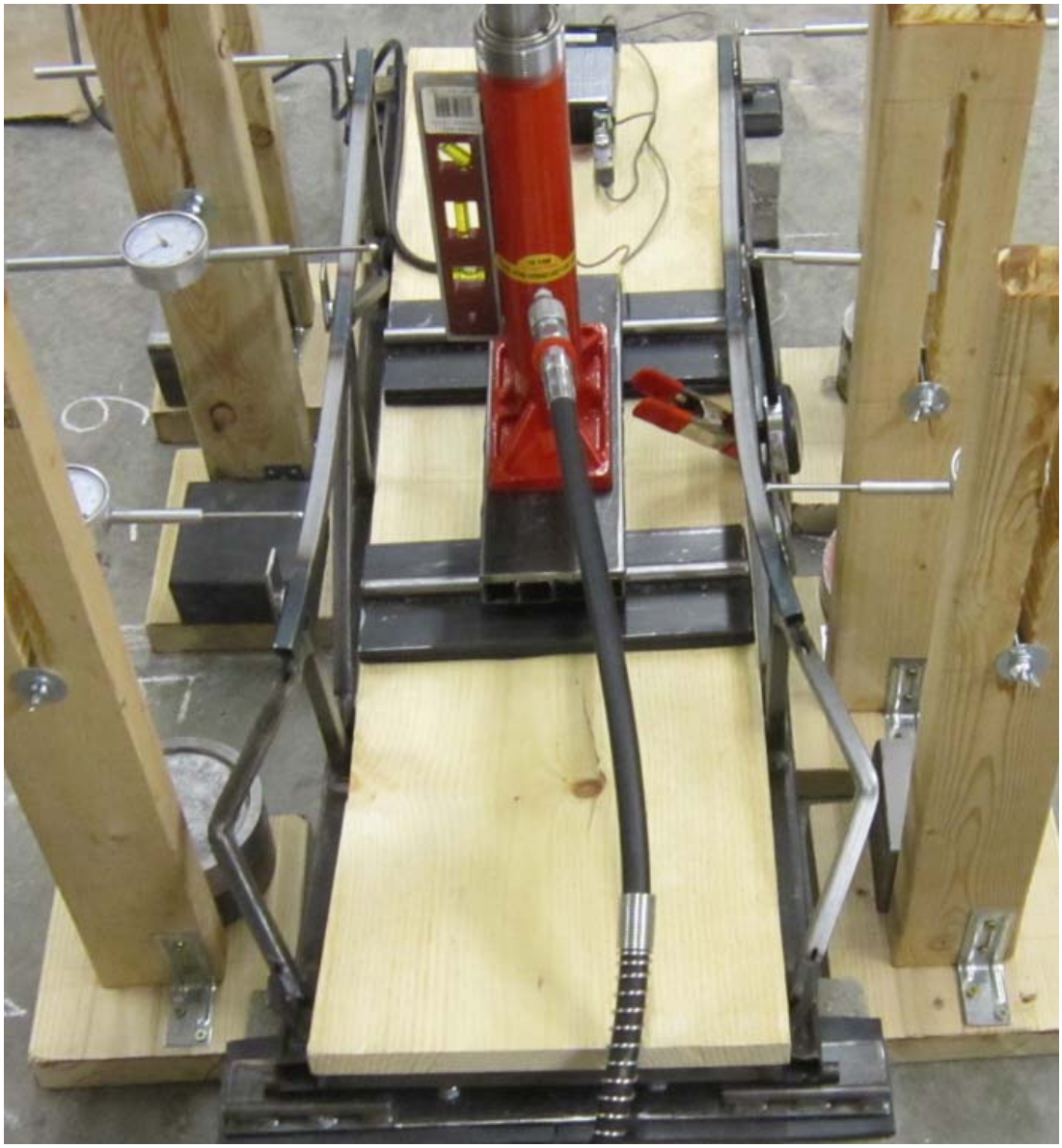

Figure 9.6 *Bridge 1* Deformed shape at failure

Table 9.6 *Bridge 1* Ratio Δ/Δ_o, theoretical results with fix-ended diagonals

Load (lbs)	NL *L*/300	NL *L*/450	NL *L*/700	B1-C1 *L*/475	B1-C2 *L*/400
0	1.000	1.000	1.000	1.000	1.000
1000	1.106	1.167	1.250	1.238	1.357
2000	1.227	1.333	1.500	1.357	1.607
3000	1.348	1.500	1.714	1.714	1.952
4000	1.470	1.690	2.000	1.952	2.190
5000	1.591	1.881	2.250	2.143	2.500
6000	1.742	2.071	2.536	2.310	2.667
7000	1.879	2.286	2.821	2.571	3.024
8000	2.045	2.500	3.143	2.810	3.381
9000	2.212	2.762	3.500	3.143	3.857
10000	2.409	3.024	3.857	3.500	4.238
11000	2.636	3.310	4.286	3.976	4.643
12000	2.879	3.667	4.750	4.452	4.976
13000	3.182	4.071	5.286	5.024	5.381
14000	3.530	4.548	5.929	5.167	6.000
15000	3.985	5.143	6.750	5.762	6.476
16000	4.576	5.929	7.786	6.476	6.976
17000	5.409	7.024	9.250	7.714	7.905
18000	6.773	8.905	11.536	9.619	10.048

NL=Notional Load

Table 9.7 *Bridge 1* Critical load, theoretical results with fix-ended diagonals

Critical Load (lbs)	NL *L*/300	NL *L*/450	NL *L*/700	B1-C1 *L*/475	B1-C2 *L*/400
	19850	19820	19840	18200	18200

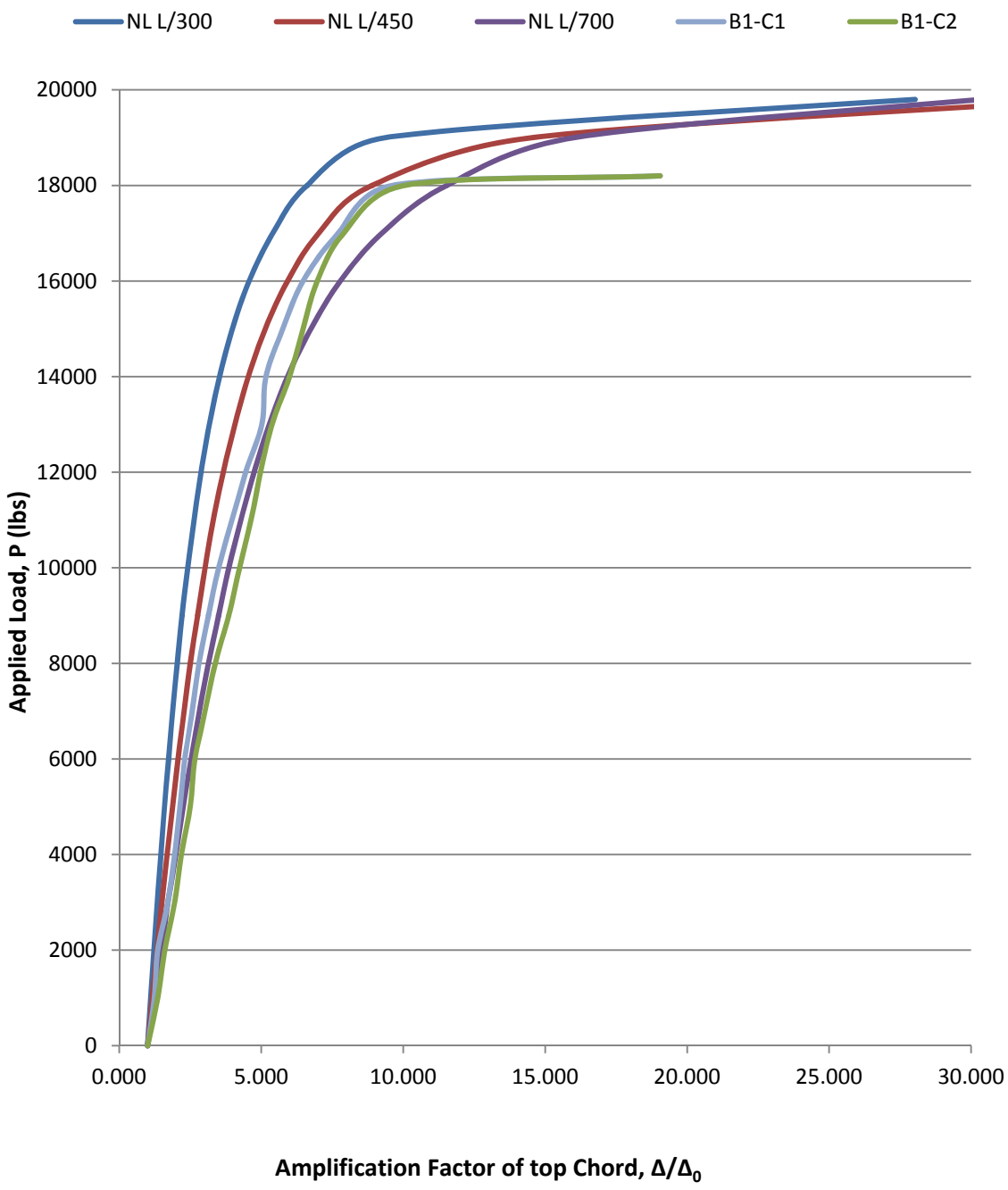

NL = Notional Load

Figure 9.7 *Bridge 1* Theoretical (fix-ended diagonals) and load test results

Figure 9.8 *Bridge 1* Deformation of end-diagonal prior to buckling (test model)

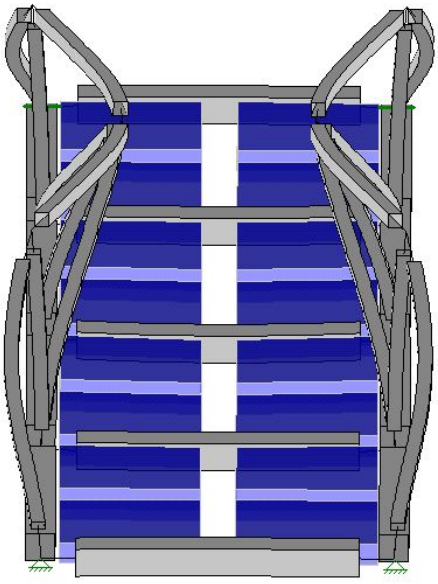

Figure 9.9 *Bridge 1* Deformation of end-diagonal (computer model) at critical load

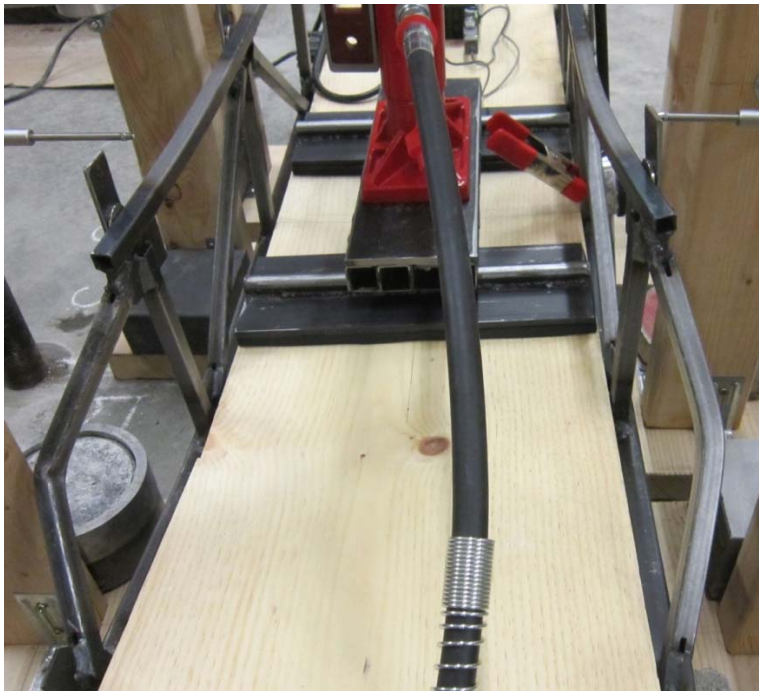

Figure 9.10 *Bridge 1* Deformation of end-diagonal at buckling (test model)

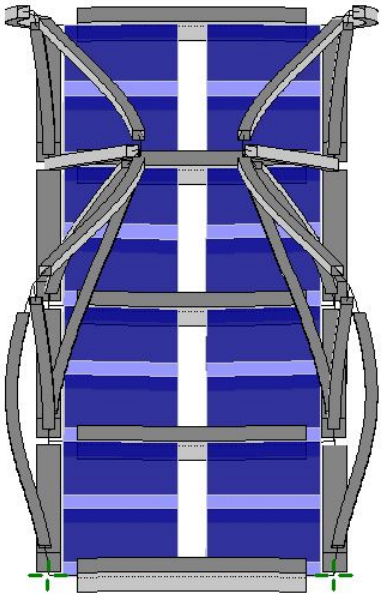

Figure 9.11 *Bridge 1* Deformation of end-diagonal (computer model) at critical load

Bridge 2 Results

Theoretical Results

Similar to *Bridge 1*, the *theoretical models* were analyzed by following the methodology presented in Chapter VI. The analysis consisted on finding the load-deformation history and critical load of *Bridge 2* with three different initial imperfections. In addition, the imperfections were modeled by using two different approaches: notional loads and modeling the imperfection directly in to the model. The results from the *theoretical model* of *Bridge 2* are compared in Table 9.8 and plotted in Figure 9.12. These results are presented as the ratio of the second-order displacement to the initial imperfection (Δ/Δ_o), of the top chord, for a corresponding gravity load. The critical loads for the theoretical models are summarized in Table 9.9.

The results between the notional load (NL) approach and the direct modeling (DM) approach correlate well. However, the difference is not as small as *Bridge 1*. At a load 3,000 lb, and for an initial imperfection of *L*/300, the top chord amplifications were 1.586 and 1.602 for the notional load and the modeled imperfection approaches respectively, compared to amplifications of 1.600 and 1.667 when an initial imperfection of *L*/450 is applied to the top chord. And for *L*/700, the top chord amplifications were 1.586 and 1.602 for the notional load (NL) and the direct modeling (DM) approaches respectively. At 4,000 lbs the top chord amplifications were 2.113 (NL) and 2.053 (DM) for *L*/300, 2.222 (NL) and 2.178 (DM) for *L*/450

and 2.456 and 2.368 (DM) for *L*/700. At 6,000 lbs the top chord amplifications were 5.489 (NL) and 4.887 (DM) for *L*/300, 5.900 (NL) and 5.244(DM) for *L*/450 and 6.702 and 6.088 (DM) for *L*/700.

The maximum difference, approximately 11%, between both approaches occurred when the initial imperfection was *L*/450 and corresponded to gravity loads of 6,000 lbs and 7,000 lbs. For the remaining load levels the difference was less than 8%. The difference, between approachess, can be seen in Figure 9.12, where the spread of results is more evident at about an amplification ratio (Δ/Δ_o) of 10 compared to the results from the *Bridge 1* test. However, all of the critical loads were only within 0.50% or less.The critical load for an initial imperfection of *L*/300 was 7,155 lbs for the notional load approach and 7,178 lbs for the direct modeling approach. For *L*/450 the critical load was 7,100 lbs and 7,140 lbs for the notional load and the modeled imperfection approach respectively, and for an initial imperfection of *L*/700, the critical load was 7,180 lbs for both, the notional load and the modeled imperfection approaches. Based on the results from the *theoretical models*, the critical load for *Bridge 2 test model* is expected to be close to 7,150 lbs.

It can be seen in Figure 9.12 that at load levels up to and less than 70% of the critical load, the structure remains reasonably stable. It is, however, beyond this point that the models start to lose significant stiffness and become instable, to the point that at about 85% of the critical load the amplification of the top chord Δ/Δ_o, is more than 5 times. For example, between 1,000 lbs and 4,000 lbs the difference in the

amplification ratio, Δ/Δ_o, is approximately 38%. Between an applied gravity load of 4,000 lbs and 5,000 lbs the difference is 49%, while between load 5,000 lbs and 6,000 lbs the difference is 78%. This difference is more than 300% when the applied load goes from 6,000 lbs to 7,000 lbs, demonstrating that significant instability occurs when the applied load approaches the critical load.

Table 9.8 *Bridge 2* Theoretical Results: Top chord ratio Δ/Δ_o

Load (lbs)	NL	DM	NL	DM	NL	DM
	$\Delta_o = L/300$		$\Delta_o = L/450$		$\Delta_o = L/700$	
0	1.0	1.0	1.0	1.0	1.0	1.0
1000	1.128	1.128	1.144	1.144	1.193	1.193
3000	1.586	1.602	1.600	1.667	1.754	1.789
4000	2.113	2.053	2.222	2.178	2.456	2.368
5000	3.098	2.872	3.311	3.078	3.667	3.456
6000	5.489	4.887	5.900	5.244	6.702	6.088
7000	22.594	21.000	23.722	22.594	25.772	22.950

NL=Notional Load DM=Direct Modeling

Table 9.9 *Bridge 2* Theoretical Results: Critical load

Critical Load (lbs)	NL	DM	NL	DM	NL	DM
	$\Delta_o = L/300$		$\Delta_o = L/450$		$\Delta_o = L/700$	
	7155	7178	7100	7140	7180	7180

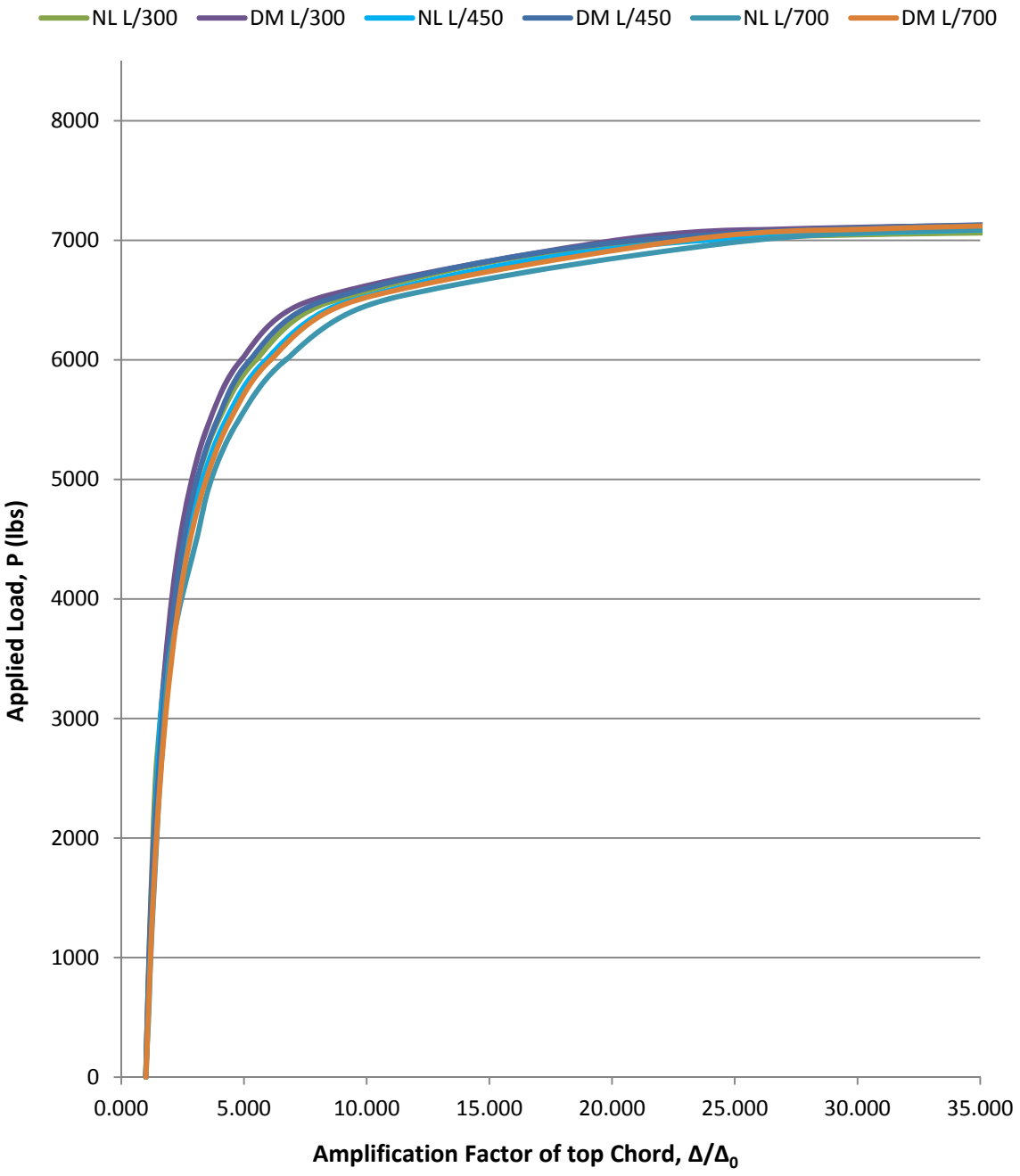

NL = Notional Load DM = Direct Modeling

Figure 9.12 *Bridge 2* Theoretical (pin-ended diagonals) results

Load Test Results

Similar to *Bridge 1*, the *test model* for *Bridge 2* was tested in accordance with the procedure presented in Chapter VIII. The results from the *test model* for both top chords (C1 and C2) are presented in Table 9.10. These results are compared to the results from the *theoretical model*s. However, only the results from the notional load (NL) approach are presented in Table 9.10 for comparison. These results are also plotted in Figure 9.13. It can be observed that up to a load level of 6,000 lbs the ratios Δ/Δ_o for both, the theoretical models and the test models, correlate very well. From this point the *test model* exhibited higher deformation capacity, although not as much as the capacity exhibited by *Bridge 1*. At this load, 6,000 lbs, the amplification factor, Δ/Δ_o, was 5.111 for chord 1 (C1) and 5.238 for chord 2 (C2) for the *test model*, compared to 5.489, 5.900 and 6.702 for imperfections *L*/300, *L*/450 and *L*/700 respectively for the *theoretical models*.

The critical loads are presented in Table 9.11. As mentioned earlier, the expected critical load of *Bridge 2*, based on the theoretical results, is approximately 7,150 lbs. The actual load from the load test was 7,902 lbs. The difference between the theoretical results and the actual model is only 10%. Although the test model exhibited higher deformation capacity during the final moments of the load test than the theoretical model, it might seem that, even though the diagonal connections provided some additional stiffness, they did not contribute with the same level of fixidity as to *Bridge 1*.

Similar to *Bridge 1*, the *test model* of *Bridge 2* remains reasonably stable up to loads of approximately 64% of the critical load. Beyond that point the model begins to lose stiffness due to second-order effects. At an applied load of 75% of the critical load, the amplification of the top chord is more than 5 times, while at 89% the amplification is more than 12 times. It can be seen that between 75% and 90% of the critical load, the secondary effects of the top chord cause significant destabilization of the structure.

Figures 9.13 through 9.17 show a series of side-by-side shots of the bridge's top chord deformed shape between the computer model and the actual model for different load values. The intent is to compare the deformed shape between both models for 53%, 78% and 91% of the critical load respectively. In addition, Figures 9.18 and 9.19 show the deformed shape of the *theoretical model* and the *test model*, respectively, at the critical load. From these pictures it can be observed that results from the computer program demonstrate good agreement with the load test.

Table 9.10 *Bridge 2* Theoretical and Load Test Results: Top chord ratio Δ / Δ_o

Load (lbs)	NL Δ_o= L/300	NL Δ_o= L/450	NL Δ_o= L/700	B2-C1 Δ_o= L/445	B2-C2 Δ_o= L/377
0	1.0	1.0	1.0	1.0	1.0
1000	1.128	1.144	1.193	1.100	1.143
3000	1.586	1.600	1.754	1.689	1.619
4000	2.113	2.222	2.456	2.378	2.238
5000	3.098	3.311	3.667	3.656	3.524
6000	5.489	5.900	6.702	5.111	5.238
7000	22.594	23.722	25.772	12.278	11.905
7500	N/A	N/A	N/A	15.033	14.762
7900	N/A	N/A	N/A	25.556	24.762

NL=Notional Load

Table 9.11 *Bridge 2* Theoretical and Load Test Results: Critical load

	NL Δ_o= L/300	NL Δ_o= L/450	NL Δ_o= L/700	B2-C1 Δ_o= L/445	B2-C2 Δ_o= L/377
Critical Load (lbs)	7155	7100	7180	7902	7902

NL=Notional Load

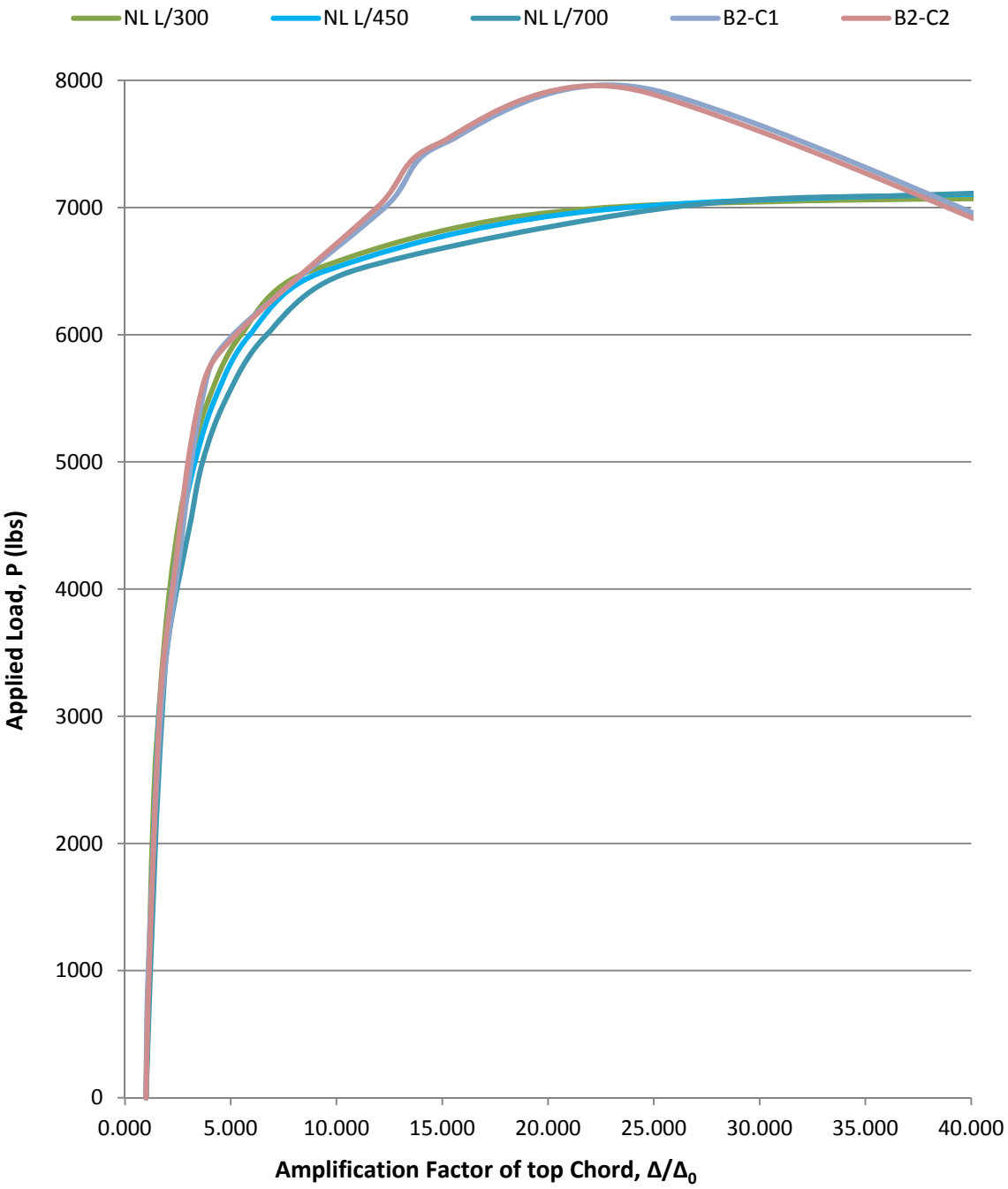

NL = Notional Load

Figure 9.13 *Bridge 2* Theoretical and load test results

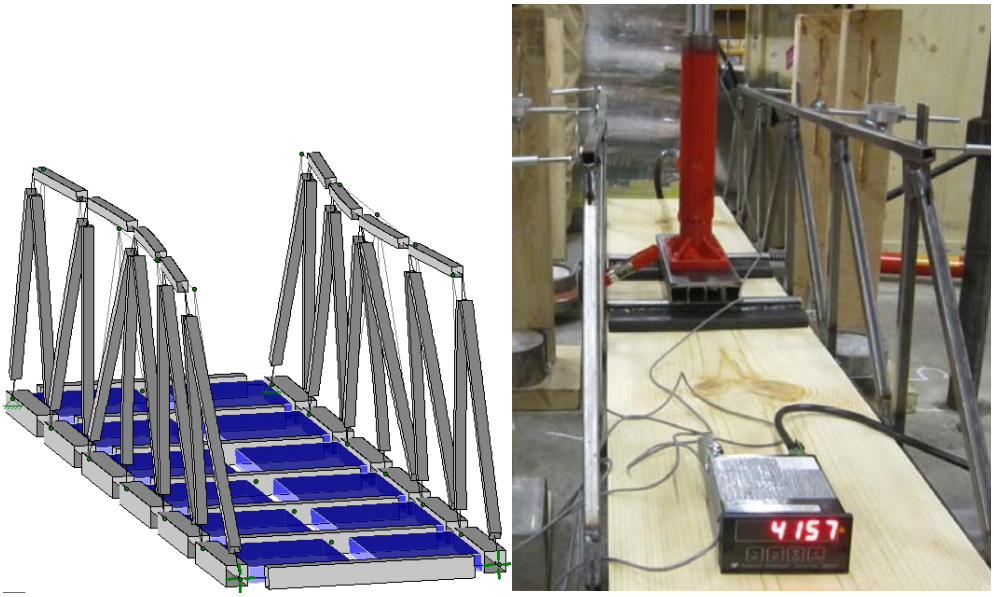

Figure 9.14 *Bridge 2* Deformed shape at 53% of the critical load

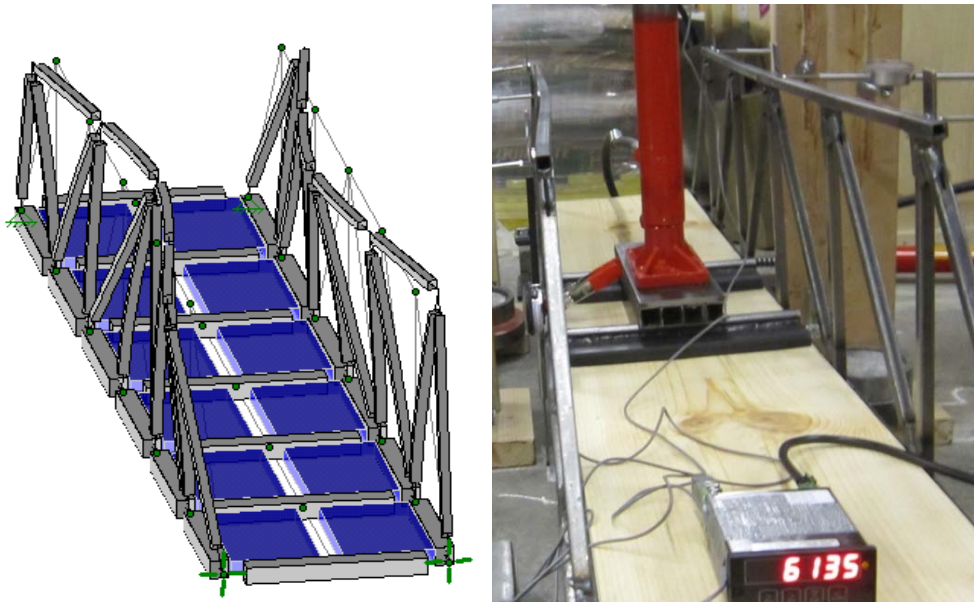

Figure 9.15 *Bridge 2* Deformed shape at 78% of critical load

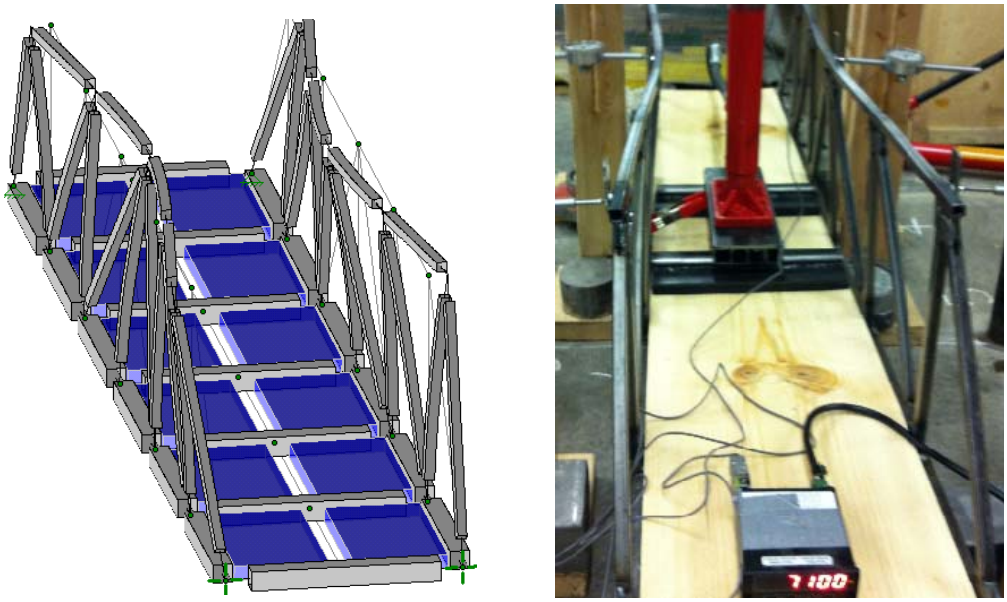

Figure 9.16 *Bridge 2* Deformed shape at 91% of the critical load

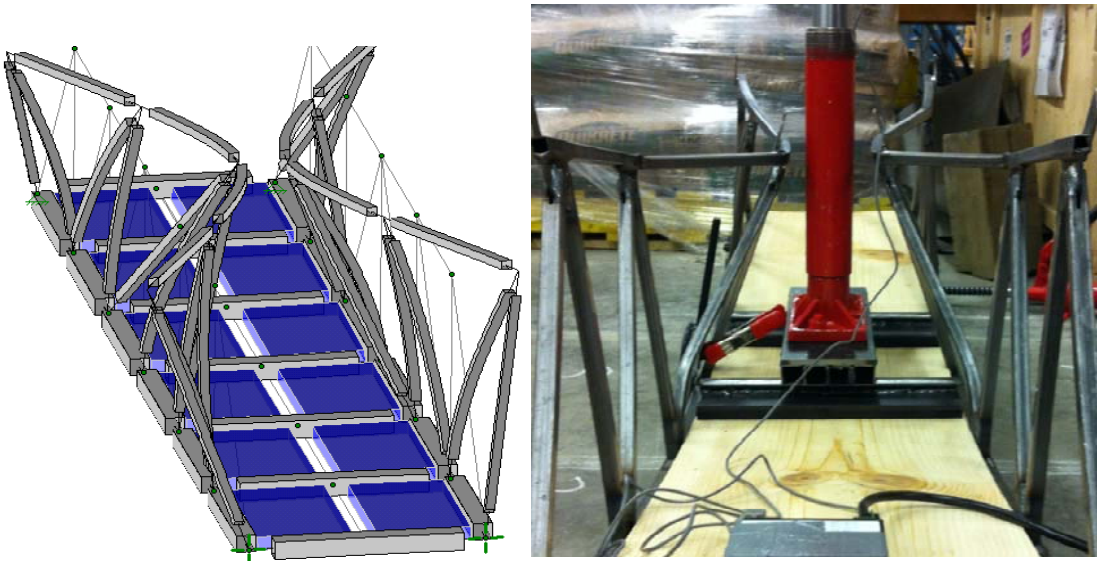

Figure 9.17 *Bridge 2* Deformed shape at critical load

CHAPTER X

CONCLUSIONS

Research Overview

The stability and load-deformation behavior of pony truss bridges were investigated using experimental testing and computational modeling, with the intent of validate an innovative methodology for critical load determination. The laboratory experiments were conducted on the pony truss bridges that were load tested without intermediate braces. The computational model was developed using the three-dimensional computer program, RISA-3D. A variety of analytical models were used to simulate both as-built and idealized truss models. The methodology computer model was verified by the laboratory test results.

A parametric investigation was developed using full-size pony truss bridge models, from hollow steel sections, with the purpose of developing expressions for determining the stiffness requirements of software generated scaled pony truss models. Based upon results from the parametric investigations, two scaled computer models were developed with the same aspect ratio, AR, of 0.20 and two different stiffness parameters, ξ, 63 for the long bridge and 97 for the short bridge. The scaled pony truss computer models were used for predicting the buckling capacity and load-deformation behavior of the laboratory experiments by following the proposed methodology.

Research Conclusions

Overall, the laboratory experiments agreed well with the computer model results and validate the results from the proposed methodology. In addition, the laboratory experiments demonstrated that the buckling capacity of the pony truss bridge is largely depended on the cross frame stiffness, the connection behavior between members and the number of intermediate panels.

Both laboratory experiments demonstrated that significant instability starts to occur at load levels above 70% of the calculated critical load. In both cases, the top chords deflected towards the center of the bridge. This is because the load on the bridge caused the cross-frame to deflect downward causing the verticals to rotate inwards.

The experimental results of *Bridge 1* demonstrated that the connection modeling assumptions of the diagonals play a critical role for the prediction of the critical load. In this case, the diagonals provided more stiffness to the cross frame than assumed. However, after modifying the connections of the theoretical models from pin-pin to fix-fix end restraints, the load-deformation behavior of the model closely matched the results from the laboratory experiment.

On the other hand, good agreement was found between the computer model and the laboratory experiment of *Bridge 2*. Although the critical load of the test model was 10% higher than the computer model, the load-deformation history of the laboratory experiment followed very closely the one from the computer model. In this

case, because the diagonals were longer than the diagonals of *Bridge 1*, the connections to the diagonals did not provide as much stiffening effects to the cross frame (U-frame) as with *Bridge 1*. However, it is still believed that some level of partial fixity, out of plane of the truss, was provided by the gusset plate.

General Recommendations

From the results of this research project, the proposed methodology gives a good indication of the critical load of a particular structure and the destabilizing effects of second-order forces due to *P-Δ*. Below are some recommendations when using the proposed methodology:

1. Verify that computer software package selected can perform a rigorous second-order analysis. This can be done with benchmark problems given in published literature, including AISC 360-10 (AISC 2010).
2. Because some computer software packages calculate secondary effects at node locations, it might be necessary to analyze the structure with different number of additional nodes between supports.
3. If moment-rotational information is available for the connections between members, this can be used to provide a more realistic analysis. Otherwise, a conservative assumption should be made.
4. It is recommended to use 75% of the theoretical critical load for ultimate design.

5. However, because actual design is based on limit states, a factor of safety needs to be incorporated for the final design. Its suggested to use the Direct Analysis Method's third constraint, which requires that the analysis be based on a reduced stiffness ($EI^*=0.80\tau_b(EI)$), where the $0.80\tau_b$ factor reduces the stiffness to account for inelastic softening prior to the members reaching their ultimate strength. For slender compression members, the critical load is most likely below 50% the yield strength, thus $\tau_b=1.0$. In this case 0.80 is roughly equivalent to the margin of safety implied by design of slender columns (AISC 2005).

REFERENCES

AASHTO (2009). *LRFD Guide specifications for the design of pedestrian bridges 2th edition*. American Association of State Highway and Transportation Officials, Washington, DC.

AASHTO (2012). AASHTO *LRFD bridge design specifications 4th edition*. American Association of State Highway and Transportation Officials, Washington, DC.

AISC (1961). *Specification for the design, fabrication and erection of structural steel for buildings*. American Institute of Steel Construction, New York, NY.

AISC (1999). *Load and Resistance Factor Design Specification for structural steel buildings*. American Institute of Steel Construction, Inc. Chicago.

AISC (2005*). Specification for structural steel buildings (ANSI/AISC 360-05)*. American Institute of Steel Construction, Inc. Chicago.

AISC (2010) Specification *for structural steel buildings (ANSI/AISC 360-10).* American Institute of Steel Construction, Inc. Chicago.

AISC (2010*) Code of standard practice for steel buildings and bridges (AISC 303-10)*. American Institute of Steel Construction, Inc. Chicago.

ASCE Task Committee on Effective Length. (1997*) Effective length and notional load approaches for assessing frame stability: implications for American steel design.* American Society of Civil Engineers, New York.

AWS (2002). *Structural Welding Code-Steel, D1.1.* American Welding Society, Miami, FL

Bjorhovde, R. (1972). *Deterministic and probabilistic approaches to the strength of steel columns*, Ph.D. dissertation, Lehigh University, Bethlehem, PA

Bjorhovde, R. (1984). "Effect of end restraint on column strength –practical applications." *AISC Engineering Journal,* 1st Qtr. 1-13

Chen, W. F., and Han, D. J. (1985). *Tubular members in offshore structures*. Pitman Publishing, Inc., Marshfield, MA.

Chen, W. F., and Lui, E. M. (1991). *Stability design of steel frames*. CRC Press, Boca Raton, FL.

Chen, W.F., Guo, Y. and Liew, J.Y.R., (1996). *Stability Design of Semi-Rigid Frames*. John Wiley & Son, Inc., New York.

Christopher, J.E. and Bjorhovde, R. (1999). "Semi-rigid frame design methods for practicing engineers." *AISC Engineering Journal*, 36 (1), 12-28.

Clark, M. and Bridge, R. Q. (1992). "The inclusion of imperfections in the design of beam-columns." *Proceedings 1992 Annual Technical Session*, Bethlehem, PA, April. Structural Stability Research Council, Rolla, MO.

Deierlein, G. G., Hajjar, J. F., Yura, J. A., White, D. W., and Baker, W. F. (2002). "Proposed new provisions for frame stability using second-order analysis." *Proceedings 2002 Annual Technical Session*, Seattle, April. Structural Stability Research Council, Rolla, MO.

Ericksen, J. R. (2011). "A how-to approach to notional loads." *AISC Modern Steel Construction,* 51 (1). 44-45.

Fernandez, P., and Rutz, F.R. (2013). "A practical method for critical load determination and stability evaluation of structures." Proceedings of the 2013 Structures Congress, ed. B. J. Leshko and J. McHugh, Structural Engineering Institute of the American Society of Civil Engineers, May 1-4, 2013, Pittsburgh, PA, ASCE, Reston VA.

Folse, M. D., and Nowak, P. S. (1995). "Steel rigid frames with leaning columns – 1993 LRFD example." *AISC Engineering Journal,* 32 (4). 125-131.

Galambos, T. V. ed (1998). *Guide to stability design criteria for metal structures, 5th Edition*. John Wiley & Sons, Inc., Hoboken, NJ.

Gere, J. M. and Goodno, B. J. (2009). *Mechanics of Materials, 7th Edition*. Cengage Learning, Toronto, ON.

Geschwindner, L. F. (2002). "A practical look at frame analysis stability and leaning columns." *AISC Engineering Journal,* 39 (4). 167-181

Geschwindner, L. F. (2009). "Design for stability using 2005 AISC specification." seminar notes, presented Sept 18, 2009, Sponsored by AISC, Chicago, IL.

Geschwindner, L. F., Disque, R. O. and Bjorhovde, R. (1994). *Load and resistance factor design of steel structures*. Prentice Hall, Inc., Englewood, NJ.

Hamberger, R. and Whittaker, A. S. (2004). "Design of steel structures for blast-related progressive collapse resistance." *AISC Modern Steel Construction,* 44 (3), 45-51.

Heyman, J. (1998). "Structural analysis a historical approach." Cambridge University Press, Cambridge, UK.

Hibbeler, R. C. (2009). *Mechanics of materials 6th Edition*. Pearson Prentice Hall, New Jersey.

Hibbeler, R. C. (2009). "Structural analysis 7th Edition." Pearson Prentice Hall, New Jersey.

Johnston, B. G. (1981). "Column Buckling Theory: Historic Highlights." *ASCE Journal of Structural Engineering*, 109 (9). 86-96

Kanchanalai, T., and Lu, L.-W. (1979). "Analysis and design of framed columns under minor axis bending." *AISC Engineering Journal,* 16 (2). 29-41.

LeMessurier, W. J. (1976). "A practical method of second order analysis part 1 – pin jointed systems." *AISC Engineering Journal,* 13 (4). 89-96

LeMessurier, W. J. (1977). "A practical method of second order analysis part 2 – rigid frames." *AISC Engineering Journal,* 14 (2). 49-67

Maleck, A.E., and White, D.W. (1998). "Effects of imperfections on steel framing systems." *Proceedings 1998 Annual Technical Sessions*, Atlanta, September. Structural Stability Research Council, Rolla, MO.

Maleck, A. E., and White, D. W. (2003). "Direct analysis approach for the assessment of frame stability: verification studies." *Proceedings Annual Technical Sessions*, Baltimore, April, Structural Stability Research Council, Rolla, MO. 18

McCormac, J. C. (2007). *Structural analysis using classical and matrix methods*. John Wiley & Sons, Inc., Hoboken, NJ.

McCormac, J. C. (2008). *Structural steel design, 4th Edition*. Pearson Prentice Hall, Upper Saddle River, NJ.

McGuire, W., Gallegher, R. H., and Ziemian, R. D. (2000). *Matrix structural analysis, 2nd Edition*. John Wiley & Sons Inc., Hoboken, NJ.

Nair, S. R. (2009). "A model specification for stability design by direct analysis." *AISC Engineering Journal,* 46 (1). 29-37

Powell, G. H. (2010). *Modeling for structural analysis: behavior and basics*. Computers and Structures, Inc. Berkeley, CA.

RISA-3D (2012). *RISA-3D v11 General reference manual*. RISA Technologies, Foothill Ranch, CA.

Salmon, C. G., and Johnson, J. E. (2008). *Steel structures: design and behavior, emphasizing load and resistance design 5th Edition*. Harper Collins, New York.

Shanmugam , N. E. and Chen, W. F. (1995). "An assessment of K factor formulas." *AISC Engineering Journal,* 1 Qtr. 3-11

Surovek, A. E. (2008). "Effects of nonverticality on steel framing systems-implications for design." *AISC Engineering Journal,* 45 (1). 73-85.

Surovek, A. E. ed (2012). *Advanced analysis in steel frame design: Guidelines for direct second-order inelastic analysis*. American Society of Civil Engineers, New York.

Surovek-Maleck, A. E., and White, D. W. (2004a). "Alternative approaches for elastic analysis and design of steel frames. I: overview." *ASCE Journal of Structural Engineering,* 130 (8). 1186-1196.

Surovek-Maleck, A.E., and White, D.W. (2004b) "Alternative approaches for elastic analysis and design of steel frames. II: verification studies." *ASCE Journal of Structural Engineering,* 130 (8). 1197-1205.

Timoshenko, S. P. (1983). *History of strength of materials*. Dover publications, Inc., Mineola, NY.

Timoshenko, S. P., and Gere, J. M. (1989). *Theory of elastic stability*. Dover publications, Inc., Mineola, NY.

White, D. W., and Hajjar, J. F. (1991). "Application of second-order elastic analysis in LRFD: research to practice." *AISC Engineering Journal,* 28 (4). 133-148.

White, D. W., Surovek, A. E., and Kin, S-C. (2007a). "Direct analysis and design using amplified first-order analysis. part 1 – combined braced and gravity framing systems." *AISC Engineering Journal,* 44 (4). 305-322.

White, D. W., Surovek, A. E., and Chang, C-J. (2007b). "Direct analysis and design using amplified first-order analysis. part 2 – moment frames and general framing systems." *AISC Engineering Journal,* 44 (4). 323-340.

Williams, A. (2009). *Structural analysis: in theory and practice*. Elsevier, Burlington, MA.

Williams, A. (2011*). Steel structures design ASD/LFRD*. McGraw Hill, Washington, DC

Yura, J. A. (1971). "The effective length of columns in unbraced frames." *AISC Engineering Journal,* 8 (2). 37-42.

Yura, J. A., Kanchanalai, T., and Chotichanathawenwong, S. (1996). "Verification of steel beam-column design based on the AISC-LRFD method." *Proceeding 5th International Colloquium Stability Metal Structures,* Lehigh University, Bethlehem, PA, Structural Stability Research Council, Rolla, MO. 21-30.

Ziemianm, R. A. ed (2010). *Guide to stability design criteria for metal structures, 6th Edition*. John Wiley & Sons, Inc., Hoboken, NJ.

Ziemianm, R. A., McGuire, W., Seo, D. W. (2008). "On the inelastic strength of beam-columns under biaxial bending." *Proceedings Annual Technical Sessions*, Nashville, April, Structural Stability Research Council, Rolla, MO. 18

APPENDIX 1: TEST MODELS PLANS

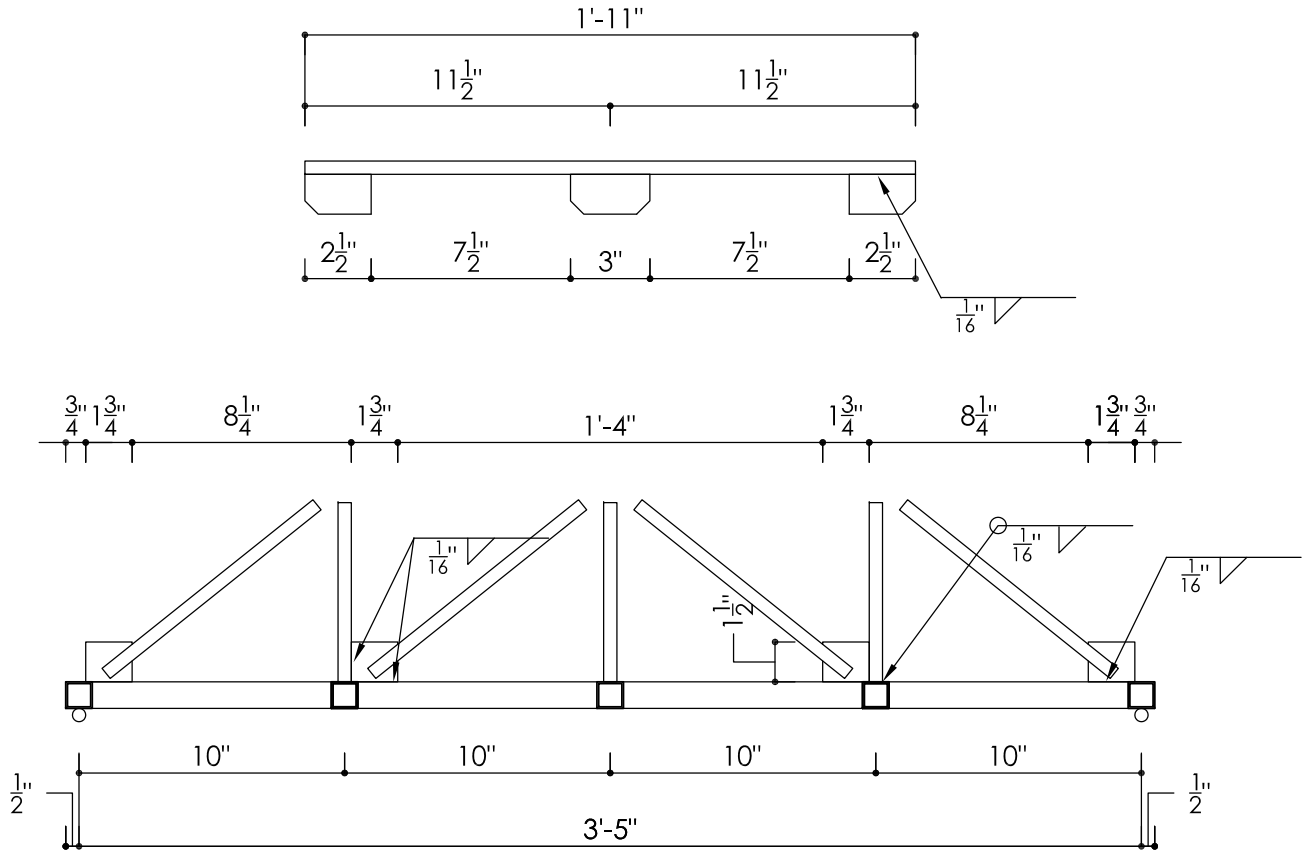

TRUSS ASSEMBLAGE

JOB NAME: PRACTICAL METHODS FOR CRITICAL LOAD DETERMINATION AND STABILITY EVALUATION OF STEEL STRUCTURES	SHEET TITLE: BRIDGE 1 PRODUCTION SHEET	DRAWING STATUS	REVISION	REVISION BY	REVISION DATE	DESCRIPTION	B1.2
	DRAWN: PEDRO FERNANDEZ						

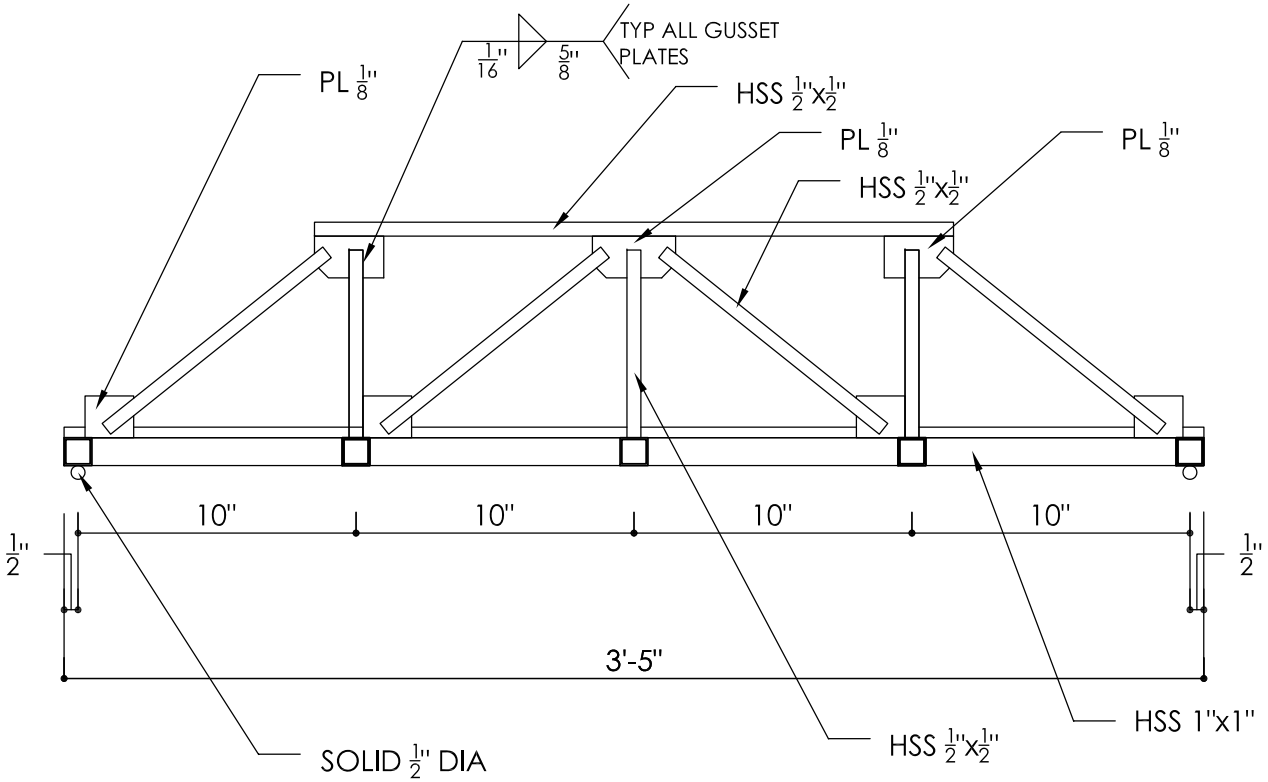

ELEVATION VIEW

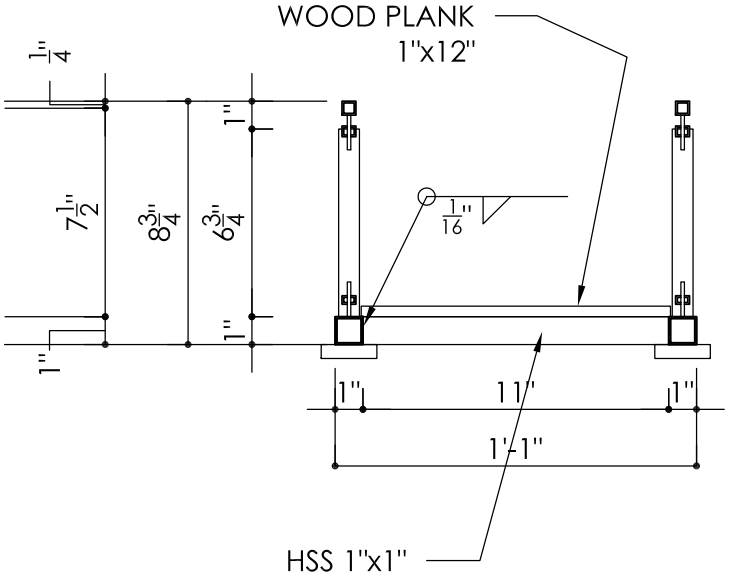

SECTION VIEW

JOB NAME: PRACTICAL METHODS FOR CRITICAL LOAD DETERMINATION AND STABILITY EVALUATION OF STEEL STRUCTURES	SHEET TITLE: BRIDGE 1 PRODUCTION SHEET	DRAWING STATUS	REVISION	REVISION BY	REVISION DATE	DESCRIPTION
	DRAWN: PEDRO FERNANDEZ		△			
						B1.1

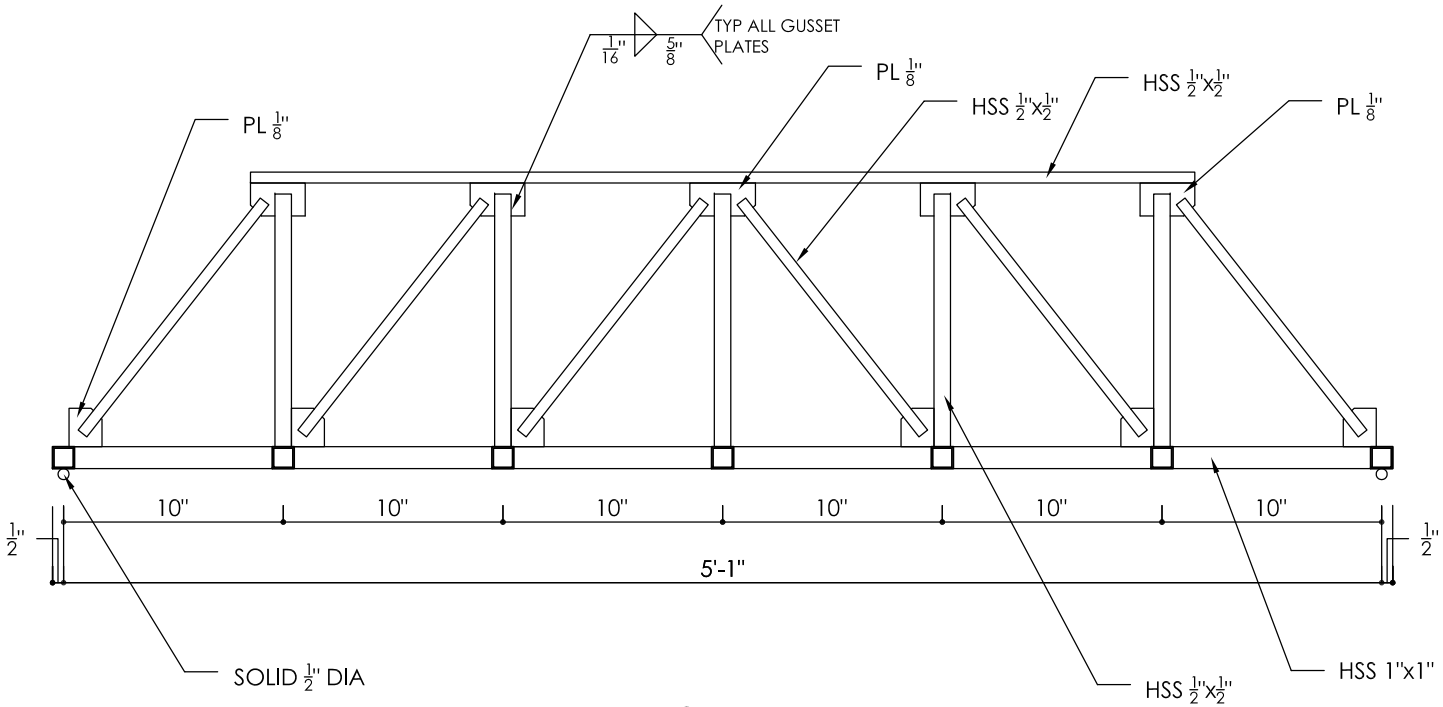

ELEVATION VIEW

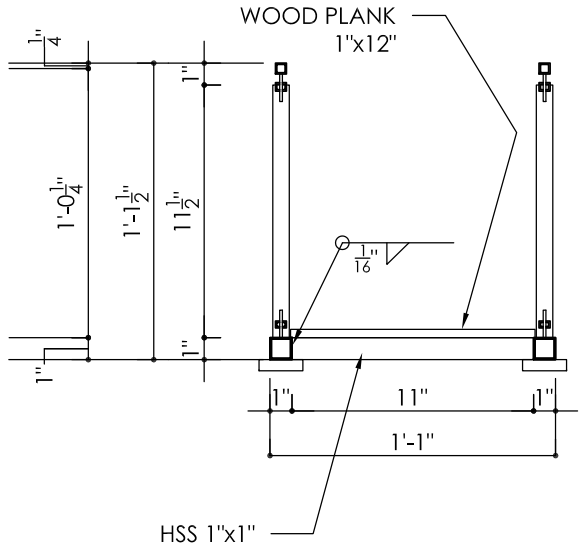

SECTION VIEW

JOB NAME: PRACTICAL METHODS FOR CRITICAL LOAD DETERMINATION AND STABILITY EVALUATION OF STEEL STRUCTURES	SHEET TITLE: BRIDGE 2 PRODUCTION SHEET	DRAWING STATUS	REVISION	REVISION BY	REVISION DATE	DESCRIPTION
	DRAWN: PEDRO FERNANDEZ		△			
						B2.1

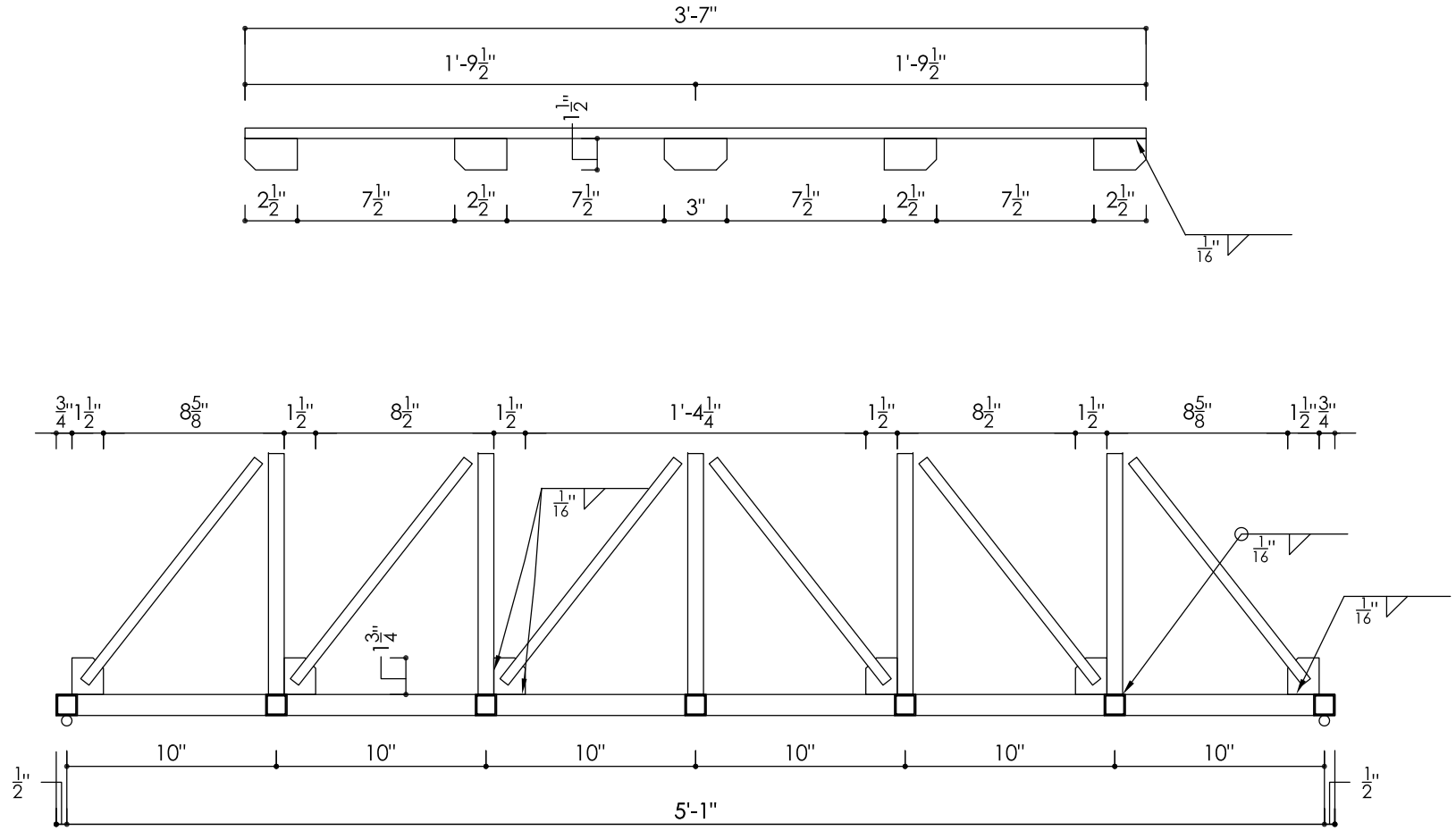

TRUSS ASSEMBLAGE

JOB NAME: PRACTICAL METHODS FOR CRITICAL LOAD DETERMINATION AND STABILITY EVALUATION OF STEEL STRUCTURES	SHEET TITLE: BRIDGE 2 PRODUCTION SHEET	DRAWING STATUS	REVISION	REVISION BY	REVISION DATE	DESCRIPTION	B2.2
	DRAWN: PEDRO FERNANDEZ						